# ANALYSIS AND DESIGN OF MODIFICATIONS FOR IMPROVED PERFORMANCE OF THE AFIT RADAR CROSS SECTION MEASUREMENT CHAMBER

THESIS

Anthony J. Hunt
Captain, USA

AFIT/GE/ENG/90J-03





DEPARTMENT OF THE AIR FORCE
AIR UNIVERSITY
AIR FORCE INSTITUTE OF TECHNOLOGY

Wright-Patterson Air Force Base, Ohio

AFIT/GE/ENG/90J-03

# ANALYSIS AND DESIGN OF MODIFICATIONS FOR IMPROVED PERFORMANCE OF THE AFIT RADAR CROSS SECTION MEASUREMENT CHAMBER

THESIS

Anthony J. Hunt
Captain, USA

AFIT/GE/ENG/90J-03

AFIT/GE/ENG/90J-03

# ANALYSIS AND DESIGN OF MODIFICATIONS FOR IMPROVED PERFORMANCE OF THE AFIT RADAR CROSS SECTION MEASUREMENT CHAMBER

THESIS



Presented to the Faculty of the School of Engineering
of the Air Force Institute of Technology
Air University
In Partial Fulfillment of the
Requirements for the Degree of
Master of Science in Electrical Engineering



Anthony J. Hunt, B.S.
Captain, USA

June, 1990

Approved for public release; distribution unlimited

*Acknowledgements*

Throughout this effort, many individuals have provided invaluable assistance. First and foremost is my advisor, Captain Philip J. Joseph, who has my greatest appreciation. His knowledge, direction and advice from conception to finish has been instrumental in my success. My sincere thanks also to my committee members, Dr. Andrew Terzuoli and Maj Harry Barksdale, who were always willing to lend their expertise.

The AFIT Fabrication Shop provided essential support. A special thanks goes to Mr. Ron Ruley for his work on the support pedestal, Mr. John Brohas and Mr. David Driscoll for their work on the translation device, Mr. Jan LeValley for his work on the translation device and the target mounting ladder, and Mr. Jack Tiffany for his technical advice and organizing the entire fabrication effort. Another individual who has my special appreciation is Mr. Robert Lindsay whose technical expertise not only contributed significantly to design considerations, but also provided the necessary support equipment to conduct the desired measurements. His willingness to lend a hand is also highly appreciated and commendable.

For that person who no amount of thanks is sufficient; my wife, Debbie, who provided constant support and encouragement. Finally, my deepest gratitude to my four sons, Anthony Jr., Eric, Daniel, and Justin for their sacrifices.

## *Table of Contents*

## *List of Figures*

# List of Tables

## Abstract

This research effort investigated improvements and characterization of the AFIT RCS measurement chamber. The two main areas of improvement included the support pedestal and antennas. Characterization included antenna and system performance as pertains to aliasing, noise floor and quiet zone definition.

Support pedestal improvement involved consideration of the three primary types used: the suspension line support, foamed plastic columns, and ogive-shaped metal pylon. Antenna improvement included installing broad bandwidth, low side-lobe antennas. These were mounted so that they could be easily rotated for polarization selection, and so that they provided a good approximation to a backscatter angle of zero degrees without incurring high antenna coupling.

System aliasing measurements and analysis was performed to ensure that the full bandwidth capacity of the antennas was achievable without causing alias error signals to enter the target zone. Noise floor data was taken to determine the degree of sensitivity improvement after modifications. Quiet zone characterization was designed to verify predictions and provide actual dimensions for measurement analysis. Additionally, the quiet zone measurements provided information as to the pedestal location relative to the focus of the antenna.

# ANALYSIS AND DESIGN OF MODIFICATIONS FOR IMPROVED PERFORMANCE OF THE AFIT RADAR CROSS SECTION MEASUREMENT CHAMBER

## I. *Introduction*

### *Background*

The radar cross section (RCS) of an arbitrary target can be measured in an anechoic chamber configured with an appropriate radar transceiver and target support fixture. The anechoic (no echo) chamber itself consists of an enclosed room lined with radar absorbing material. Transmitting and receiving antennas are typically placed side-by-side (in one wall) to measure radar backscatter. A target support pedestal is placed at the opposite end of the room, to provide maximum downrange distance from antenna to target. Other factors such as clutter levels and target/room interactions also impact the desired pedestal position. In this configuration, the pedestal provides a means of supporting and rotating targets to measure their RCS.

The measurement of RCS depends on the signal seen at the receive antenna for both the unknown target and a calibration target. This received signal is corrupted by energy transmitted into the room which scatters off the walls, floor, ceiling, pedestal, or anything else in the room. Energy received from all objects other than the target are, of course, unwanted. Fortunately, radar absorbing material exists which can be placed on the walls, floor, and ceiling to greatly reduce the unwanted energy returned to the receiver. Also, measurement techniques such as time gating (range gating) discount energy that returns too early or too late to be a target return. Background nulling and background subtraction techniques also exist which help eliminate unwanted returns from the room. For example, to improve the raw target measurement, a measurement is made with the target mount but without the target. This "target background" is then vectorially subtracted from the target measurement.

Although these techniques work very well for most of the unwanted signals, there is still a major contributor that is not eliminated. This is the interaction between the target and its mount and the support pedestal. Since the target is not present during the background measurement, the target/support interactions can not be subtracted. Since the target, mount, and pedestal top are all in relative close proximity, these interactions can not be range gated out. Thus, a mount and pedestal configuration is needed which will minimize the target support interaction.

The need to approximate a plane wave incident on the target results from the equation used to define the RCS, which is given by

$$\sigma = \lim_{R \to \infty} 4\pi R^2 \frac{| E_s |^2}{| E_i |^2} \tag{1}$$

In actuality, this plane wave is approximated by placing the target far enough away from the antenna, which radiates spherically, so that the target illumination meets some allowable amplitude and phase variation.

*Problem Statement*

The purpose of this research is to improve the measurement capability of the AFIT chamber through three primary efforts. These consist of installing broadband, low sidelobe antennas; reworking the target support pedestal for lower direct return and lower interactions; and characterization of the target zone. Additional considerations include a convenient means of placing targets on the pedestal and software control of antenna polarization.

*Approach*

The first effort is to improve system performance by installing new transmit and receive antennas. These antennas were chosen by the need for greater bandwidth and lower sidelobes. The increased bandwidth allows for the measurements of RCS over a larger range of frequencies. Also, given the (complex) frequency response of a target over some bandwidth, a bandlimited impulse response can be calculated. The resolution of this impulse response improves as system bandwidth increases. The requirement for low sidelobes serves to concentrate energy on the target and minimize clutter returns. The installation must provide a mounting configuration which allows computer-controlled rotation from horizontal to vertical polarization and back. As will be discussed later, a side benefit in the choice of antennas and mounting configuration was a reduction in antenna coupling which increases system dynamic range.

The second effort concerns the upgrade of the target support pedestal. The old design for the pedestal, as shown in Figure 1, was based on the use of a very large rotator. To support the rotator a box-shaped frame was built under the desired pylon shape. Unfortunately, the frame was too large for the pylon shape to cover. Thus, a skirt was formed along the bottom. In addition, pyramidal absorber was placed upright around the bottom of the support pedestal to reduce returns. This set-up had two major drawbacks. The first was that the leading edge of the pedestal directed energy down into the side of a piece of absorber which is designed to absorb best when the energy is directed normal to its surface. The second drawback was the practical problems associated with target installation with absorber at the pedestal base. The new design will take advantage of a smaller target rotator currently in use. The goals of the new design are to reduce the RCS of the pedestal itself, to reduce target/support interactions, and to allow an improved technique for mounting targets. The RCS of the pedestal will be reduced by extending the ogive shape all the way to the floor so that the leading edge directs all energy down normal to

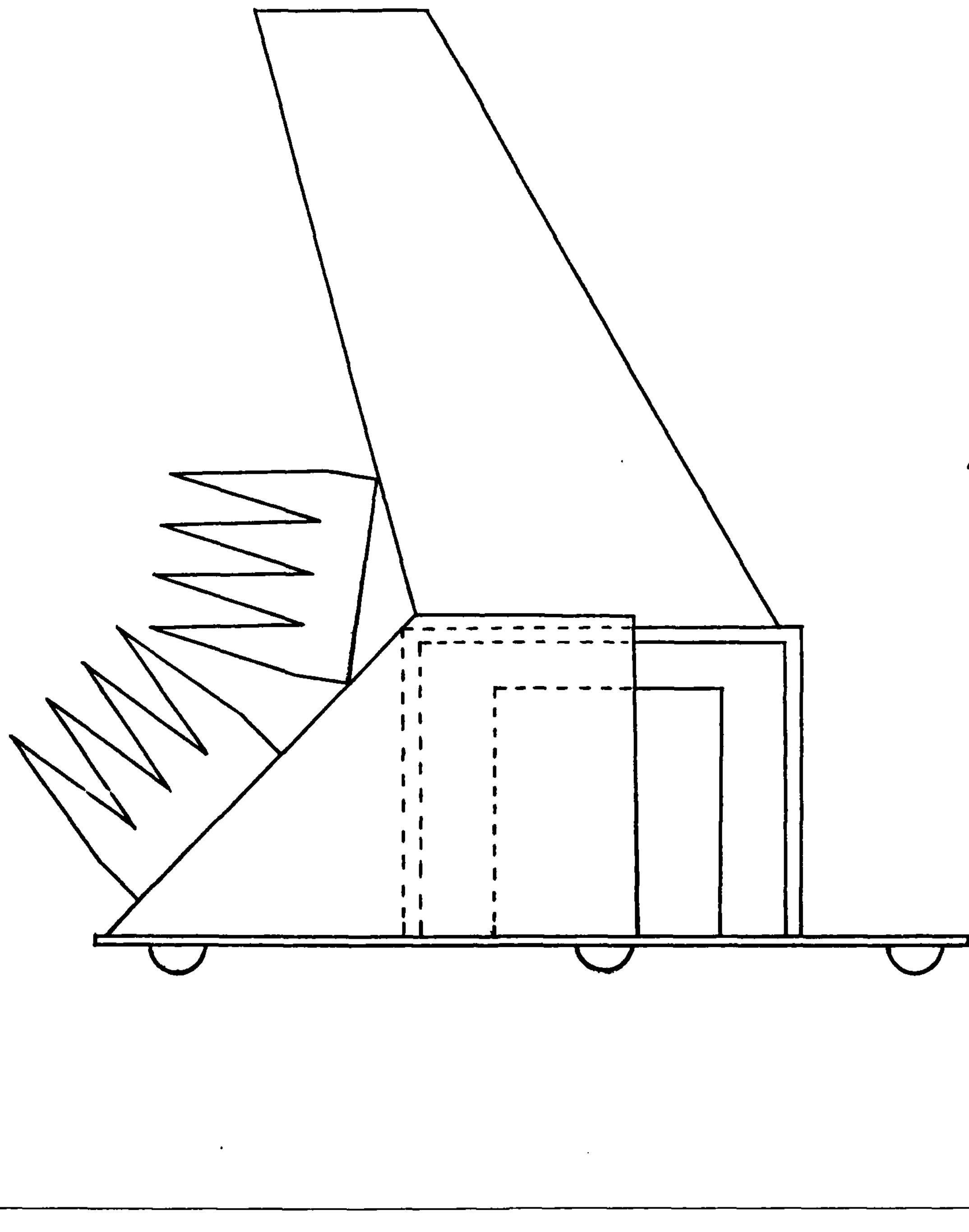

Figure 1. Old Pedestal in AFIT RCS Chamber

the floor where pyramidal absorber can absorb best. Target support interactions will be reduced through the use of an absorber cap, and can be further reduced by proper target mount designs. The absorber cap will also further reduce the RCS of the pedestal. The pedestal redesign will consider a means of easily mounting and removing targets

The final step is verification of the range. Measuring the amplitude and phase of our incident field at several frequencies will verify our predicted quiet zone size. Measurements of system noise floor will also be made.

*Literature Review*

This research effort is primarily directed at engineering design improvements to enhance the capability of the AFIT RCS chamber. The current literature is very consistent in basic design techniques for RCS chambers. The variations that do exist depend upon the expected use for the RCS chamber. The AFIT chamber is a far-field CW range where target RCS as a function of frequency and azimuth angle is desired. The frequency response also provides a bandlimited impulse response. The transmit and receive antennas are clearly an integral component of the system.

The primary considerations in choosing the antennas are radiation pattern and frequency response. Separate transmit and receive antennas are needed because the AFIT system is continuous wave. This means that the transmit antenna can not be turned off to listen for the receive signal. The usual approach in backscatter RCS measurements is to place two identical antennas as close together as possible. This essentially allows measurement of the backscattered fields. The problem that arises is that the receive antenna signal consists not only of reflections from the target and from the anechoic-chamber walls, but also of a component that is coupled directly from the transmit antenna. Robinson (10) points out that choosing an antenna with low sidelobes at 90 degrees off the main beam and placing an absorbing baffle between the antenna apertures will reduce the cross-coupling to an acceptable level.

The target support pedestal is also a key component of the system. Installing a support in an RCS chamber requires consideration of many factors. First, the support must present a low cross section in certain directions. There are three schools of thought along this line. One is to shape a metal pedestal in such a way that it directs any incident energy away from the receive antenna to where it is absorbed. Another is to make the pedestal of some material, such as plastic foam, which is transparent to the frequency range of interest. The third is a nylon string suspension system.

In (3) Ross states that the conventional suspension-type target support consists of two towers, a main suspension line, a vertical support line, a target sling and target control lines; as shown in Figure 2. Ross also states that cross-section accuracy is maintained by

1. Minimizing tower effects through shaping, absorber materials, location of towers in nulls of the field pattern, and range gating techniques.
2. Reducing main suspension-line interaction by means of aspect control and placement above the main beam.

This technique is very good for targets which are large or have a very high RCS with respect to the suspension lines; however, in the AFIT chamber, the targets become quite small and the desired RCS contributions would start to reach the same level as the support system.

Plonus (9) points out that support pedestals of cellular plastic materials are widely used in RCS chambers. Plonus goes on to show that these materials have a total RCS

$$\sigma = \sigma_i \left| \int_0^{\infty} \bar{n}(r) e^{-2ikr} dr \right|^2 + \sigma_i \int_0^{\infty} \bar{n}(r) dr \tag{2}$$

where $\bar{n}(r)$ is the time average of the distribution function, $n(r,t)$, which represents the number of particle scatterers per unit length at any given time. The first term

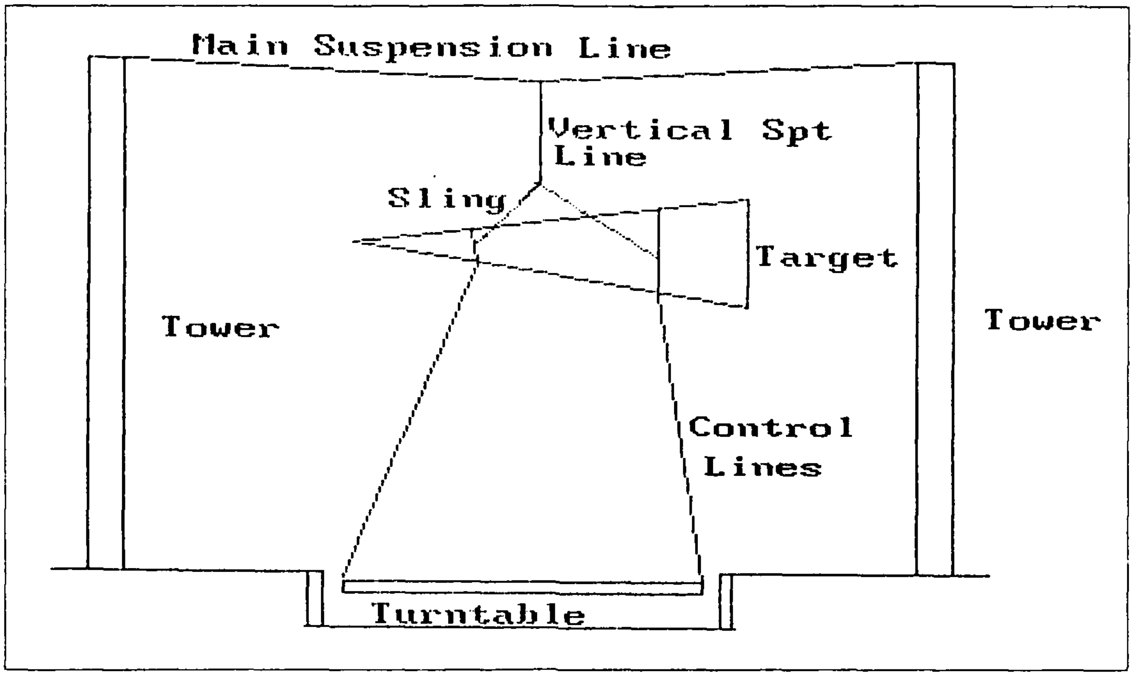


Figure 2. Conventional Suspension Support (3)

represents *the* coherent *scattering. The second term is* just $N\sigma_i$, the cross section per scatterer ($\sigma_i$) times the number of scatterers ($N$), and therefore represents the incoherent scattering. In (11); Thomas, Plonus, and Knott demonstrate that different foams perform differently with respect to coherent and incoherent scattering. They examined six foams and their results indicated that performance in one category did not correlate to performance in the other. This is shown in Table 1 (11). The best choice of these foams, which are representative of what is available, seems to be Pelaspam with its low coherent RCS and moderate incoherent RCS in cases where bistatic measurements are desired. This stems from the necessity to keep the foam symmetrical vertically for stability. The alternative is to choose Thurame which has a very low incoherent RCS and shape the pedestal into something low in RCS for monostatic RCS measurements.

Knott, Shaeffer, and Tuley (5) describe a metal pedestal (Figure 3) that is shaped like an aircraft wing which has edges forward and rear and is inclined at the top toward the transmitter. In this configuration, most of the energy is directed

Table 1. Comparison of Cylindrical Pedestals at X Band

| Material | Dia.(in) | Coherent (dbm ) | Incoherent (dbm ) |
|---|---|---|---|
| Tyrilfoam | 26.04 | -15.4 | -33.8 |
| Pelaspam | 13.98 | -12.5 | -48.0 |
| Styrofoam FB | 14.66 | - 9.9 | -49.0 |
| Styrofoam DB | 15.40 | - 7.5 | -49.3 |
| Styrofoam FR | 13.34 | - 9.3 | -53.2 |
| Thurame | 19.13 | - 9.7 | -50.2 |

down (into absorber) and back (into absorber). The metal pedestal has the distinct advantage of strength, thus allowing the incline which has a theoretical return of zero (5).

The next consideration with pedestal installation is its placement. Ideally, a target is illuminated by a plane wave. In a far field range, the target is placed at some distance such that the spherical wavefront approximates a planar wavefront (to some specified degree) over the extent of the target.

Kouyoumjian and Peters (6) discuss the minimum range as a function of tolerable deviation from a planar wavefront. The two main criteria are crossrange amplitude ($A$) and phase ($\phi$) variation. The crossrange amplitude and phase variation are the change in amplitude and phase of the incident field from the center to the edge of the quiet zone, respectively. The minimum range, found from amplitude and phase considerations, is given by

$$R_m(A) = \frac{\pi}{\sqrt{24(1-A)}}\left(\frac{l}{L}\right)\left(\frac{L^2}{\lambda}\right) \tag{3}$$

$$R_m(\phi) = \frac{\pi}{4\phi}\left\{1 - \frac{\phi^2}{3}\left[\left(\frac{l}{L}\right)^2 + \frac{1}{3}\left(\frac{l}{L}\right)^4\right]\right\}\left(\frac{L^2}{\lambda}\right) \tag{4}$$

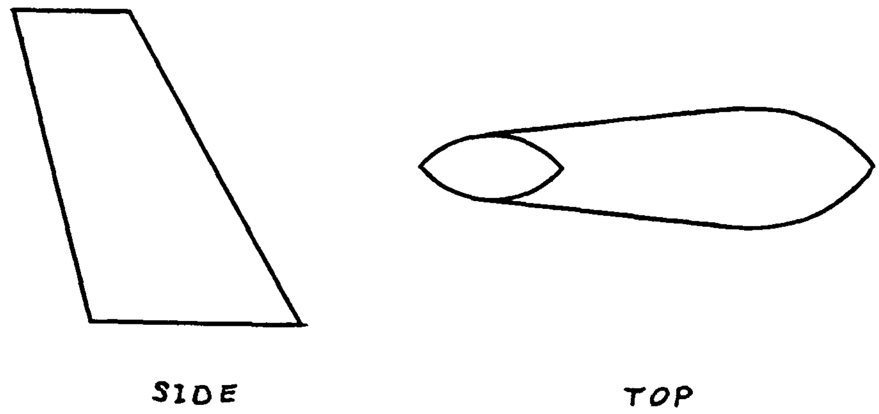


Figure 3. Metal Support Pylon

with the following restrictions:

$$R_m > 0.41^2/\lambda \tag{5}$$

$$A > 0.3 \tag{6}$$

$$\frac{\phi^2}{3}\left[\left(\frac{l}{L}\right)^2 + \frac{1}{3}\left(\frac{l}{L}\right)^4\right] < 0.25 \tag{7}$$

where $L$ is the largest dimension of the target, $\lambda$ is the wavelength of the incident field, and $l$ is the maximum antenna aperture dimension (6). These results were found assuming uniform aperture fields in a square aperture transmitting antenna. As stated in (6), the allowable variation in crossrange amplitude and phase depends on the type of target to be measured, the required accuracy of the RCS data, and the type of processing that will be performed on the RCS data. $R_m(A)$ and $R_m\phi$ for several values of $A$ and $\phi$ are depicted in Table 2. Common choices are $A = .9$ and $\phi = \pi/8$.

Finally, target-support interactions significantly affect system performance. These are error signals that usually cannot be removed with background subtraction or range gating. For this research, "target-support interactions" includes interactions between the target and the mount and the target and the pedestal. The AFIT chamber uses a calibration technique which includes background subtraction. The calibrated (complex) target response ($\sigma$) is found from

$$\sigma = E(T - B_T)/(R - B_R) \tag{8}$$

where $E$ is the exact response of the calibration target, $T$ is the target measurement, $B_T$ is the target background measurement, $R$ is the calibration target measurement, and $B_R$ is the calibration target background measurement. Background measurements are made with the appropriate mount attached to the pedestal. This is important because mounts may be different for the target and calibration target. This procedure does not, however, remove interactions which occur between a target and its mount, and the target and the pedestal. Thus, a matter of finding a mount and pedestal treatment combination which yields interactions well below the target return is desired.

The work in (9) with foamed plastics for support pedestals covered earlier is applicable to mount design also. Since mounts are much easier to change than pedestals, the tuned right circular cylinder presented in (11) may be a good choice for a mount.

*Organization*

Chapter II discusses the theoretical performance of the AFIT chamber and its improvements. The first discussion concerns the chamber structure and how that contributes to the chamber's performance. Next the function of the processing equipment is described. Then the antenna's part in the system is presented with a detailed explanation of the advantage of the diagonal horn antenna. This is followed by a quiet zone analysis with the theoretical dimensions given in tabular form. Next is an analysis of aliasing. Finally, discussions of the pedestal, absorber cap. and absorber placement are presented.

Chapter III discusses the actual chamber improvements. The first discussed is the diagonal horn antenna and its demonstration of improved performance in coupling and alias free operation in the target zone. The next section discusses the noise floor improvement which was realized by the antennas. Finally, the pedestal's absorber cap is discussed in terms of its contribution to improved measurements.

Chapter IV discusses the measurement of the plane wave in the quiet zone. It begins with a description of the equipment used. Then the software used to control the measurements is discussed in some detail. Finally, the methodology of the measurements is discussed.

Chapter V discusses the results of the plane wave measurements and analyzes the results based on the theoretical data presented in Chapter II. Chapter VI contains the recommendations for further study and or modifications and conclusions drawn from this effort.

# II. Theoretical Performance

## Chamber Description

*Physical Dimensions* The physical dimensions of the AFIT chamber are illustrated in Figures 4 and 5. The tapered design of the chamber walls and ceiling is evident. At the time the AFIT chamber was designed and built, the current thought was that a taper-l room was beneficial in that it would eliminate specular reflections from the walls or ceiling (5). However, more recent investigations of pyramidal absorber indicate it is a diffuse scatterer (12). In fact, converting the room from a tapered to a rectangular design would help reduce absorber clutter levels through increased spatial attenuation and through the resulting change in absorber bistatic scattering angles (4). For practical reasons, the room configuration will not be changed.

*Measurement Equipment* The AFIT chamber uses Hewlett Packard hardware to make measurements. The system (less the antenna, which will be covered in the next section) consists of the source, amplifier, frequency converter, network analyzer, controllers and peripherals as shown in Figure 6. The chamber uses the HP 8340B Synthesized Sweeper to generate a continuous wave (CW) microwave signal. This signal is input to a directional coupler; the "coupled" signal is sent to the HP8511A (RF to IF frequency converter) to serve as a reference, the "through" signal is sent to the HP 8349B Microwave Amplifier. The amplifier boosts the signal to roughly 24 dBm and sends it to the transmit antenna. The test signal received on the receive antenna is then sent to the frequency converter. The frequency converter then converts the (RF) reference and test signals to an intermediate frequency, preserving the relative phase and amplitude of the signals. The IF signals are then sent to the network analyzer. The HP 8510B Network Analyzer (NWA) is the receiver which measures the amplitude and phase of the test signal (relative to the reference signal).

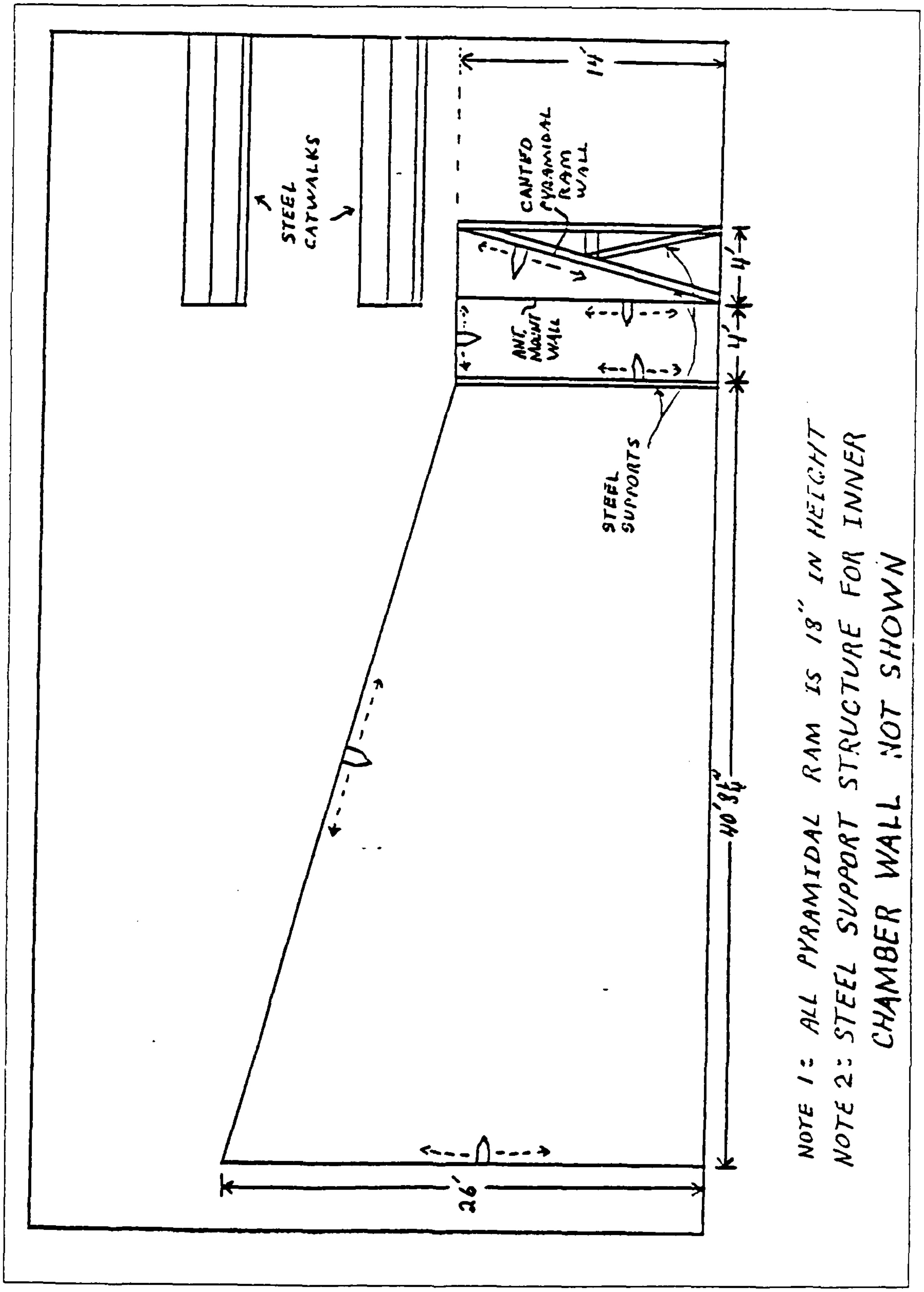


Figure 4. Side view of AFIT chamber

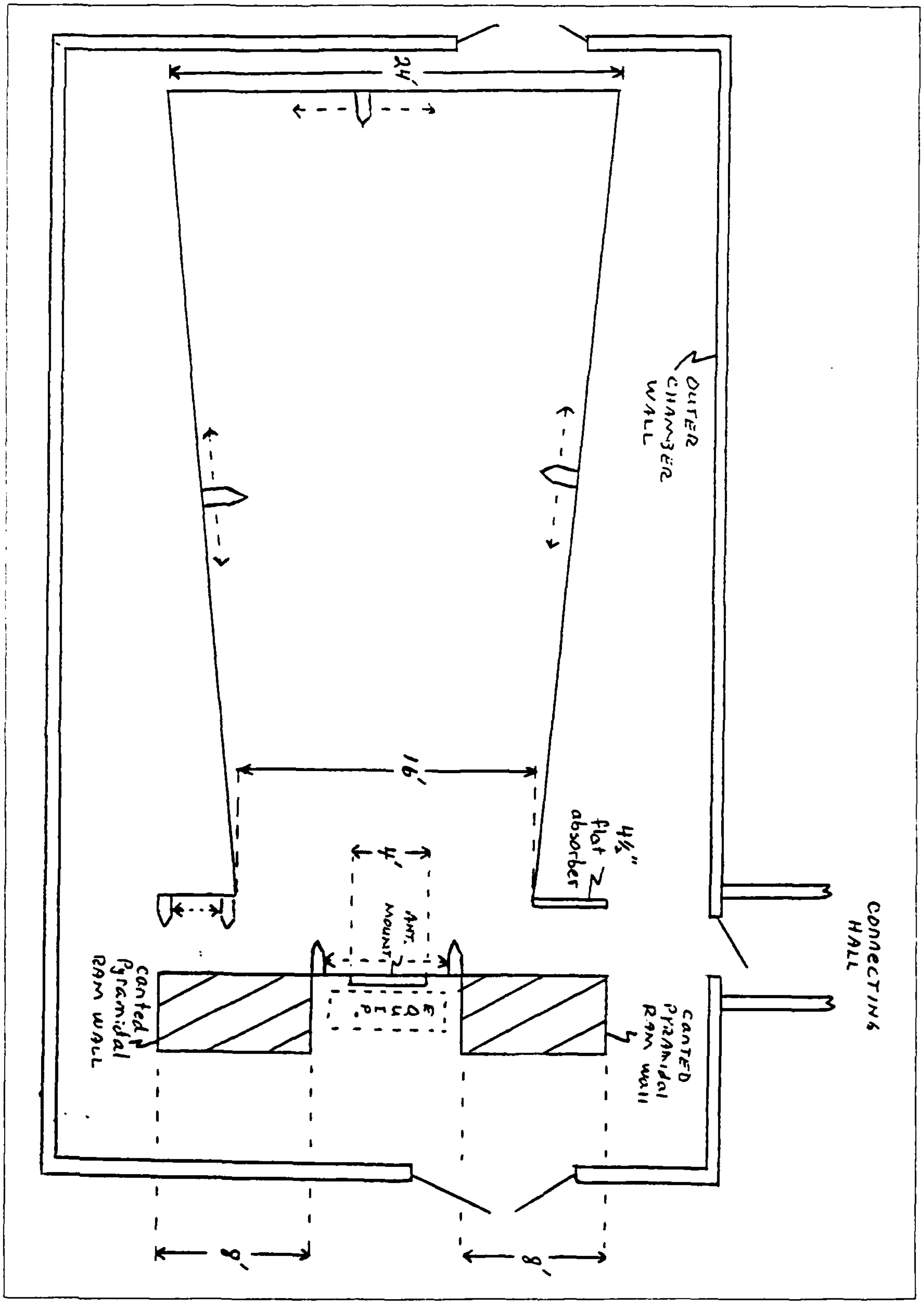


Figure 5. Top View of AFIT Chamber

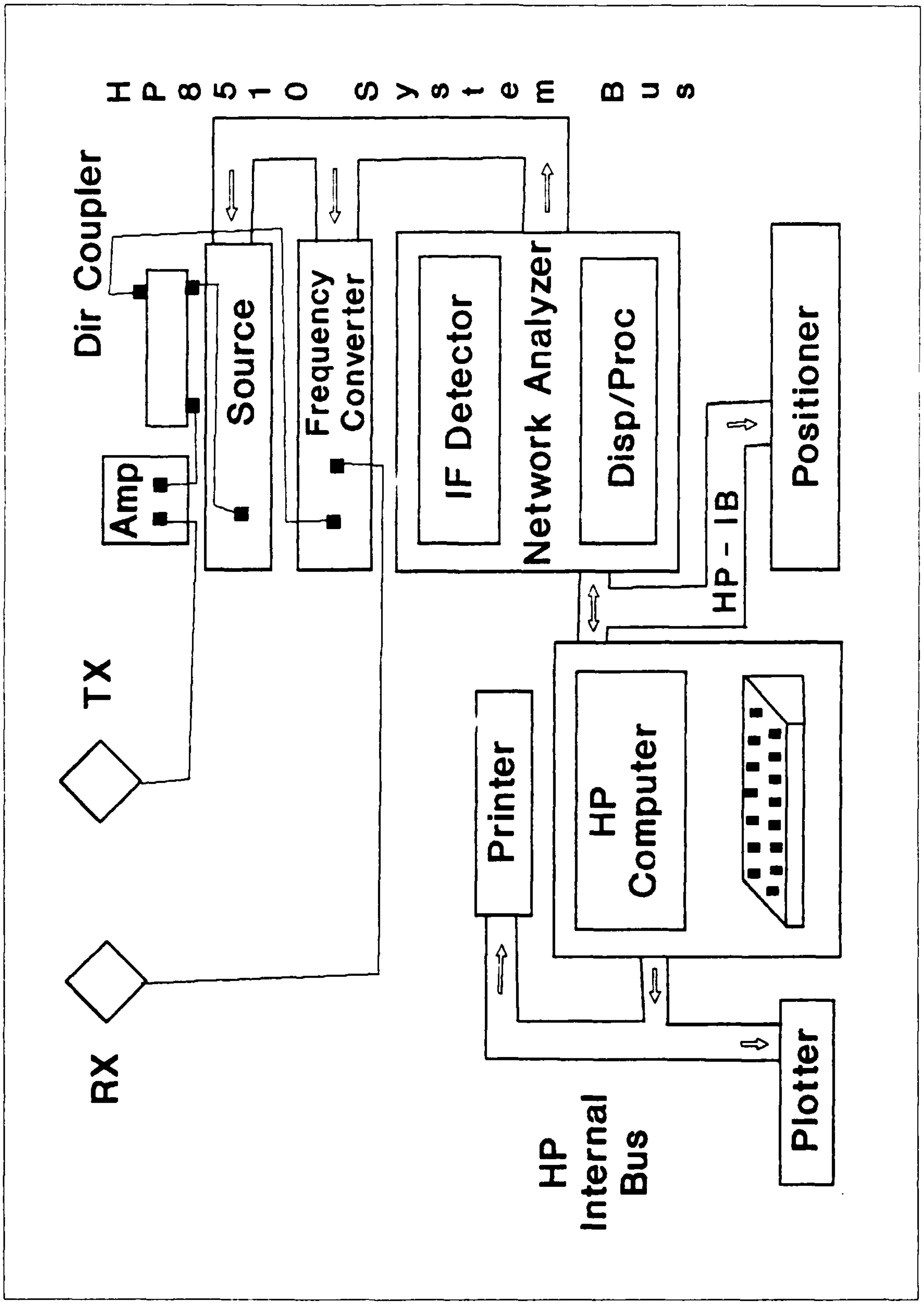


Figure 6. Equipment Configuration

The system is controlled by the HP 9000 Series 236 Computer. The computer allows for software control of the entire system and augments the processing functions of the NWA. Servo-motor controllers direct rotation of the target on the pylon and of the antennas to the proper polarization. These controllers can be software or manually controlled. For hardcopy output, a plotter and printer are also connected to the system.

*Diagonal Horn Antennas*

As discussed earlier, an acceptable approximation to a plane wave is achieved over a limited region (quiet zone) by simply placing the target at some distance from the antennas. The size of the quiet zone depends on the range distance and on the allowed deviation from an ideal plane wave. The sidelobes of the transmit antenna illuminate the walls, and thus contribute to absorber scatter into the quiet zone. Analogously, the sidelobes of the receive antenna can pick up target scattering which illuminates the walls. A highly directive antenna by nature has relatively low side lobes which reduce these clutter signals. Traditionally, RCS chambers have used the pyramidal horn antenna. However, as part of this thesis effort, the AFIT chamber has switched to diagonal horn antennas. These were chosen primarily for their increased bandwidth and low sidelobe levels. As described in (2), a chamber has four primary dimensions of interest, the two cardinal dimensions (horizontal and vertical) and the two intercardinal dimensions (diagonals). The pyramidal horn dimensions correspond to these dimensions while the diagonal horn has its diagonal dimensions corresponding to the cardinal dimensions of the room. In (7), Love states that the diagonal horn possesses an almost perfectly circular radiation pattern, and thus, its beamwidth is equal in both cardinal and intercardinal dimensions. Additionally, Loves' work showed that the diagonal horn antennas had side lobes in the cardinal planes of the room measured at least 30 dB down and in the intercardinal planes from 23 to 27 dB down from the main beam. Conversely, the pyramidal horn antennas exhibited an H-plane 3dB beamwidth about 35 percent wider than the E-plane and the E-plane side lobe levels were noted to be at only 12 to 13 dB down relative to the main beam. It should also be noted that the diagonal horn antenna had its higher side lobe in the intercardinal dimensions of the chamber which are a factor of $\sqrt{2}$ greater in distance. This means that reflections from these lobes must propagate approximately 41 percent further to reach the quiet zone and therefore are attenuated more.

*Quiet Zone*

The ideal quiet zone is a volumetric area in the anechoic chamber in which a plane wave passes from only one direction when the transmit antenna is excited (2). In actuality, the imperfectly absorbing walls will scatter energy from multiple paths into the quiet zone which causes distortions in the plane wave. Also, the antenna is transmitting a spherically shaped beam which has an inherent amplitude and phase variation dependent on the propagation distance.

In Chapter 1, Equations 3 and 4 give the minimum down range distance required for a given amplitude or phase variation, respectively, as a function of wavelength, antenna aperture, and target dimension. Let the target dimension become the quiet zone dimension and the minimum range become the actual down range distance so that Equations 3 and 4 can be rewritten to solve for the theoretical crossrange quiet zone dimension ($L$) for the AFIT chamber. Doing so for Equation 3 yields

$$L = R\left(\frac{\lambda}{l}\right)\frac{\sqrt{24(1-A)}}{\pi} \tag{9}$$

In the AFIT chamber, $R = 25$ ft. For a crossrange amplitude variation of 1 dB, $A = .9$. Using our horn dimensions of $l = 0.943$ feet, and considering the lower and upper frequencies of 6 and 18 GHz, the quiet zone dimension $L$ is found from Equation 9 to be 2.16 and .72 feet, respectively. Figure 7 shows these dimensions

Table 2. Quiet Zone Dimension, $L$ (ft)

| Frequency (GHz) | | | | | | | |
|---|---|---|---|---|---|---|---|
| | 6 | 8 | 10 | 12 | 14 | 16 | 18 |
| A=.9 | 2.14 | 1.61 | 1.29 | 1.07 | .92 | .80 | .71 |
| $\phi = \pi/8$ | 1.43 | 1.24 | 1.11 | 1.03 | .94 | .88 | .83 |
| $\phi = \pi/16$ | 1.01 | .88 | .78 | .72 | .66 | .62 | .58 |

as they apply to the chamber. Equation 4, which considers phase variation, is much harder to simplify into a solution for $L$. In this case, we consider our source to be a point source, and the resulting expression for $L$ is given by

$$L = \sqrt{R\left(\frac{4\phi}{\pi}\right)\lambda} \tag{10}$$

For an allowed crossrange phase variation of $\phi = \pi/16$, the AFIT chamber quiet zone crossrange dimension ($L$) for 6 and 18 GHz is 1.01 and .58 feet, respectively. If the allowed phase variation is relaxed to the still acceptable $\pi/8$, then the dimension ($L$) becomes 1.43 and .83 feet, respectively. Note that $A$ and $\phi$ are defined by

$$\frac{E^i(L/2)}{E^i(0)} = Ae^{j\phi} \tag{11}$$

Table 2 shows the quiet zone dimension ($L$) for A = .9, $\phi = \pi/8$ and $\phi = \pi/16$ versus frequency. These calculations show that the theoretical quiet zone dimensions are limited by the phase variation except for $\phi = \pi/8$ and frequency greater than or equal to 14 GHz, where the dimension is limited by the amplitude variation. An additional dimension with respect to the quiet zone is downrange distance (D). In this direction, the only variable of concern is amplitude. A constant amplitude is desired; a 1 dB variation is usually accepted. The downrange amplitude decays as $1/R$, which results in $D = R/8.2$ or $D = 3$ feet.

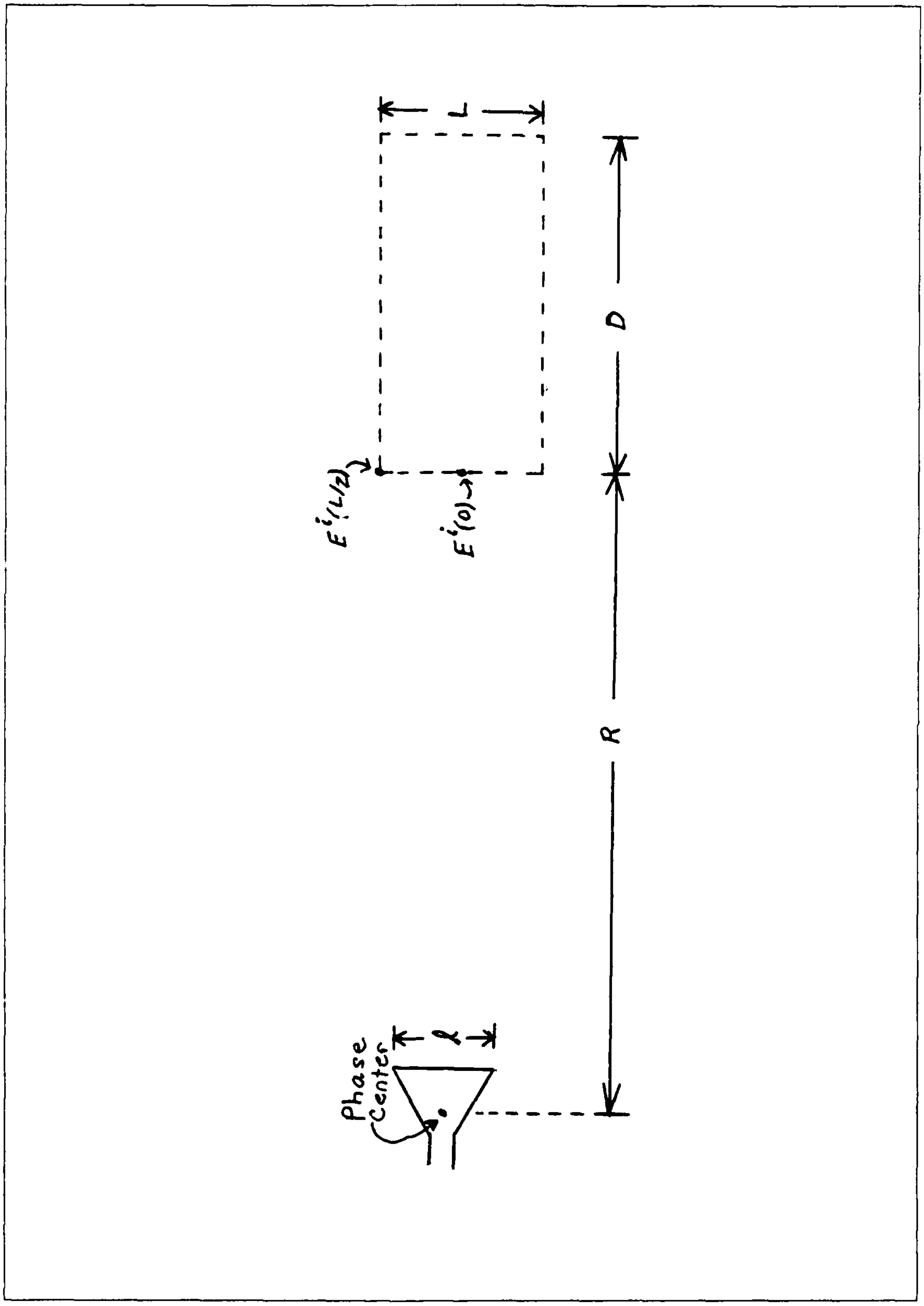


Figure 7. Quiet Zone and Pertinent Parameters

*Aliasing*

The AFIT RCS chamber makes 801 discrete measurements while sweeping from 6 to 18 GHz. This is a limitation in the network analyzer. Care must be taken to ensure time domain aliasing does not corrupt the target response. The alias free range is determined by dividing the speed that the wave travels ($c$) by the width of the frequency bins ($\Delta f$). This width is determined by the bandwidth and the number of points that the signal processor samples (8). The AFIT chamber's signal processor takes 801 points of data which equates to 800 bins. The width of the frequency bins is given by

$$\Delta f = B/800 \tag{12}$$

where $B$ is the system bandwidth. Thus for a bandwidth of 12 GHz (6 to 18 GHz) $\Delta f$ equals 15 MHz. Since the RCS measurement is a reflection measurement,

$$R_{aliasfree} = c/2\Delta f \tag{13}$$

represents the down range distance at which aliasing occurs. For the AFIT chamber, the range turns out to be 10 meters or 32.8 feet. Therefore, with the pedestal placed at 25 feet down range, there should be no problem with aliasing in the target area (quiet zone).

*Pedestal and Cap*

It would be ideal to be able to set a target in a chamber's quiet zone in mid-air with no support and to be able to rotate it on command. Since the AFIT chamber is only currently interested in monostatic RCS measurements, the ideal is approximated with a properly designed support pedestal. Of the three pedestal types described in the introduction, the metal ogive shaped pylon was chosen for the AFIT chamber. This type pylon has a very low backscatter RCS and can support sufficient weight for any target which can fit into the quiet zone. Another advantage to this design is

Table 3. AFIT Pylon RCS vs Frequency

| Frequency GHz | | | | | | |
|---|---|---|---|---|---|---|
| 6 | 8 | 10 | 12 | 14 | 16 | 18 |
| -41.54 | -44.04 | -45.97 | -47.56 | -48.90 | -50.06 | -51.08 |

that a rotator system can be incorporated inside the pylon for rotating the target.

In (1), Burnside states that the RCS of an ogive shaped support pylon (as shown in Figure 3) can be found in an approximate manner. The assumption is made that only the top portion of the pylon is illuminated with a plane wave. This is reasonable if you consider that the area all around the pylon is covered with absorber reducing multipath reflections to a minimum. Also, the transmitted beam does taper off as one moves toward the pylon base. With this approximation, the expression for the RCS of the pylon in terms of wavelength $\lambda$ and forward edge tilt angle $\theta$ becomes (1),

$$\sigma_{mount} = \frac{\lambda^2}{16\pi^3} cot^2\theta \qquad (14)$$

This expression is for the mount terminated in free space. An absorber cap should reduce the RCS. The AFIT pylon has a 15 degree forward edge tilt angle, thus, the theoretical RCS (dBsm) is as shown in Table 3.

*Absorber*

Radar absorbing material attached to the walls, floor, and ceiling play a key role in reducing energy scattered into the quiet zone and to the receive antenna. For the purposes of this work, two types of absorber are of primary interest. These are pyramid and wedge absorber. Pyramid absorber is most effective at reducing scattering at normal incidence. Wedge absorber is most effective reducing backscatter at grazing incidence. Generally, the ideal placement in a chamber would be to have pyramid absorber from the antennas to a point just past half-way to the quiet zone

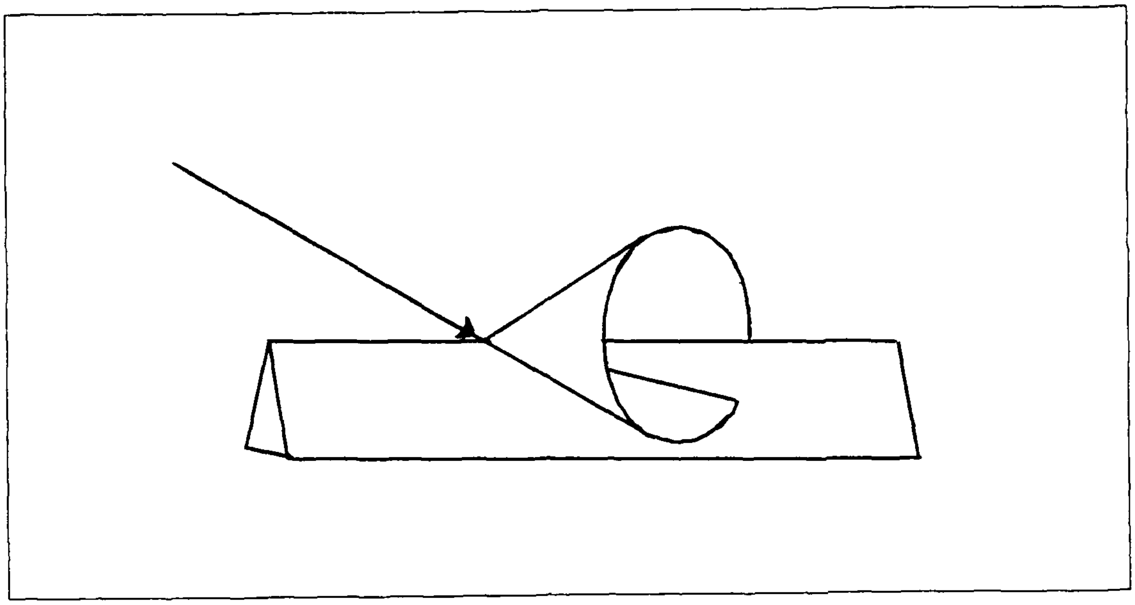

Figure 8. Keller Cone Reflection of Wedge Absorber

on all sides, then wedge absorber the rest of the way back to the rear wall, and lastly, pyramid absorber on the back wall and a small area directly under the pedestal's leading edge incline. The wedge absorber scatters in "Keller cones" as shown in Figure 8. With the wedge absorber placed as described, the incident energy is directed to the back wall at an angle very close to normal incidence. Incident energy hitting the leading edge of the pedestal is directed down in "Keller cones" which for that distance become incident very near normal to the floor, thus, the placement of pyramidal absorber.

Originally, in the AFIT chamber, the entire chamber was covered with pyramid absorber except for a pathway which passed across the chamber directly under the antennas, turned up the left wall, and then near the target area began to guide toward the pylon. At the pylon a square-like area existed to stand a step stool for mounting targets on the pylon. The new absorber pattern will incorporate wedge absorber and a path change to the pylon.

Due to a limited amount of wedge absorber being available, placement of the wedge absorber is restricted to the floor. The wedge absorber will be placed from a point half the distance from the antennas to the quiet zone to as far back past the quiet zone as supplies last. The path will enter the chamber on the right and continue down the right side to the back where it will turn across the back and then come up to the pylon from the rear. A new collapsable ladder design will provide easy access to the top of the pylon from the rear.

# *III. Chamber Improvements*

*Antenna*

The bandwidth of an antenna affects two primary characteristics associated with RCS measurements. These are time domain aliasing and range resolution. The original antennas used in the AFIT chamber operated from 8 to 12.4 GHz. This bandwidth resulted in an alias free down range distance of 89.5 feet, according to Equation 13. The range resolution, $\Delta R$, is inversely proportional to the bandwidth

$$\Delta R = \frac{c}{2B} \tag{15}$$

where the $B$ is the bandwidth and $c$ is the speed of light (5). Given this, the range resolution of the old antennas is 1.34 inches. This means that all scatterers on a target within a 1.34 inch down range distance are indistinguishable.

The Flam and Russell antennas installed in the chamber have a bandwidth of 12 GHz. The alias free range is estimated at 32.8 feet which is still sufficient for the AFIT range which has the target 25 feet down range. The range resolution is .49 inches, which is a significant improvement.

Figures 9 through 13 demonstrate the aliasing in the chamber as the bandwidth is increased. These measurements were taken at 801 sample points and vertical polarization. These are uncalibrated time domain views of the entire room scatter. The points of interest are marked to make visualizing the aliasing easier. Beginning with Figure 9, the antenna coupling is labeled 'A'. The pylon, which contains a five inch sphere mounted on top, is marked with 'C'. The back wall is marked with a 'B'. This point was verified by placing a corner reflector in the absorber on the back wall. The reflector was then removed so that the data would pertain to the rear wall only. In Figures 10 through 13, the marker 'a' represents the antenna coupling alias signal and 'b' represents the back wall alias signal. The figures show that as

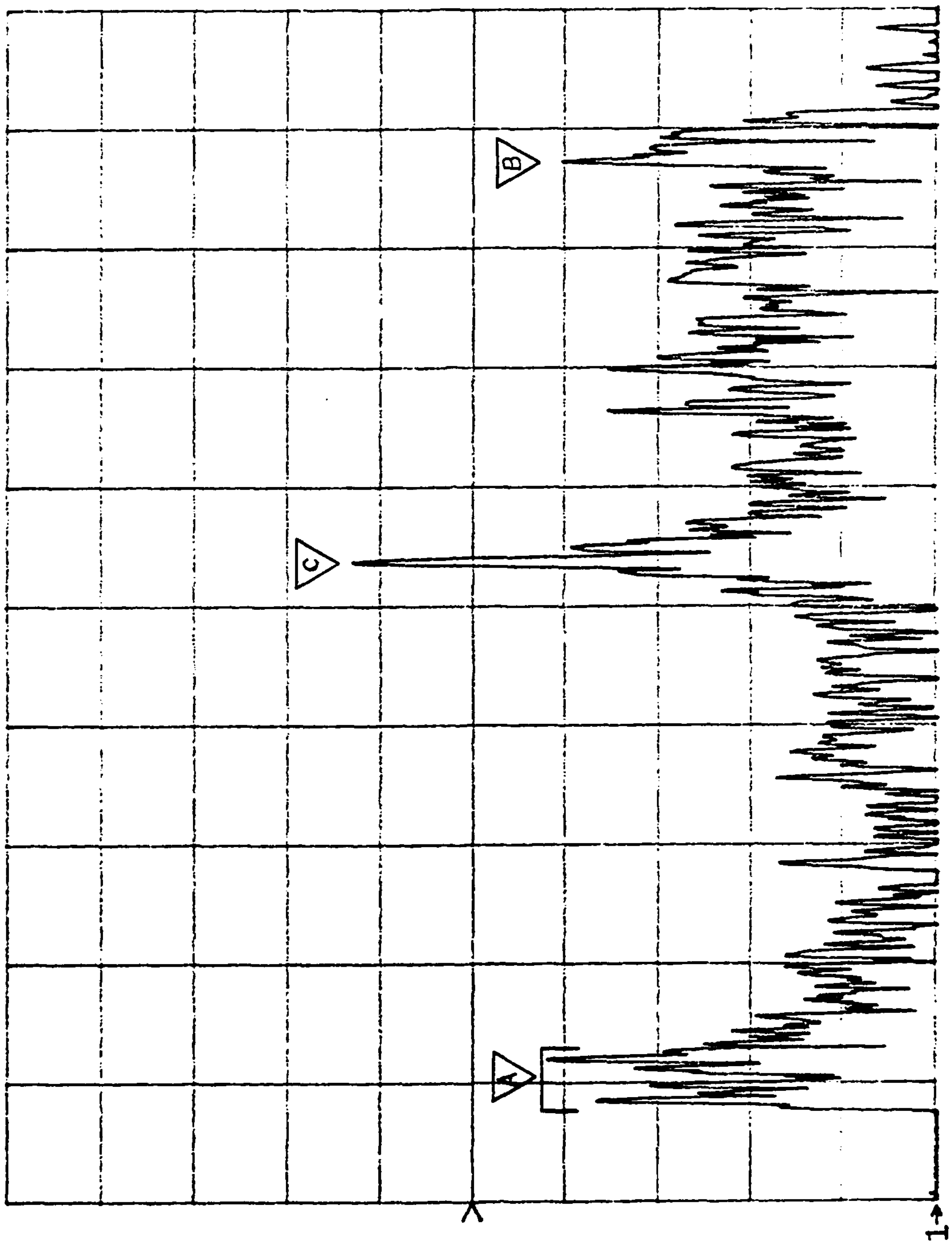


Figure 9. Time Domain of Chamber with 4.4 GHz (8-12.4) Bandwidth, uncalibrated

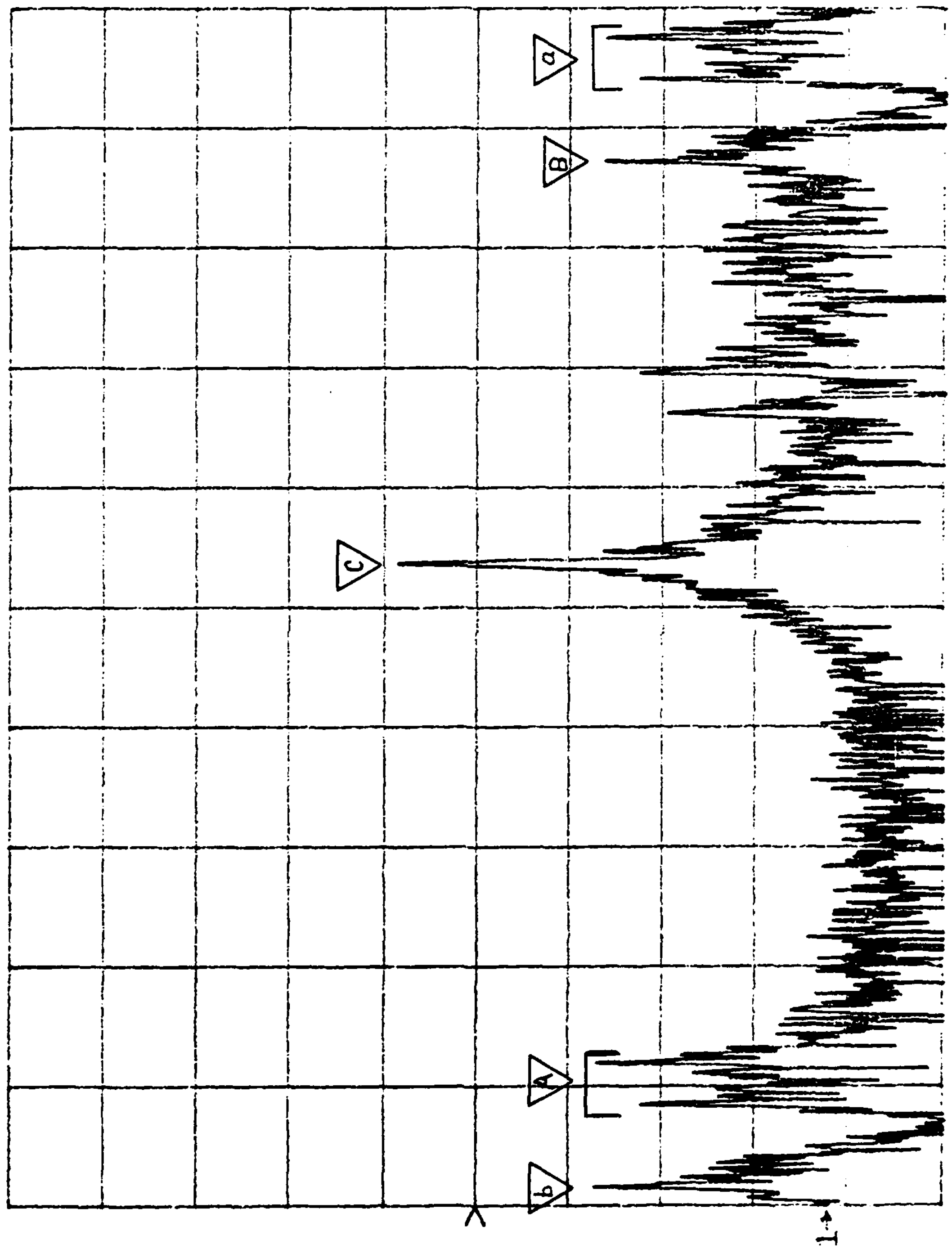

Figure 10. Time Domain of Chamber with 8.5 GHz (7.5-16) Bandwidth, uncalibrated

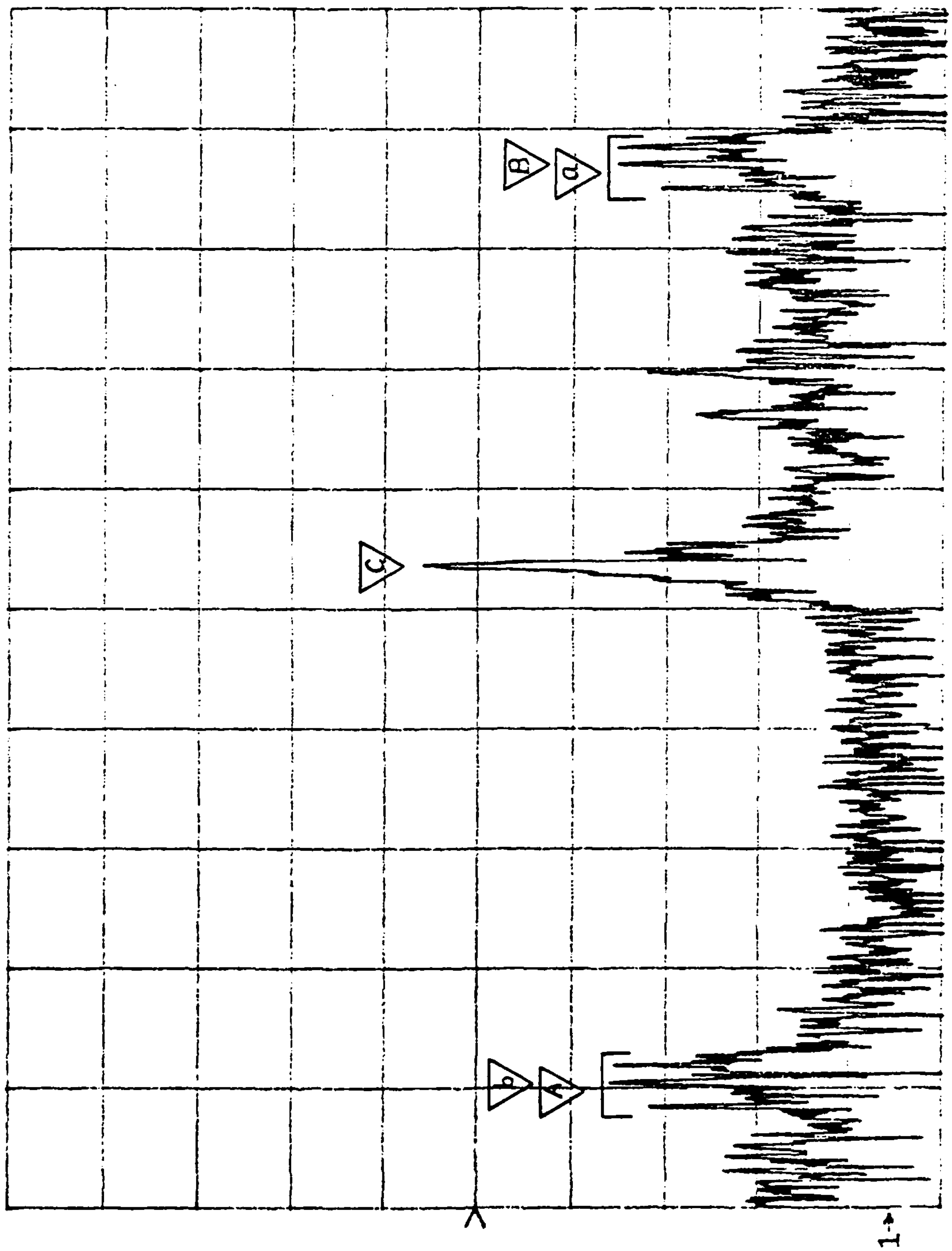

Figure 11. Time Domain of Chamber with 9.5 GHz (7.5-17) Bandwidth, uncalibrated

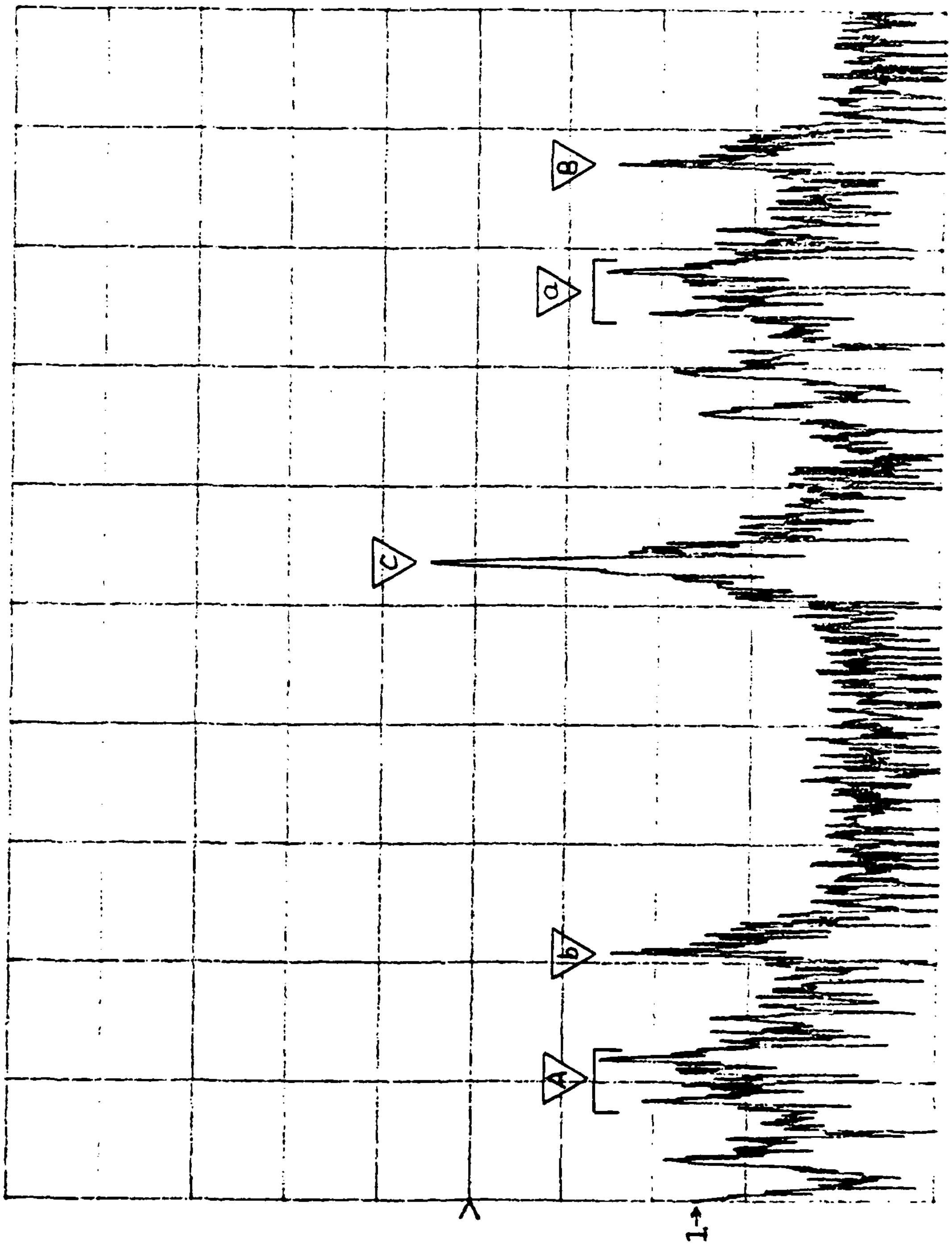


Figure 12. Time Domain of Chamber with 11 GHz (6-17) Bandwidth, uncalibrated

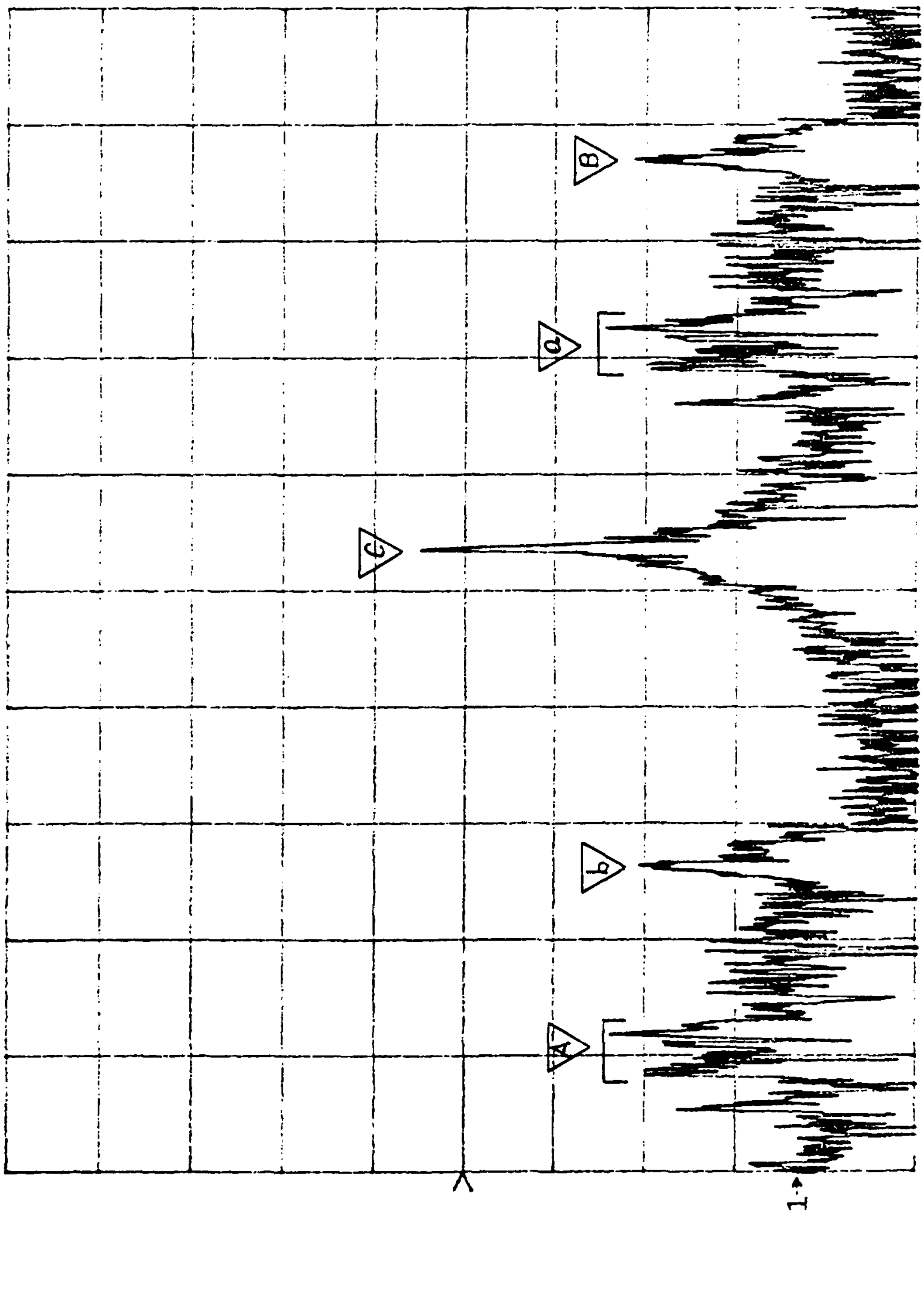


Figure 13. Time Domain of Chamber with 12 GHz (6-18) Bandwidth, uncalibrated

the bandwidth increases, the patterns begin to overlap, and the antenna coupling and back wall alias signals start to approach the pylon. Figure 10 clearly shows the back wall alias signal approaching the antenna coupling signal from the left. In Figure 11 the back wall alias signal and antenna coupling signal are directly over each other and the antenna coupling alias signal and back wall signal are likewise overlapping. Figure 12 shows the back wall alias signal approaching the quiet zone from the left and the antenna coupling alias signal approaching the quiet zone from the right. Finally, in Figure 13 the back wall and antenna coupling alias signals are at their closest position to the quiet zone. On the figures, each block represents 11 ns, therefore, the first part of the antenna coupling alias signal is about 17 ns away and the closest the back wall alias signal gets is approximately 32 ns away from the pylon signal in the quiet zone. To convert to distance from the pylon, multiply the speed of the signal times the time traveled. In feet per second, the speed is

$$v = 3.2808c(\frac{ft}{sec}) \tag{16}$$

where $c$ is the speed of light in meters per second. Since the measurement is a reflection, the actual distance separating the signals is half the product of the velocity given in equation 16 and the time separation shown in figure 13. Thus, the antenna coupling alias signal is 8.3 feet away and the back wall alias signal is 15.7 feet away from the pylon signal. Where the expected quiet zone is no more than about one foot to either side of the pylon, it is clear that there is no aliasing interference in the general area of the pylon, thus, the chamber can handle the increased bandwidth.

Figure 14 illustrates the range resolution available with the new antennas. The plot is the impulse response of a generic airplane as shown. For this target, the tail fins extend past the cylindrical portion of the airplane .50 inches. The plot shows that the responses from these two points are clearly resolvable. Thus, the predicted range resolution of .49 inches is accurate.

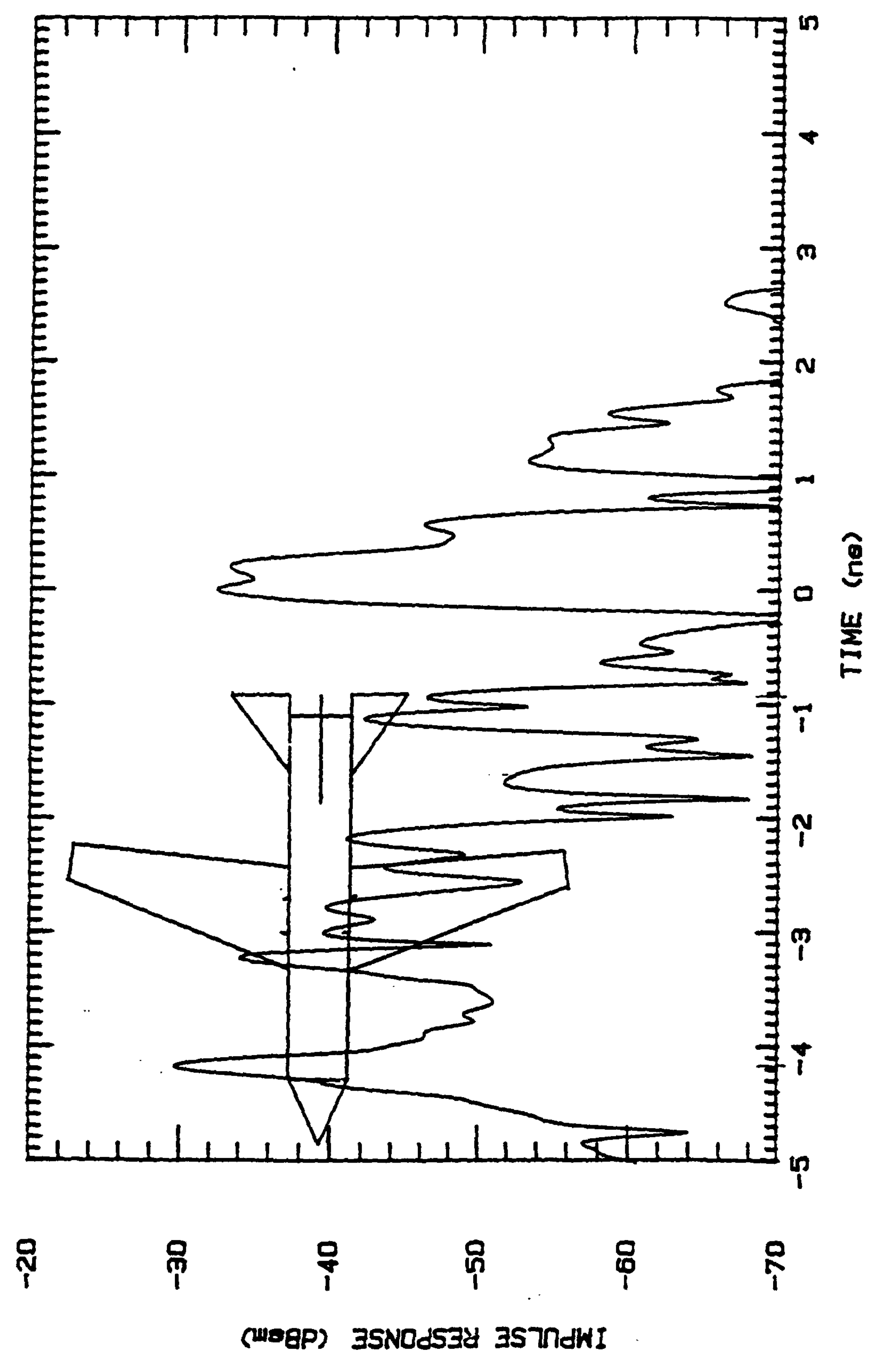


Figure 14. Impulse Response of Generic Airplane

Additional improvements in the chamber as a result of the new antenna installation were a reduced antenna coupling and an easier means of controlling antenna polarization. The original antennas were designed for a uniform amplitude across the aperture. This uniform amplitude results in a nonzero field strength at the edges of the antenna which causes coupling if the antenna are not properly isolated. For a backscatter measurement, the antennas need to be as close to each other as possible. This requirement causes the transmit and receive antenna to be very close to each other. (In this configuration, coupling can be reduced by placing an absorbing baffle between the antenna.) The new antennas have a tapered amplitude across the aperture resulting in a theoretical zero field strength at the edges. This means that the antenna can be placed tip to tip with greatly reduced coupling.

Figures 15 and 16 show the relative difference in the antenna coupling. Figure 15 is an uncalibrated time domain cut of the chamber with the old antennas. Marker 1 shows the point where antenna coupling occurs. In this configuration, the antenna are spaced about 4 inches apart and have a piece of flat absorber taped between them. Figure 16 is the same type measurement with the new antennas. Here the antenna coupling is clearly about -40 dB lower. In this configuration, the antennas are mounted with the E-plane tips virtually touching. The low coupling level removes the need for an absorbing baffle.

The old antenna mounting configuration had the antenna mounted on a circular disk in the wall. The operator had to climb up and turn the disk by hand, aligning hash marks, to set polarization for vertical or horizontal. The new mounting platform has the antenna mounted on a disk which is driven by a rotator controlled by the hand-held controller. Computer control gives not only accurate horizontal and vertical settings, but also allows for measurement at any angle in between. The one limitation which still exists is that measurements must be made with the transmit and receive antenna in the same orientation: no cross polarization measurements are possible without physically removing one antenna and turning it in its mount.

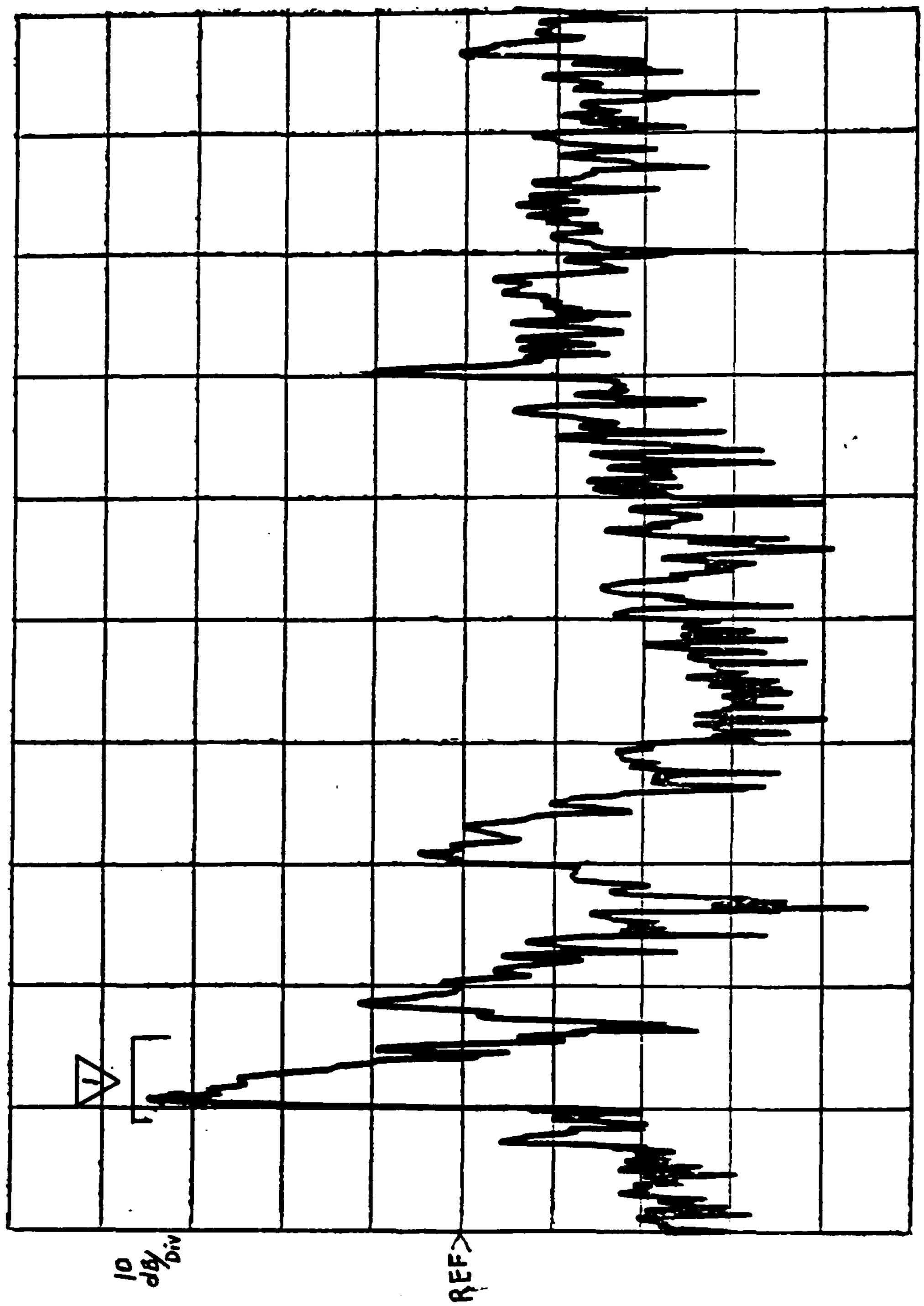


Figure 15. Uncalibrated Time Domain View of Chamber - Old Antennas

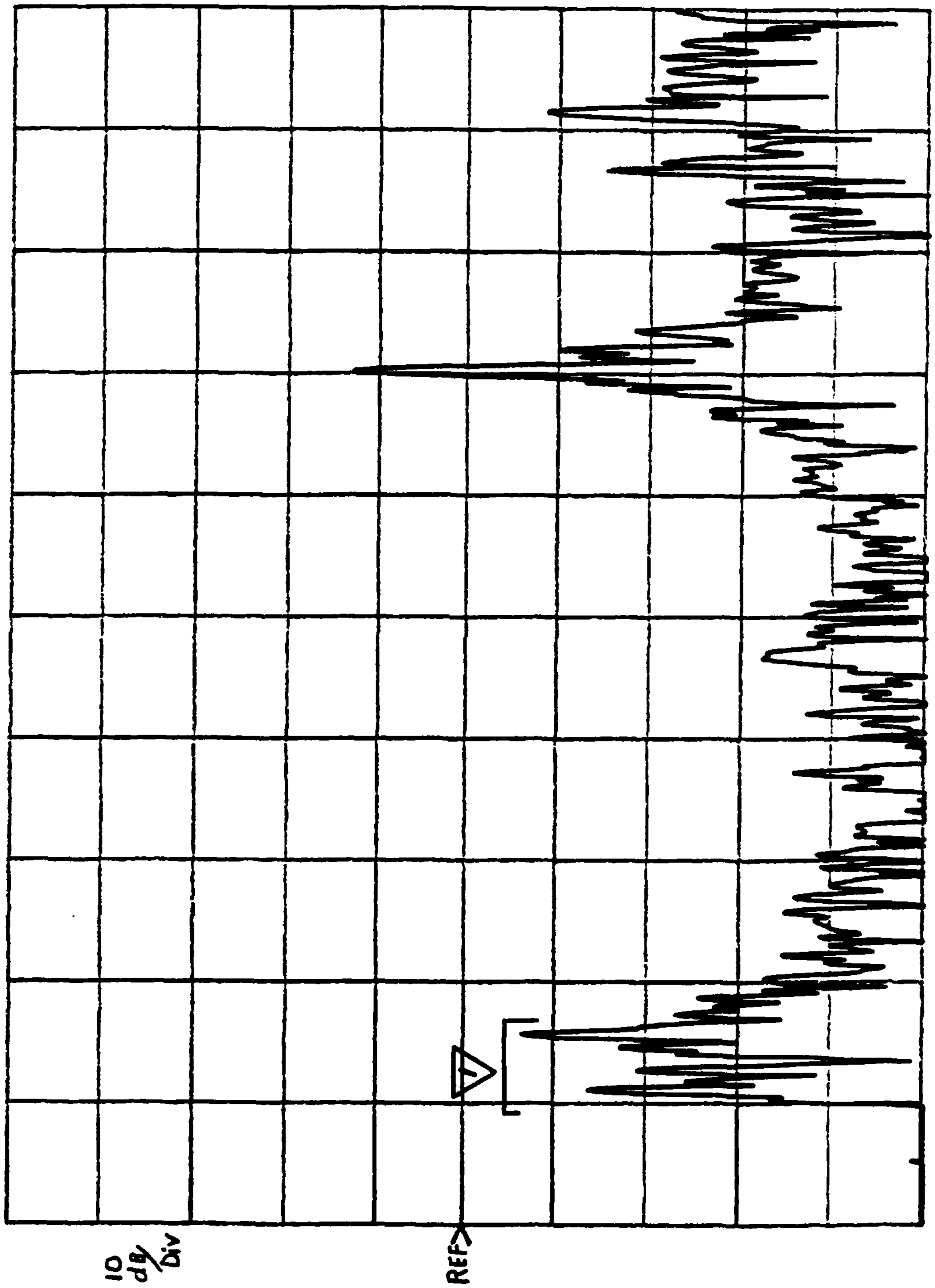


Figure 16. Uncalibrated Time Domain View of Chamber – New Antennas

### *Chamber noise floor*

The primary expectation from the new pedestal and absorber placement in the chamber is to reduce the noise floor. Originally, in the AFIT chamber, the entire chamber was covered with pyramid absorber except for a pathway which passed across the chamber directly under the antennas, turned up the left wall, and then near the target area began to guide toward the pylon. At the pylon, a square-like area existed to stand a step stool for mounting targets on the pylon. This absorber pattern with the old pedestal (described in Chapter 1) and the old antennas provided a noise floor of about -50 to -60 dBsm as shown in Figure 17.

The current chamber configuration includes the new pedestal, antennas, and a new absorber pattern which incorporates wedge absorber and a path change to the pylon. Due to a limited amount of wedge absorber being available, placement of the wedge absorber is restricted to the floor. The wedge absorber is placed from a point half the distance from the antennas to the quiet zone to approximately 3 feet passed the base of the pylon. The width of the wedge strip is 12 feet. The path enters the chamber on the right and continues down the right side to the back where it turns across the back and then comes up to the pylon from the rear. A new collapsable ladder design provides easy access to the top of the pylon from the rear. The noise floor associated with this configuration is -70 to -80 dBsm as shown in Figure 18. While each noise floor measurement is different, Figure 18 is representative of typical values.

### *Pedestal Cap*

As said in Chapter 2, the RCS of the pedestal is further reduced by terminating its top with an absorbing cap. This addition also provides a reduction in target-support interactions which can not be subtracted out. To demonstrate the effect of a RAM cap, a sphere was measured under three separate cap conditions. The target chosen was a sphere because it would provide a strong specular reflection

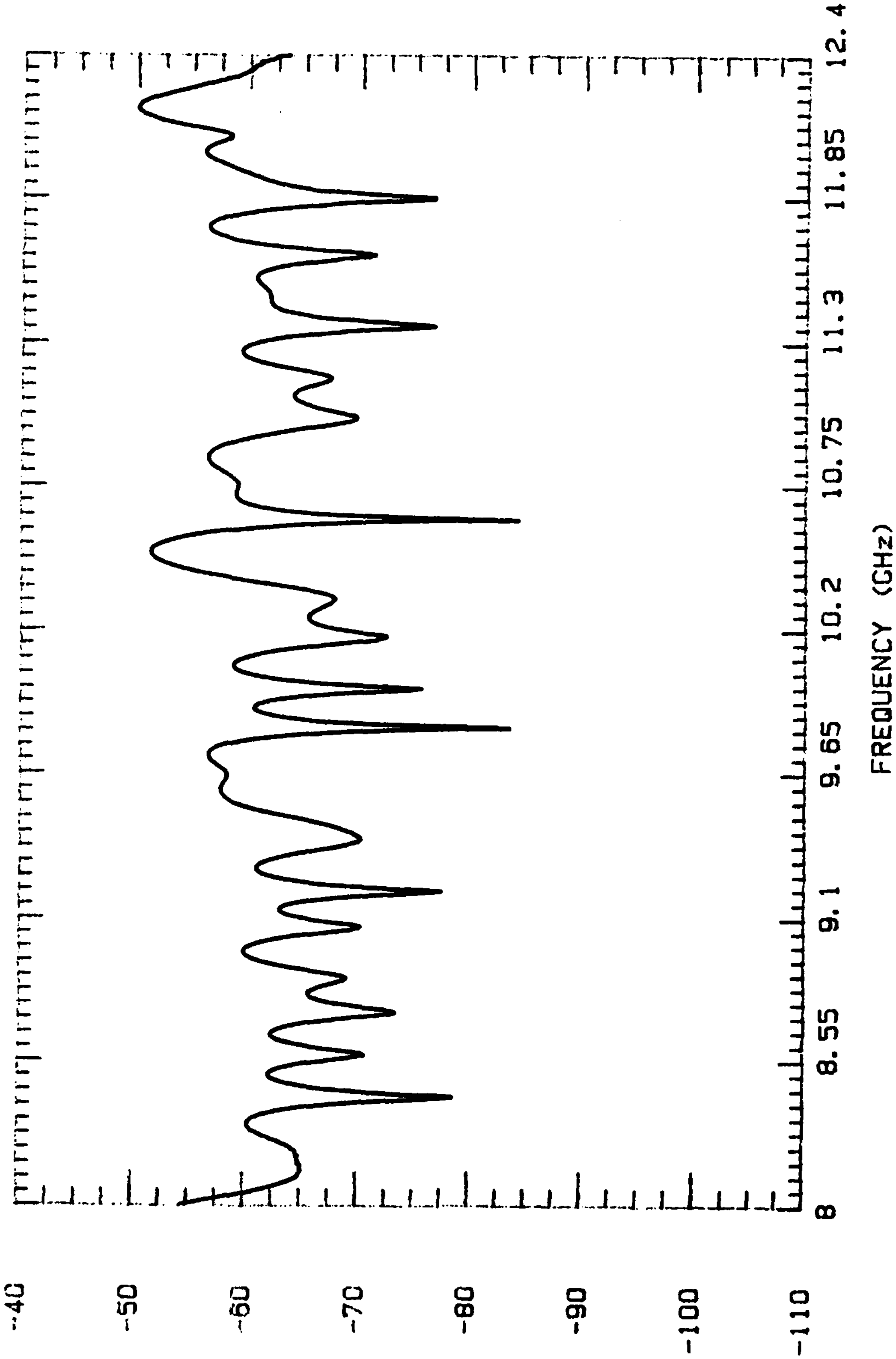


Figure 17. Chamber Noise Floor in Old Configuration

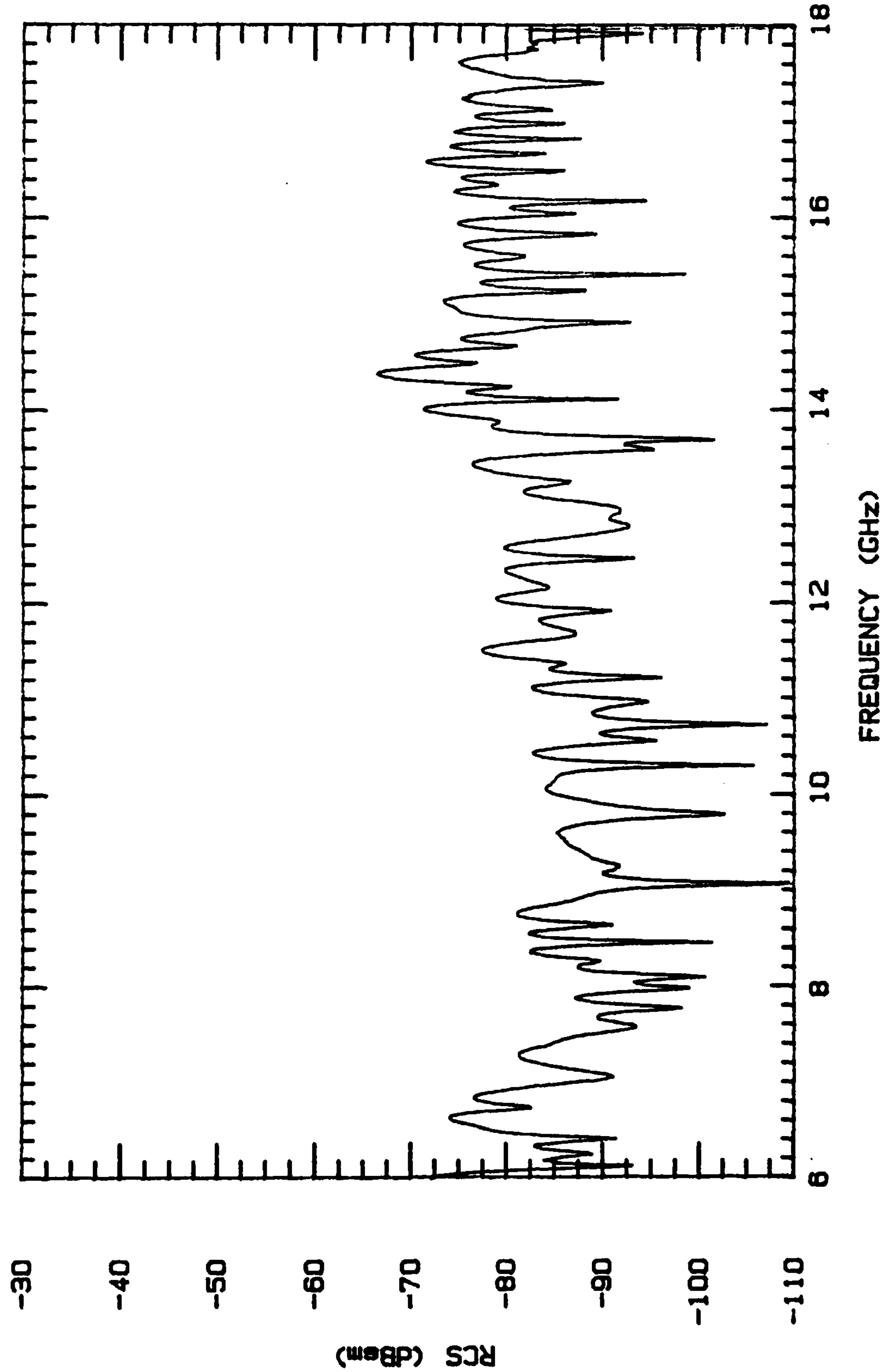


Figure 18. Chamber Noise Floor with Current Set-up

and a second order mechanism, a creeping wave. The measurements were taken over a bandwidth of 8-12.4 GHz at horizontal polarization. Figure 19 shows the time domain result of all three measurements. Point A is the specular reflection and point B is the creeping wave. The creeping wave appears at a later time due to a $(2 + \pi)a$ longer round trip path, where $a$ is the radius of the sphere. In this case the creeping wave return would be approximately 1.1 nanoseconds after the specular return. The first measurement involved no cap. Here the flat metal surface of the pedestal top interacted with the target to a large degree as shown in trace 1. In this trace, there is a high intermediate return between the reflection point and the first creeping wave which, without other information, could be mistaken as a target feature. The second measurement used an ogive shaped absorber cap over the pedestal top. The cap was cut from a 6 inch thick piece of absorber. The absorber was constructed so that the top four inches of the pedestal was covered with approximately 2 inches of absorber. Trace 2 shows the intermediate return about 10 dBsm lower and now the reflection and first creeping wave are much clearer. The last measurement consisted of the absorber cap with an ogive sheet of magnetic RAM cut to fit over the top flat portion of the pedestal (under the absorber cap). As trace 3 indicates, the intermediate return is reduced another 10 dBsm and now the reflection and first creeping wave are evident. Hence, the sphere, which scatters in all directions, has a return that more precisely matches the exact solution when the top of the pedestal is covered with absorber. An additional measure would be to raise the sphere higher off the top. In this way the path from the scattered rays to the top of the pedestal and back to the antenna would be further back in time where it could be range gated out. Note that these measurements were made when the chamber was in the old configuration. This explains the poorer range resolution.

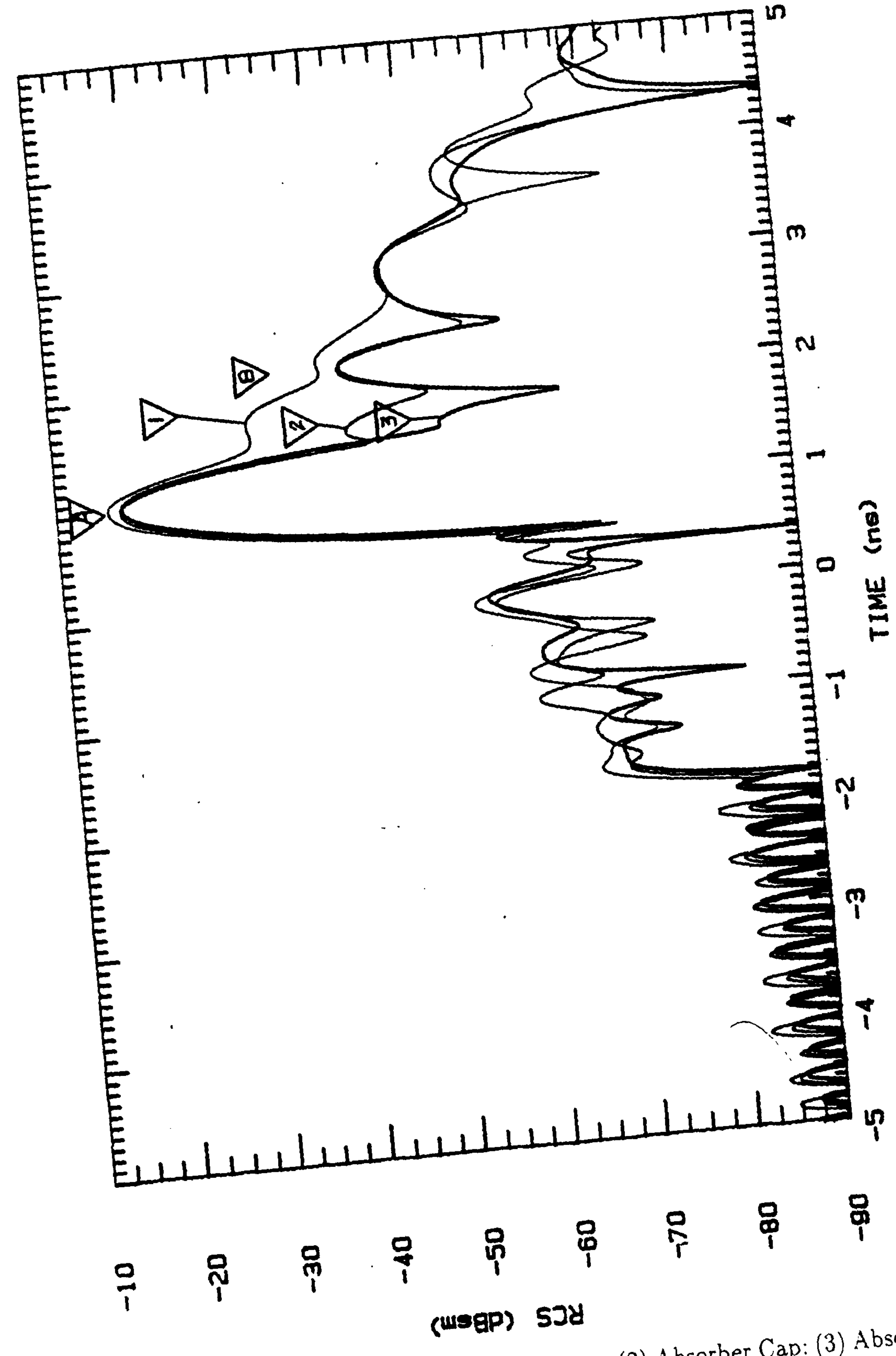


Figure 19. Time Domain of 5" Sphere: (1) No Cap; (2) Absorber Cap: (3) Absorber Cap and Magnetic RAM Sheet

# *IV. Quiet Zone Measurement*

The final phase of this effort was to characterize the quiet zone. To do this, a method of translating an antenna across the quiet zone without interfering with the incoming wave had to be engineered, software had to be written for controlling the measurements, and a plan of attack was necessary for the data to be collected.

## *Equipment Set-up*

An ogive shaped translation device was designed and built as shown in Figure 20. This device is capable of translating a probe 120 cm (4 feet). The field can be measured in a horizontal or vertical scan. Since the nature of the diagonal horn antennas is to produce a circular-shaped beam, the two scans should be adequate for determining the quiet zone of the chamber. The shape of the translator negligibly perturbs the incident field measured by the probe.

The only difference in equipment set-up from the RCS measurement (Figure 6) is that the receive antenna is now in the quiet zone. Also, the translator contains a rotator. This required laying antenna coaxial cable and a rotator control cable down the length of the chamber to the translation device. The translation directions and antenna positions for horizontal polarization are shown in Figure 21. For vertical polarization, antenna 1 becomes the bottom antenna and antenna 2 the top.

## *Software*

Portions of the AFIT RCS measurement (ARMS) code were adapted and incorporated into a program called AFITFP (AFIT field probe). A flow chart of the code is in Figure 22. The actual code is listed in Appendix A. The primary purpose of the code is to determine the amplitude and phase of the field relative to the field at the center of the translation. The main program consists of initialization and a

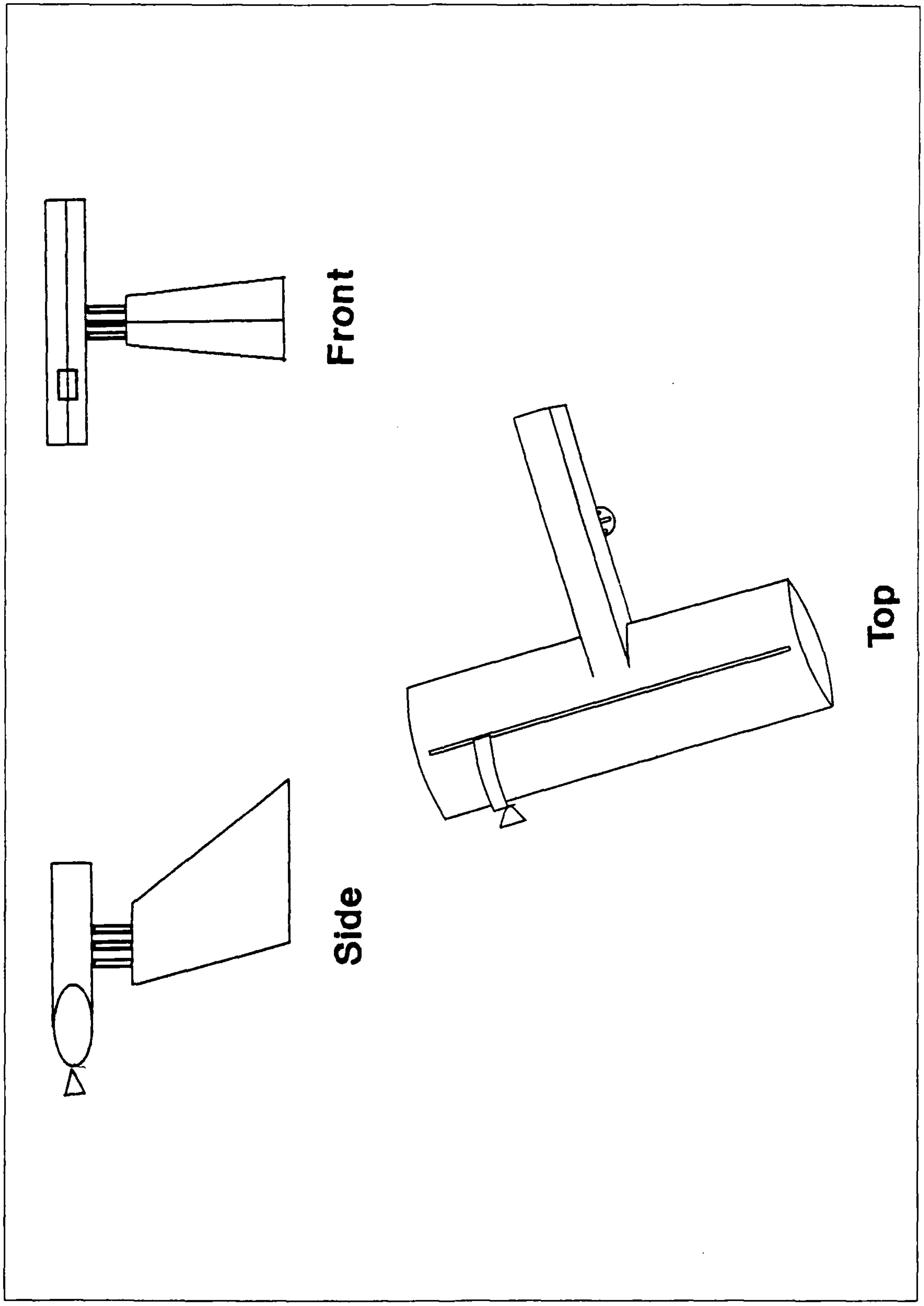


Figure 20. Translation Device

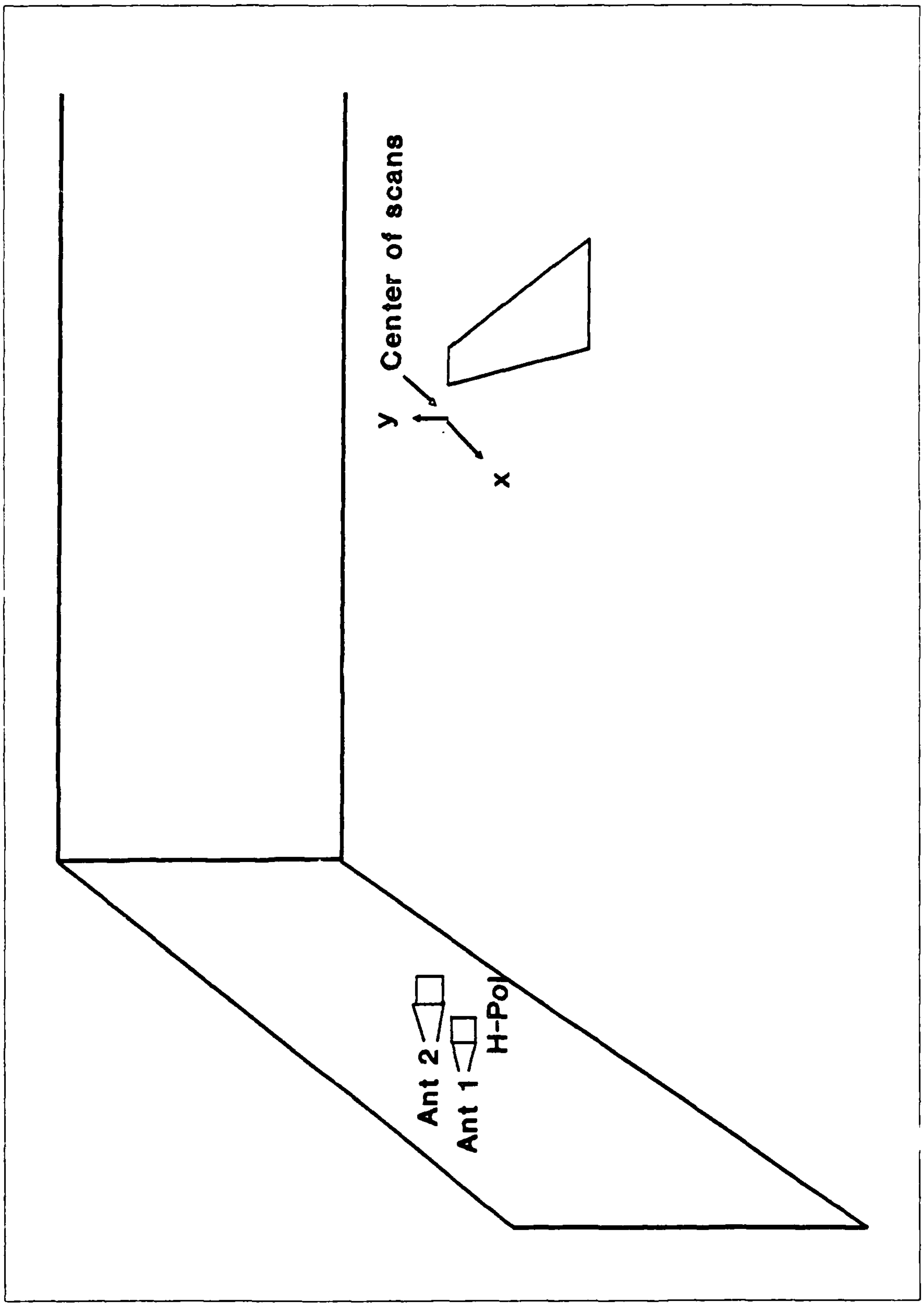


Figure 21. Antenna and Translation Orientation

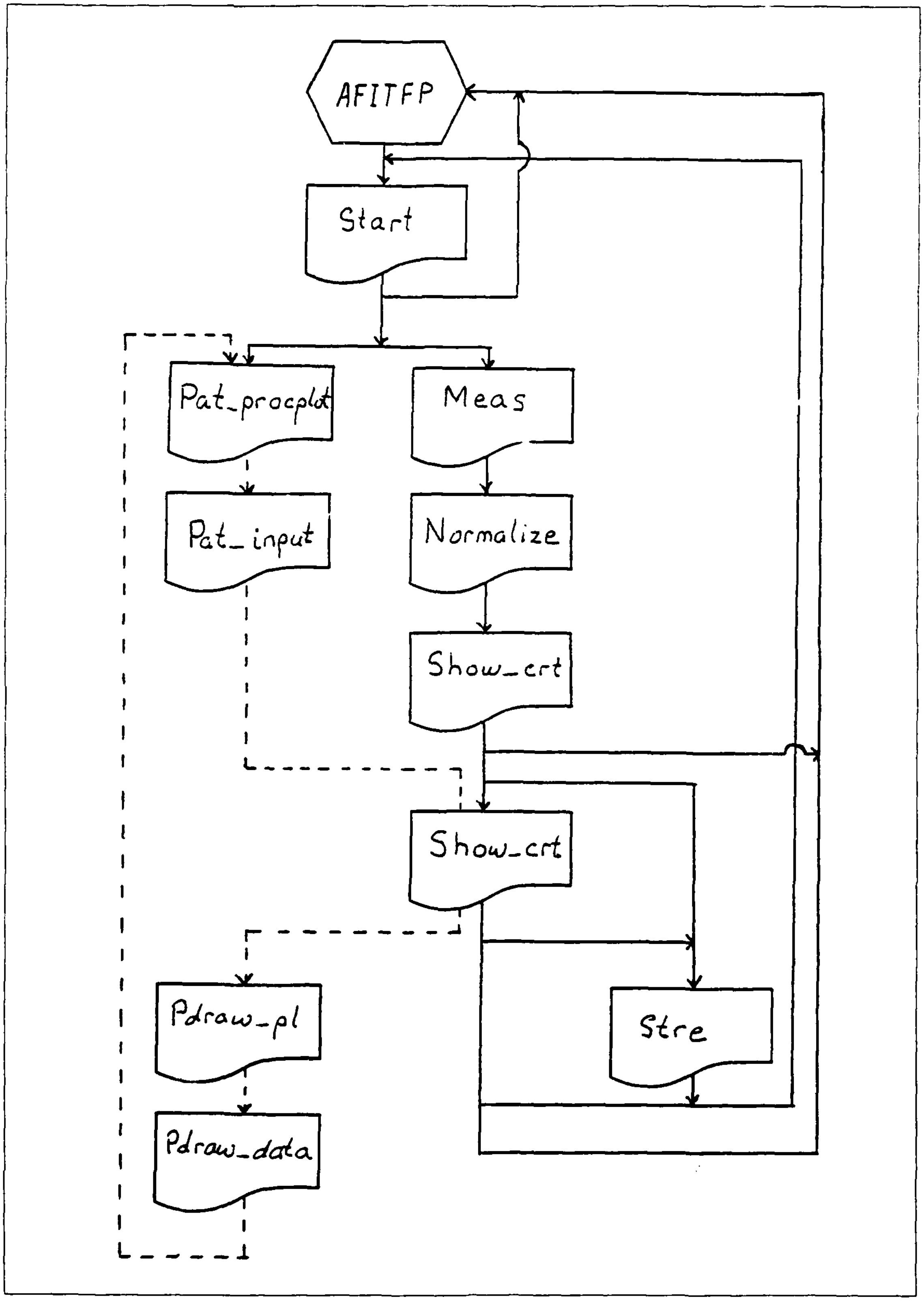


Figure 22. AFITFP Flow Chart

call to a main subroutine which takes the measurement parameters and calls subroutines which measure the field, normalize the data, and show the results on the HP computer screen. Additional menus allow for saving and plotting the data.

The main subroutine (start) begins by asking for the date which gets printed on the plots. Then a menu appears which allows selection between taking a measurement, plotting saved data, or returning to basic. If a measurement is chosen, the program prompts the user for the required measurement data. This includes selection of a frequency from 6 to 18 GHz and whether the user wants the data taken in 1 or 10 cm increments. The next input is the polarization followed by the direction the translator will be moving: left to right (top to bottom) or right to left (bottom to top) for horizontal (vertical) translation. The remainder of the main subroutine is a sequence of calls to subroutines.

The first measurement subroutine (Meas) sends the measurement parameters to the network analyzer, initializes the rotator controller, and takes the measurement. In the measurement, the network analyzer measures magnitude in dB and phase in degrees. The next call is to the normalization subroutine (Normalize). Here the data collected at the center point of the scan is subtracted from all other data points; this normalizes the data as specified earlier. At this point, a characteristic of the HP 8510 generates the need for further processing of the phase data in order to get a clean trace. The HP 8510 only records angles between -180 and +180 degrees. Thus, at the 180 degree point, the trace will display a 360 degree jump after normalization whenever the unnormalized phase passes through 180 degrees. This was corrected by taking the normalized array and checking the difference between the points. Since a change of more than 40 degrees between any two points was never expected, that was chosen as the threshold for detecting 360 degree jumps. If the difference was greater than 40 degrees, 360 degrees was subtracted from the second point. If the difference was less than -40 degrees, 360 degrees was added to the second point. In this way a smooth trace was achieved. However, it was now possible for the phase at the center of the scan to be ±360 degrees. Thus, a check is made of that center point and if it is not 0, then it is again subtracted from all the points. At this stage, a smooth trace with the desired normalization is obtained. There now was only one more check to make. The plotter used only plots from left to right, thus the measurements taken from right to left or bottom to top were reversed for proper plotting. The final two measurement subroutine calls are to display the data on the screen (Show-crt). The first call displays the magnitude on the screen. At this point a menu is available which allows selection of storing the data, taking a new field probe measurement, dumping the data to a printer (low quality output), looking at the phase trace, or returning to Basic. Choosing the phase trace results in the second call to Show-crt. At this point, the trace on the screen is the phase and the menu choices are store, new measurement, dump to printer, or return to Basic. The new measurement choice is actually a return to main menu where the plot choice may also be selected.

The plot choice on the main menu calls a plotting subroutine (Pat-procplot) which controls the plotting of data stored on disk. The first subroutine called inputs the data from a disk. Since the magnitude and phase data are stored in separate files, this sequence must be done for each plot. The data is shown on the screen by the next call to the Show-crt subroutine and a menu becomes available which allows a choice of line type (for multiple traces on the same grid), grid plotting, data plotting, and exit. The grid must be plotted before selecting the data plotting choice. Once the trace is plotted, the exit choice returns to the main menu where further plotting or more measurements may be made.

*Methodology*

The 1 cm increment option obtains the most accurate measurement of the quiet zone. This allowed the ripples in the quiet zone to become apparent and determine where the edges were based on the 1 dB amplitude and $\pi/8$ or $\pi/16$ phase criteria discussed earlier. First, horizontal axis measurements were made at 6,8,10,12,14,16, and 18 GHz. Then a 10 GHz measurement on the vertical axis was made. This was done first for vertical polarization and then repeated for horizontal polarization. Only one measurement in the vertical translation direction was taken as comparison of it with its horizontal translation counterpart would be similar for all frequencies.

# *V. Quiet Zone Analysis*

The final product of this effort was the quiet zone characterization. For this effort, quiet zone illumination measurements were made and compared to predicted values. Good agreement was seen in the measurements and predictions of the phase of the illumination. Then the two way path of the RCS measurement was considered since the round trip phase is more significant than the one-way (measured) phase. There is confidence in these round trip predictions due to the agreement seen previously in the one-way case.

## *Results and Analysis of Quiet Zone Illumination*

The results of the quiet zone measurements are magnitude and phase plots of the transmitting antenna which are normalized to 0 dB magnitude and 0 degrees phase at the center of the scan; not the peak of the beam. Appendix B contains plots of all the measurements that were made. Selected data is presented and discussed here. Analysis of the individual plots produces the illumination pattern over the quiet zone with respect to the amplitude and phase variation criteria discussed in Chapter II. The analysis of the illumination patterns provides data which can be compared to that in Table 2. For this analysis only the horizontal translation data was used, since the vertical data is only repeated in the opposite polarization. Close examination of the plots reveals that the traces are not completely smooth. Thus, the estimation of the beam peak and the points at which amplitude and phase exceed the criteria is not exact. The method used to find the peak of each trace in turn was to look first at the 10 to 15 cm portion of the top of the trace. Then, pick the center of that spread as the identified peak even though it may not be the highest point on the trace. For the amplitude traces a line was drawn 1 dB down from the identified peak. For the phase traces a line was drawn at a point 11.25 degrees down and 22.5 degrees down for the $\pi/16$ and $\pi/8$ phase variation criteria.

Table 4. $L$ (ft), Beam Peak Method, V-polarization

| | Frequency (GHz) | | | | | | |
|---|---|---|---|---|---|---|---|
| | 6 | 8 | 10 | 12 | 14 | 16 | 18 |
| A=.9 | 2.94 | 2.20 | 2.49 | 1.94 | 1.87 | 3.38 | 2.72 |
| $\phi = \pi/8$ | 1.35 | 1.20 | 1.05 | .98 | .95 | .85 | .57 |
| $\phi = \pi/16$ | .95 | .85 | .75 | .71 | .59 | .52 | .49 |

Table 5. $L$ (ft), Beam Peak Method, H-polarization

| | Frequency (GHz) | | | | | | |
|---|---|---|---|---|---|---|---|
| | 6 | 8 | 10 | 12 | 14 | 16 | 18 |
| A=.9 | 2.95 | 2.89 | 1.76 | 1.90 | 1.28 | 3.08 | 3.38 |
| $\phi = \pi/8$ | 1.50 | 1.28 | 1.05 | 1.02 | .89 | .82 | .74 |
| $\phi = \pi/16$ | 1.13 | .82 | .77 | .75 | .59 | .58 | .52 |

respectively. Where these lines intersected the apparent smooth curve fit of each trace was the point chosen as the cut-off point. Finally, the distance between these cut-off points for each trace was measured to determine the dimension $L$ for that particular amplitude or phase variation. This methodology allowed for the random fluctuations of the measurement. My observations of the results is that the curve fitting approach rarely differed by more than one centimeter. In most cases, what was gained on one side was lost on the other side of the trace. Table 4 shows the results of the vertically polarized data. Table 5 contains the horizontally polarized results.

Tables 4 and 5 show the measured quiet zone crossrange dimension as a function of frequency for the amplitude and phase criteria shown. This data can be compared to the prediction in Table 2. It is immediately obvious that the phase predictions are better than the magnitude predictions. This is because the magnitude predictions assumed uniform aperture fields in a square aperture. The data clearly shows that

Table 6. Percent Deviation of Measured Data to Predicted Data

| Frequency (GHz) | | | | | | | |
|---|---|---|---|---|---|---|---|
| | 6 | 8 | 10 | 12 | 14 | 16 | 18 |
| H-Plane $\pi/8$ | -2.88 | -1.64 | -2.78 | -2.49 | 0.53 | -1.73 | -18.6 |
| $\pi/16$ | -3.06 | -1.73 | -1.96 | -0.70 | -5.60 | -8.77 | -8.41 |
| E-Plane $\pi/8$ | 2.39 | 1.59 | -2.78 | -0.49 | -2.73 | -3.53 | -5.73 |
| $\pi/16$ | 5.61 | -3.53 | -0.65 | 2.04 | -5.60 | -3.33 | -5.45 |

the tapered illumination and defocussed aperture of the diagonal horn antennas produce a more constant gain across the beamwidth than the square aperture horns. Also evident is the dramatic increase in beamwidth at the 16 and 18 GHz level due to the modification of the horn near the apex.

The design of the diagonal horn antennas should not affect the phase results as drastically since the point source assumption is still a good one. Comparison of the data reveals that this is true. Table 6 shows the percent deviation in each value from Tables 4 and 5 to the values in Table 2. In all but one case the percent deviation is less than 10. This is acceptable considering that there are many factors affecting the measured data which are not taken in to account in the prediction. The one undesired outcome is that the measurement values are for the most part less than the predicted values. Thus, the ideal quiet zone is smaller than expected. However. RCS measurements have a path which is twice the illumination path length. Also. the use of separate transmit and receive antennas causes the actual quiet zone to be some combination of the two antenna's patterns.

*Results and Analysis of Actual Quiet Zone*

If the beam peaks for both the transmitter and receiver were centered on the pedestal. then the quiet zone dimension would match the values obtained in Tables 4 and 5. For this to happen the transmit and receive antenna would have to

Table 7. $L$ (ft), Round Trip Method, Target Pedestal Along Antenna Centerline

| | Frequency (GHz) | | | | | | |
|---|---|---|---|---|---|---|---|
| | 6 | 8 | 10 | 12 | 14 | 16 | 18 |
| $\phi = \pi/8$ | .72 | .62 | .56 | .49 | .47 | .43 | .42 |
| $\phi = \pi/16$ | .49 | .43 | .39 | .36 | .32 | .30 | .27 |

be the same. Since they are not in the AFIT chamber, the actual quiet zone is a result of the combination of the two patterns. The actual quiet zone as determined by phase of a two antenna system taking an RCS measurement can be predicted by determining the phase of the two way path reflected from an imaginary line across the quiet zone as shown in Figure 23. The equation for the phase, in degrees, at the receive antenna at each point across the quiet zone is

$$\phi = \left(\sqrt{(14.3684 + X)^2 + 580644} + \sqrt{(14.3684 - X)^2 + 580644}\right) 360/\lambda \qquad (17)$$

where 14.3684 is half the separation of the phase centers in centimeters, $X$ is the translation increment (centimeters) across the quiet zone, 580644 is the square of the downrange distance to the quiet zone in centimeters, and $360/\lambda$ is the degrees per wavelength (centimeters). Running $X$ from -60 to 60 and taking the resulting array of $\phi$ and normalizing by subtracting the $\phi$ value when $X$=0 from the entire array leaves a trace of the beam pattern due to the combination of the two antenna. Using a similar method of determining the cut-off points as described for the illumination traces, the cross-range dimension of the quiet zone due to a $\pi/16$ and $\pi/8$ phase variation for various frequencies can be determined. Table 7 shows the cross-range dimension, $L$, of the quiet zone due to the combination effect of the two antennas. Given the relatively high confidence level of the illumination predictions, particularly in the center portion of the frequency band, it is safe to assume that these predictions are similarly accurate.

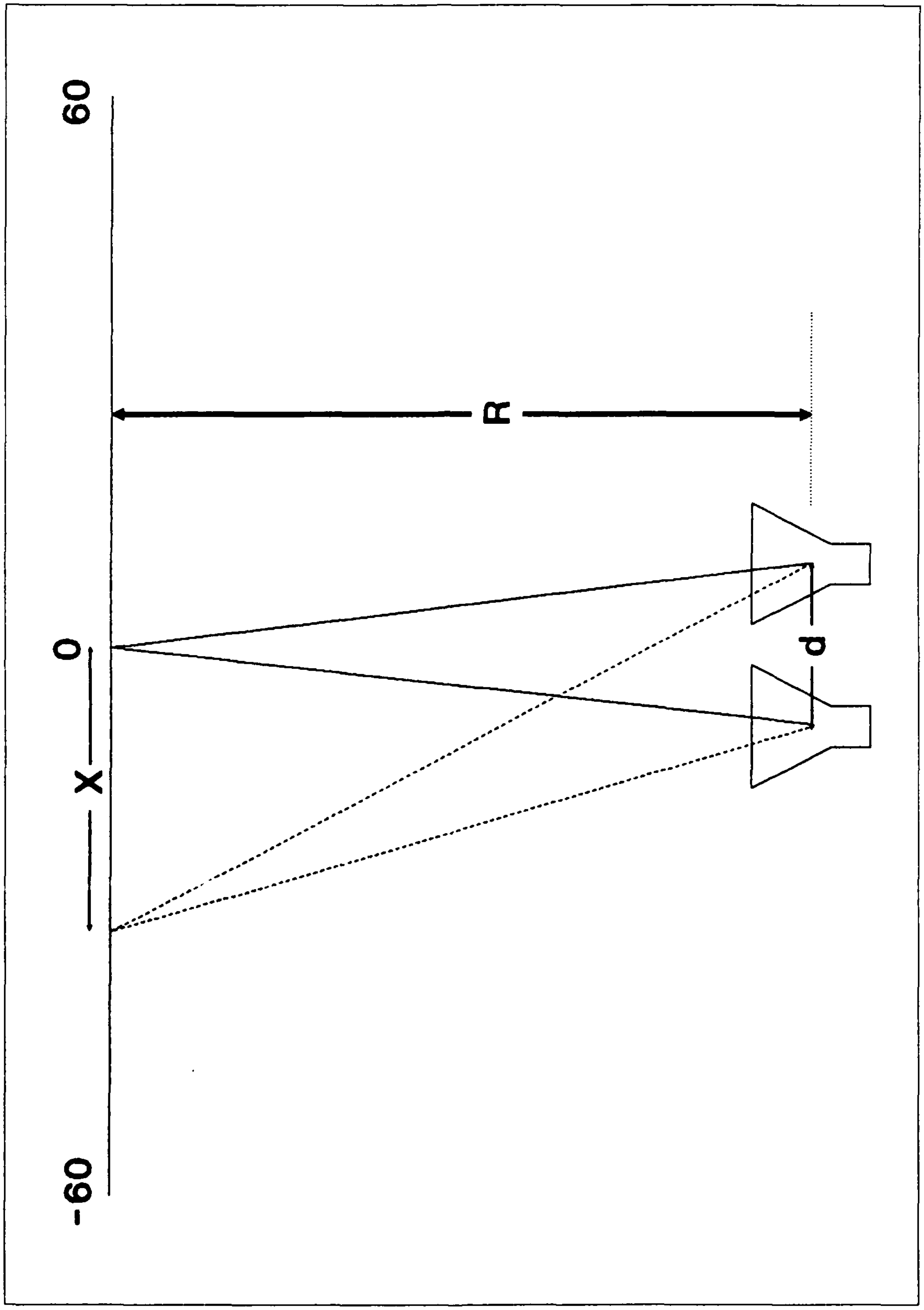


Figure 23. Two-way Path of RCS Measurement

The data from Table 7 assumes that the center of the quiet zone is aligned with the center point between the two antennas' phase centers. In the AFIT chamber, the data shows that the center point of the antennas does not coincide with the center of the pedestal. This places the target zone and thus the quiet zone on the edge of the combined antenna trace. To demonstrate the distance the antennas are shifted off the center of the pedestal, measurements were taken at 10 GHz translating horizontally and vertically at horizontal and vertical polarization, respectively, transmitting from first antenna 1 and then repeating with antenna 2 (Figure 21). The phase plots from these measurements are in Figures 24 through 27. Figure 24 is taken with horizontal translation and polarization and transmitting through antenna 1. Figure 25 is under the same conditions transmitting through antenna 2. Figure 26 is the vertical translation and polarization measurement taken with antenna 2 transmitting, while Figure 27 is taken with antenna 1 transmitting. Figures 24 and 25 are plotted to the same scale as are the remaining two to their scale. In both sets of plots, antenna 2 has a shorter minimum phase length than antenna 1. This results from the fact that the center point of the translation path (used for normalization) is off center from the line of the center point between the two antennas. Overlaying these pairs of plots, it becomes easy to see that the center point between the beam peaks is not at 60 cm. For the vertical translation (Figure 29), the shift is merely an adjustment up or down over the pedestal which is important to know; however, the horizontal translation (Figure 28) shows the shift from the desired center point to be approximately 8.5 cm (3.3 in) to the side of antenna 1. Taking this shift into account the values for the quiet zone as the AFIT chamber is currently configured are as shown in Table 8. This data indicates that the pedestal should be realigned with the antennas in order to achieve the quiet zone dimension shown in Table 7.

Since the quiet zone dimensions have been pessimistic due to pedestal misalignment, it seems appropriate to demonstrate the ability of the system to measure a relatively large target. Consider a 1 foot right circular cylinder, rotated on its side.

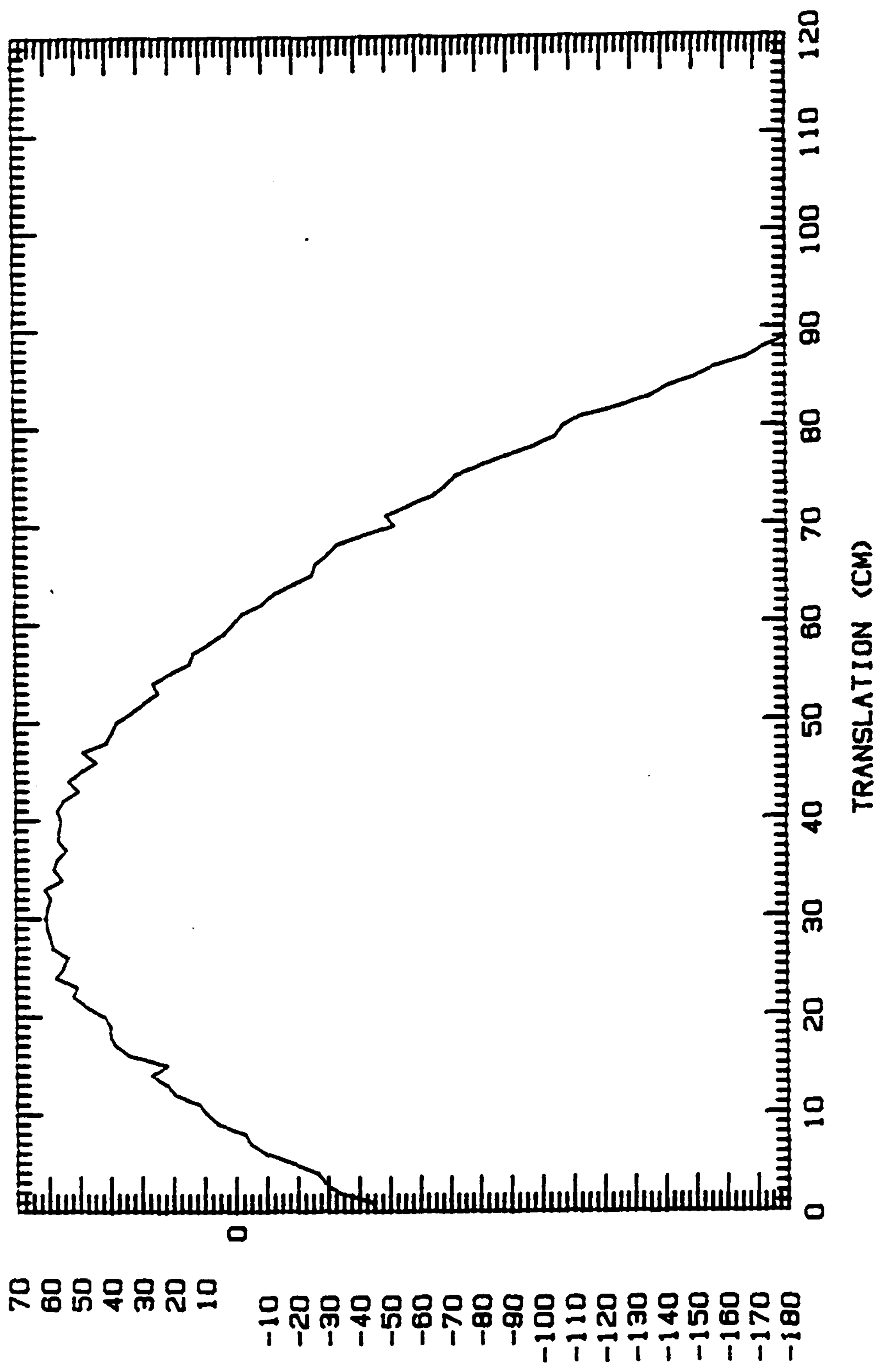


Figure 24. Phase Plot, H-translation, H-polarization, Antenna 2 TX

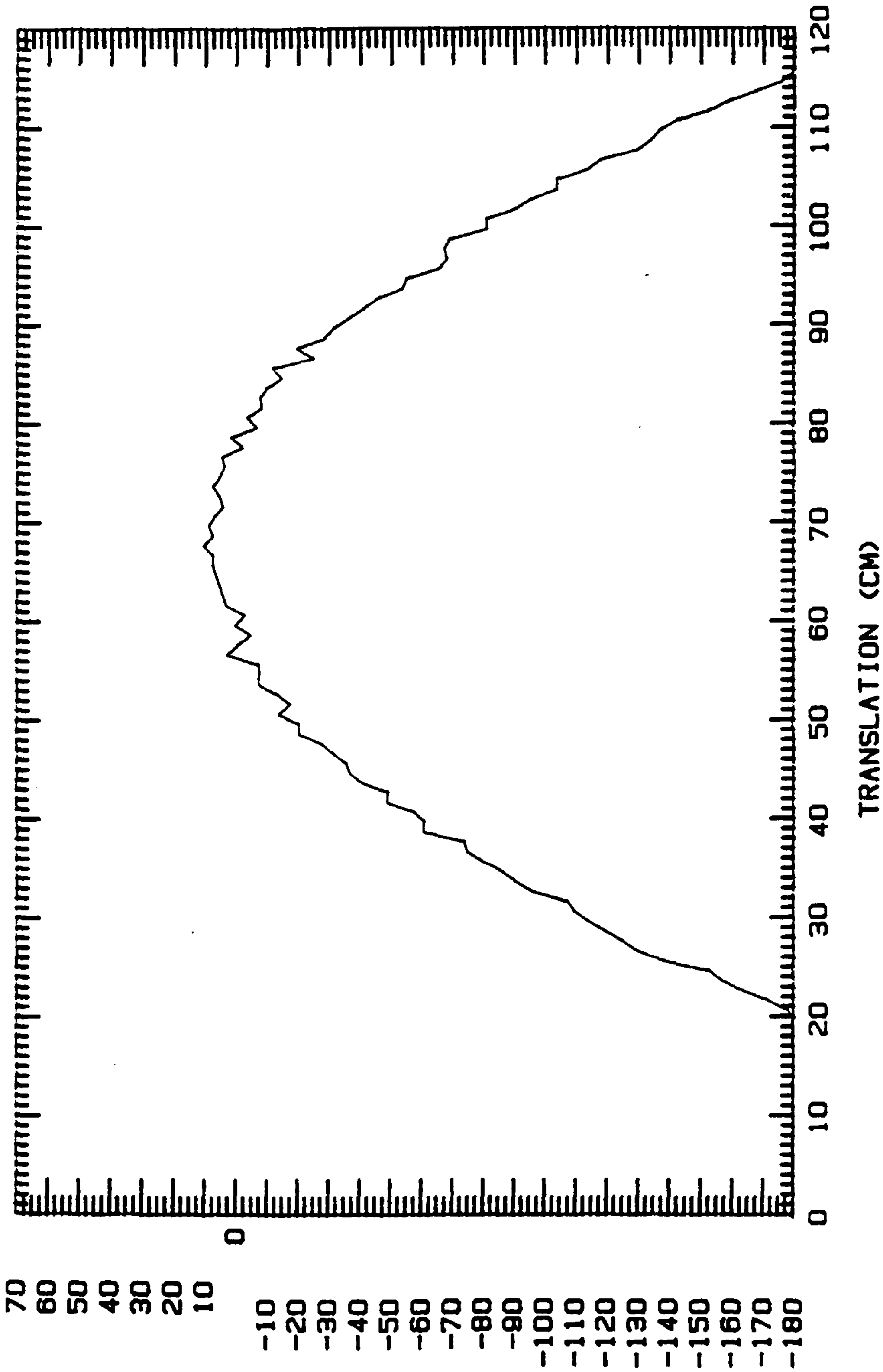


Figure 25. Phase Plot, H-translation, H-polarization, Antenna 1 TX

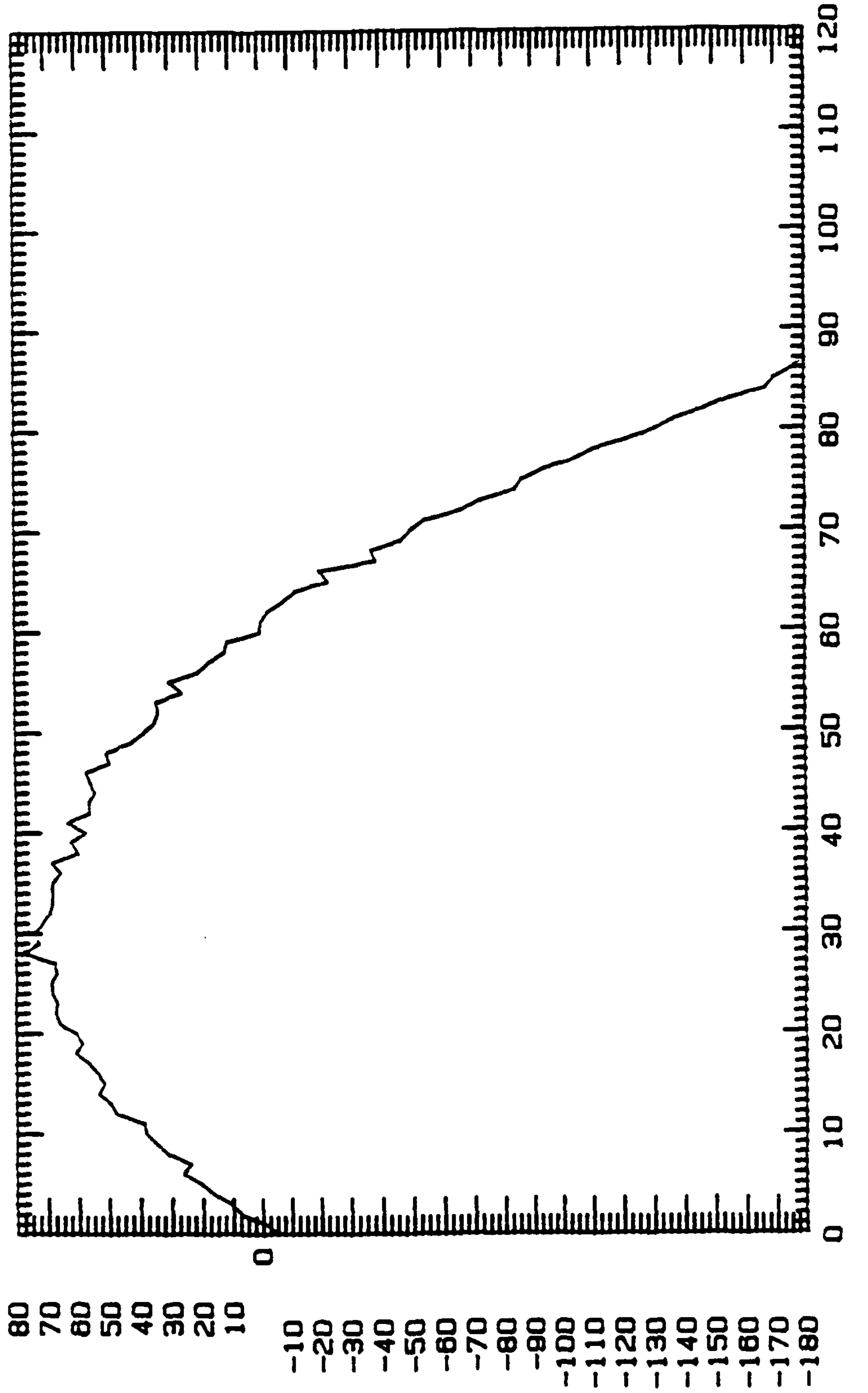


Figure 26. Phase Plot, V-translation, V-polarization, Antenna 2 TX

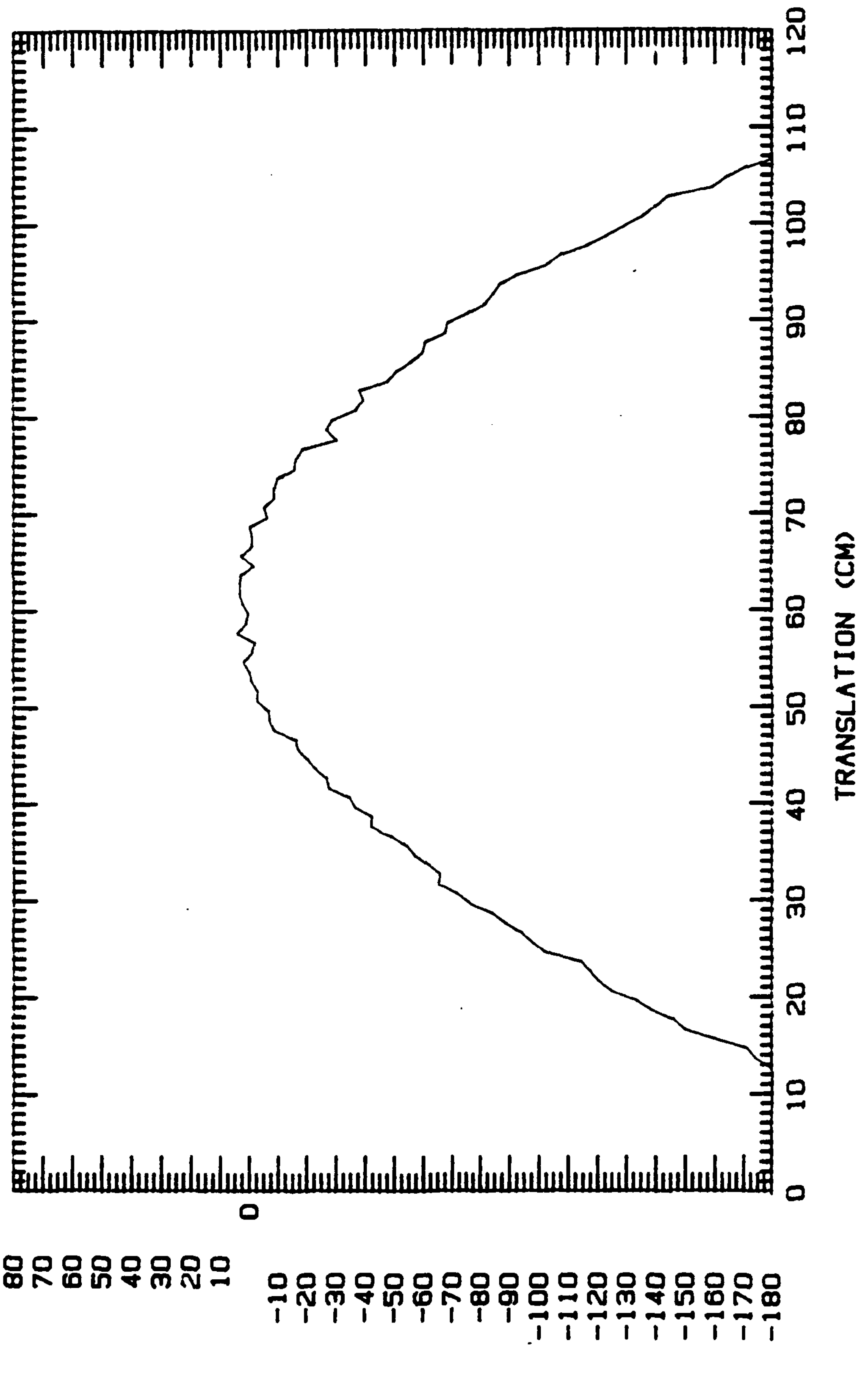


Figure 27. Phase Plot, V-translation, V-polarization, Antenna 1 TX

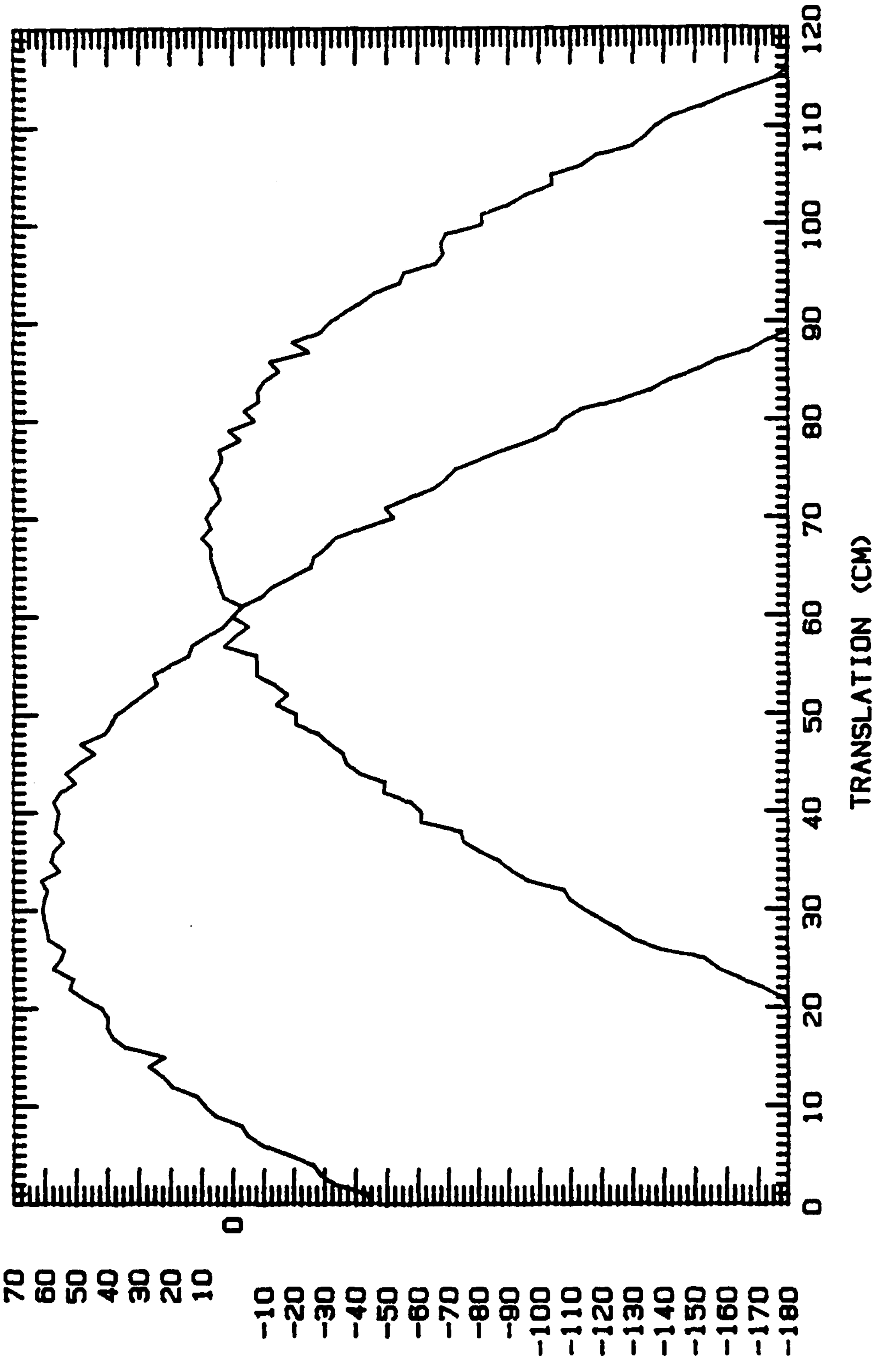


Figure 28. Phase Overlay Plot from Horizontal Translation

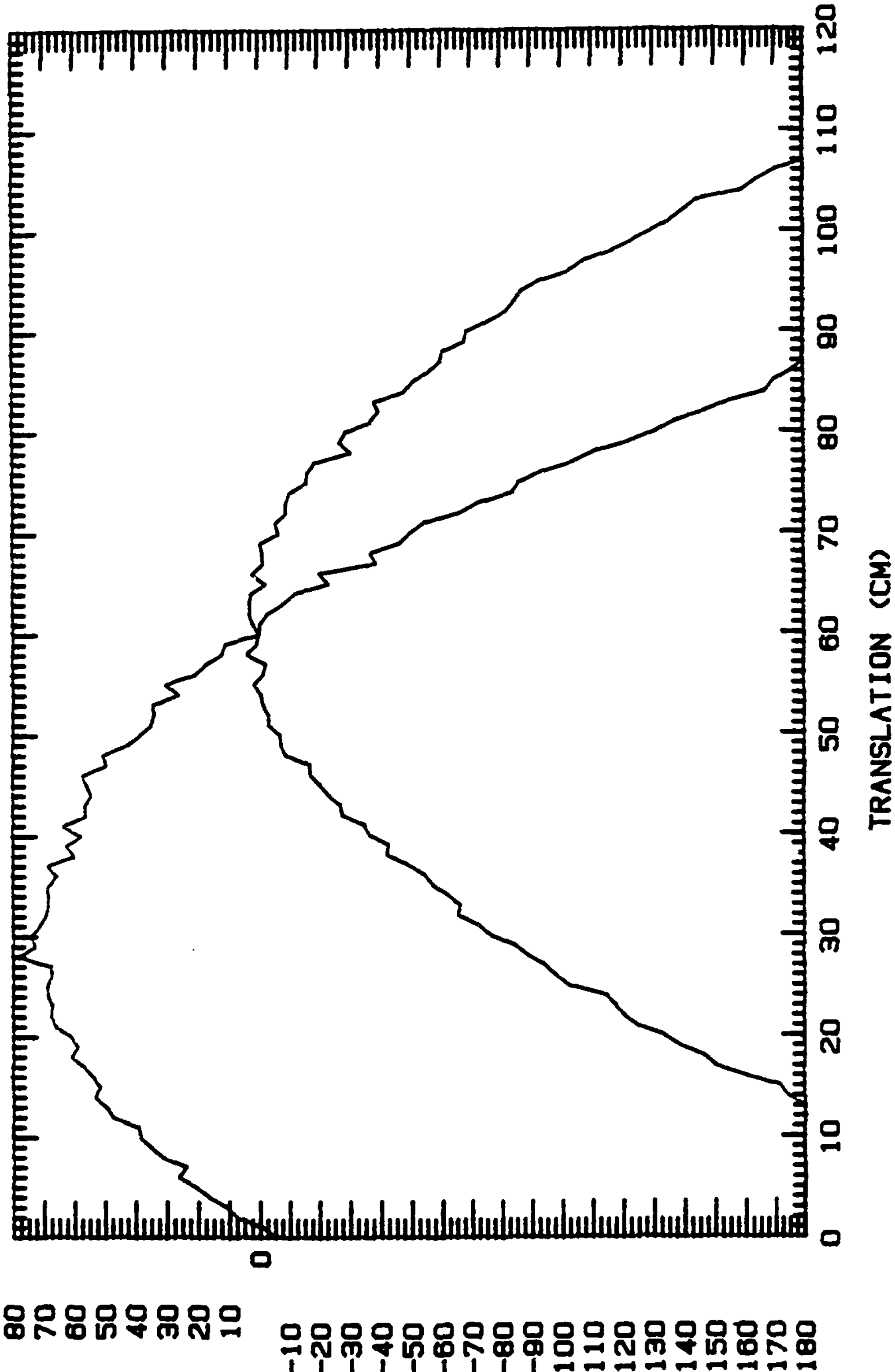


Figure 29. Phase Overlay Plot from Vertical Translation

Table 8. $L$ (ft). Round Trip Method. Target Pedestal Off Antenna Centerline

| | Frequency (Ghz) | | | | | | |
|---|---|---|---|---|---|---|---|
| | 6 | 8 | 10 | 12 | 14 | 16 | 18 |
| $\phi = \pi/8$ | .46 | .34 | .28 | .21 | .20 | .17 | .16 |
| $\phi = \pi/16$ | .23 | .21 | .13 | .12 | .10 | .08 | .07 |

Since this is a "clean" target, its RCS pattern should be very susceptible to phase errors. Figures 30 and 31 show measurements of the 1 foot cylinder, vertical polarization, in the AFIT range and a compact range, respectively. The compact range measurement had extremely small phase and amplitude variation, and can be considered as the correct RCS pattern. Both plots are oriented so that the incident wave was normal to an endcap at 180 degrees and to broadside at 90 and 270 degrees. A comparison shows that the portion of the plots around 180 degrees are very much alike. This is expected since the phase variation across the target is the smallest at this point. When the cylinder is broadside; however, the maximum phase variation across the target is experienced. Comparing the plots at these points reveals that the AFIT chamber results do not reflect the symmetrical lobing off the main peak as well as the compact range results. Still, the AFIT chamber results do show a good representative plot of a cylinder. Furthermore, the AFIT measurements might be improved by taking more data points per degree and/or more smoothly rotating the target.

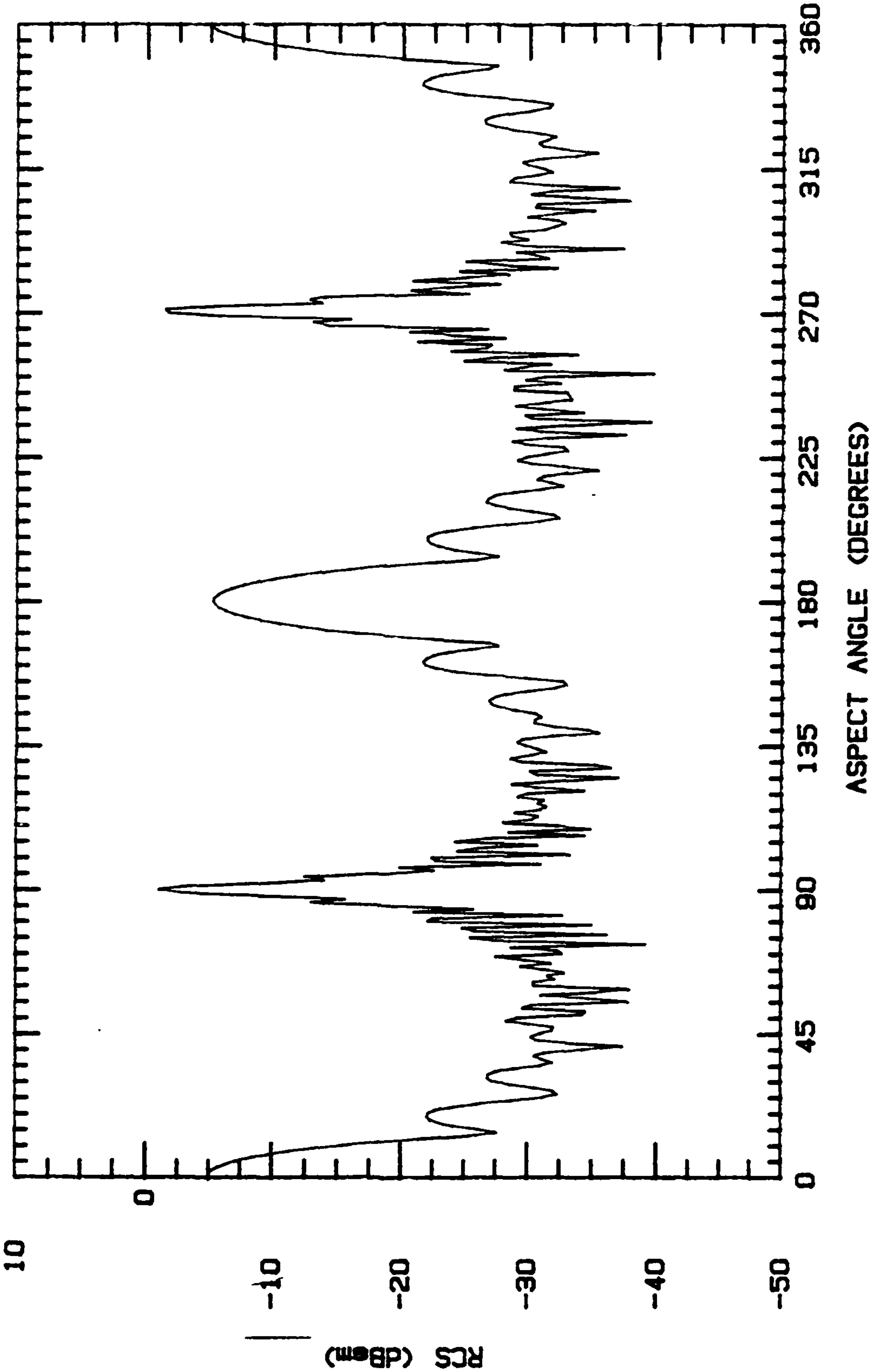


Figure 30. Pattern Cut, 1 foot Cylinder. Vertical Polarization. AFIT

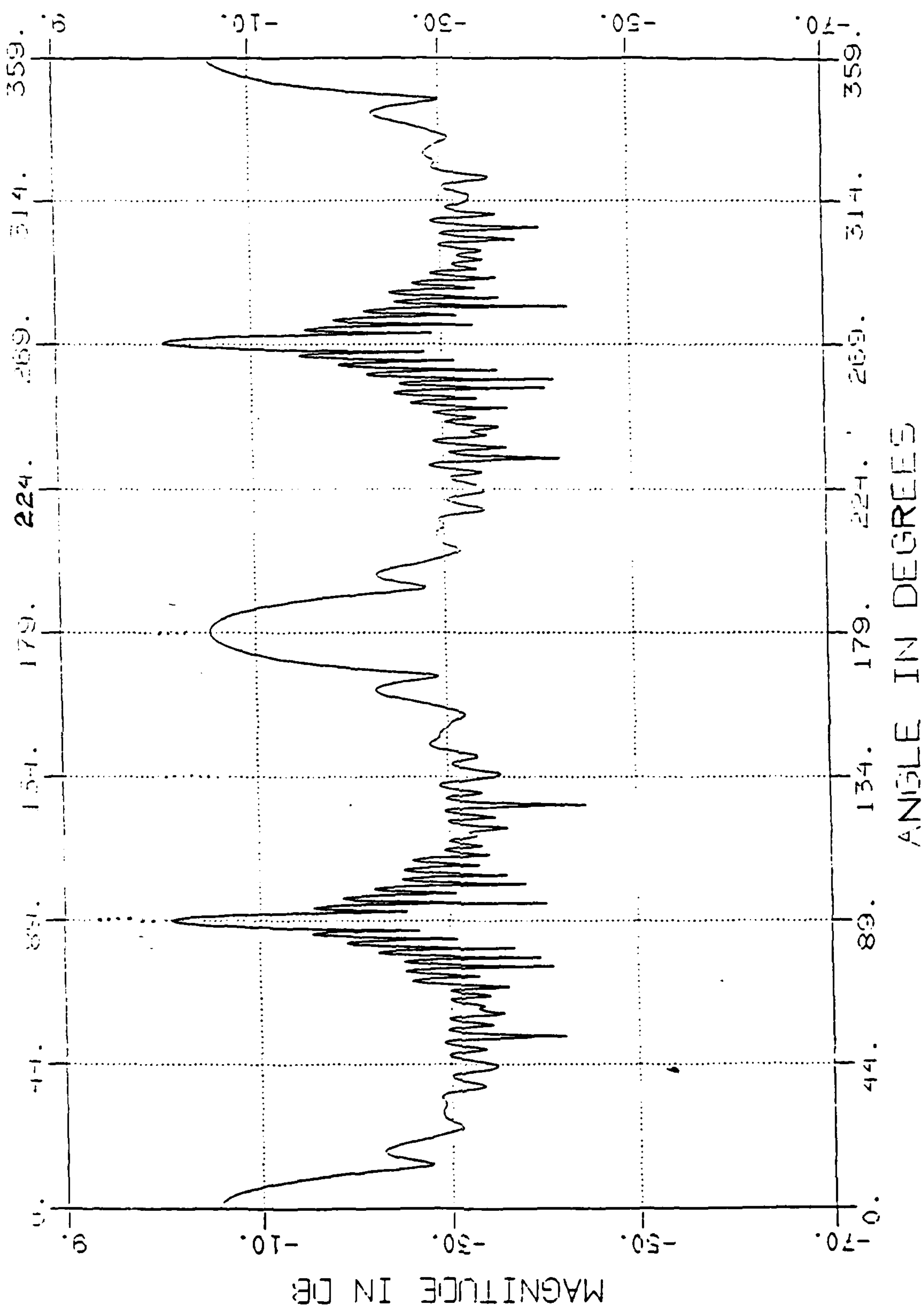


Figure 31. Pattern Cut, 1 foot Cylinder, Vertical Polarization, Compact Range

# VI. Conclusions and Recommendations

## Conclusions

The conclusions drawn from this thesis effort are:

- The diagonal horn antenna are significantly better than the pyramidal horn antenna for a far field range. This is due to the diagonal horn's much reduced side lobe levels which reduced scattering from the room, amplitude taper across the aperture which allowed mounting the antennas closer together creating a backscatter angle nearer to zero degrees, and an increased bandwidth which improved range resolution by almost a factor of three.
- The quiet zone of a chamber is a dynamic area that is influenced by many factors, one of which is frequency. Antenna alignment, beam shape, polarization, and antenna rotation are four more which were discovered during this effort.
- Absorber types properly placed also reduce scattering into the quiet zone area. Background subtraction and range gating take much of the unwanted scattered signals out of the measurement. However, error signals which arrive close in time to the target signal can not be time gated out.
- The magnitude predictions were derived from an assumed square aperture antenna with constant amplitude across the aperture and were invalid for comparison with the diagonal horn antenna magnitude measurements. However, the phase predictions were fairly good in that the phase variation from both types of antenna can be accurately modeled with the point source approximation method.

## Recommendations

Much work can be done to continue the effort of improving the AFIT RCS chamber. The problem of measuring horizontally long targets with horizontal polarization and vertically long targets with vertical polarization is one very important concern. Two approaches which could be investigated are:

1. Modifying the system to use only one antenna. This would require a circulator or a means of pulsing the transmitted and received signals.

2. The system currently has the antenna looking straight out into the chamber. Perhaps if they were tilted so that they focussed on the quiet zone it would alleviate the parallax problem. Investigation would have to be done to see if the angular orientation introduced different error.

Absorber placement is another area of concern. To be done properly, this would require funds to purchase the proper type of wedge absorber in sufficient quantities to install properly. In the meantime, much could be done to cut and fit the existing absorber for maximum benefit.

Continued work toward better characterizing the chamber could also be performed. A more complete mapping of the quiet zone would lead to a much better picture of the beam patterns in the two polarizations. This could be done with the existing translator by having a number of mounting rods in 1 cm increments made. I believe that the rods could be as high as 50 cm with a lead brick counter balance. This would allow 50 horizontal traces at 1 cm intervals. Something would have to be designed to do the same for vertical traces. Improvements in the code which runs the translator could be implemented to make it more user friendly and less volatile. For instance, when a measurement is complete and the magnitude plot shows on the screen. If the phase option is selected before the magnitude is saved that magnitude data is lost. Other sequences of key strokes also result in undesired or unanticipated responses. The program works if one just takes the data, saves it, and then plots it.

# Appendix A. *AFITFP Code*

```
10     ! AFITFP                    version 1.0  Apr 1990
20     !LINES 20 TO 100 ARE THE MAIN PROGRAM
30     OPTION BASE 1
50     MASS STORAGE IS ":INTERNAL.4.0"
60     OFF KEY
70     CALL Clear_crt
80     CALL Start
81     CALL Clear_crt
90     PRINT "You are now back in BASIC."
100    END
110    !
120    !THIS SUBROUTINE IS THE MAIN MENU FOR 'AFITFP'.
130    !
140    SUB Start
150    PRINT ""
151    REAL View(365)
160    CALL Clear_crt
170    INPUT "Enter today's date.",Date$
180 Start:DISP CHR$(129)
190    CALL Clear_crt
200    PRINT ""
210    PRINT "This program is designed to translate the AFIT field"
220    PRINT "probe apparatus through a 120 cm range and provide a"
230    PRINT "measure of the field in dB and Phase normalized to"
240    PRINT "0 dB magnitude and 0 degrees phase at the center."
250 Startt:  PRINT ""
260    PRINT "At this time ensure (by manually operating the"
270    PRINT "rotator) that the probe antenna is positioned to the"
280    PRINT "left or right end"
300    PRINT ""
310    PRINT "Also ensure the antenna are set for the desired "
320    PRINT "polarity."
330    PRINT ""
331    ON KEY 0 LABEL "MEASURE" GOTO B
332    ON KEY 1 GOTO Idle
333    ON KEY 2 LABEL "PLOT" GOTO C
334    ON KEY 3 GOTO Idle
335    ON KEY 4 LABEL "BASIC" GOTO D
336 Idle:    DISP "ENTER APPROPRIATE SOFT KEY"
337          GOTO Idle
339 C:     CALL Clear_crt
340         OFF KEY
341         Icount=120
342         J=1
344         CALL Pat_procplot(Icount,J,Choice)
349         IF Choice=0 THEN SUBEXIT
350         GOTO Startt
```

```
351 D:     CALL Clear_crt
352        OFF KEY
353        SUBEXIT
360 B:CALL Clear_crt
361    OFF KEY
370    INPUT "Enter probe frequency  (between 6 & 18 GHz)".Meas_freq
371    IF Meas_freq<6 OR Meas_freq>18 THEN GOTO B
380 A:   CALL Clear_crt
390    PRINT "Enter the measurement interval."
400    PRINT ""
410    PRINT "      1  . . . . . . .  1 cm"
420    PRINT "      2  . . . . . . . 10 cm"
430    PRINT ""
440    PRINT "1 cm is the default"
450    Mrange=1
451    INPUT Mrange
460    IF Mrange<>1 AND Mrange<>2 THEN GOTO A
470    IF Mrange=2 THEN Mrange=10
471    Pol$=""
472    INPUT "Type the polarization of the field (H or V : Default is horizontal)
.".Pol$
473    IF Pol$<>"H" AND Pol$<>"V" AND Pol$<>"" THEN Goto472
474    IF Pol$="" OR Pol$="H" THEN
475      Pol$="HORIZONTAL"
476      Pol=0
477    ELSE
478        Pol$="VERTICAL"
479        Pol=1
480    END IF
482    !
483    CALL Clear_crt
485    PRINT "Enter measure direction-"
486    PRINT "1 ... 0 TO 1"
487    PRINT "2 ... 1 TO 0"
488    INPUT Dir$
489    IF Dir$<>"1" AND Dir$<>"2" THEN Goto483
490    !
491    REAL Viewm(365),Viewp(365),Pdata(365),Mdata(365)
502    FOR I=1 TO 365
503      Viewm(I)=0
504      Viewp(I)=0
505      Mdata(I)=0
506      Pdata(I)=0
507    NEXT I
510    Deg_cm=35300
520    Length=120
521    Icount=(Length/Mrange)
530    Fmin=6
531    Fmax=18
532    Istep=Mrange*Deg_cm
533    IF Dir$="2" THEN Istep=-Istep
535    Choice=2
536    Tmegte=7
540    Pre_gate$=VAL$(Tmegte)
550    CALL Meas(Meas_freq,Tmegte,Istep,Pdata(*),Length,Mrange,Mdata(*),Fmin,Fmax
)
```

```
570    CALL Normalize(Pdata(*),Length,Mrange,Viewp(*),Mdata(*),Viewm(*),Dir$)
571    J=0
572    CALL Clear_crt
576    CALL Show_crt(Meas_freq,Pol,Date$,Pre_gate$,Choice,Viewm(*),J,Icount,Retrn
,Coord)
577    IF Choice=0 THEN SUBEXIT
578    IF Choice=1 OR Choice=3 THEN GOTO Startt
580    J=1
581    CALL Clear_crt
582    CALL Show_crt(Meas_freq,Pol,Date$,Pre_gate$,Choice,Viewp(*),J,Icount,Retrn
,Coord)
583    IF Choice=0 THEN SUBEXIT
585    CALL Clear_crt
586    GOTO Startt
587    SUBEND
588    !
4040   SUB Meas(Meas_freq,Tmegte,Istep,Pdata(*),Length,Mrange,Mdata(*),Fmin,Fmax)
4050   OPTION BASE 1
4060   ASSIGN @Nwa TO 716
4090   ASSIGN @Nwa_data1 TO 716;FORMAT OFF
4110 New: CALL Clear_crt
4111         OUTPUT @Nwa;"RECA2;"
4120         OUTPUT @Nwa;"STAR";Fmin;"GHZ;STOP";Fmax;"GHZ;"
4730         OUTPUT @Nwa;"MARK1";Meas_freq;"GHz;"
4740         OUTPUT @Nwa;"GATESPAN";Tmegte;"ns;"
4750         OUTPUT @Nwa;"ENTO;"
4751         OUTPUT @Nwa;"LOGP;"
4752         WAIT 10
4760         OUTPUT 709 USING "K";"V34.0"
4770         OUTPUT 709 USING "K";"S3";Istep
4780         OUTPUT 709 USING "K";"C30.0"
4800         !
4810         FOR I=1 TO Length/Mrange
4811         CALL Clear_crt
4813         PRINT "          TAKING MEASUREMENT #";I
4820         OUTPUT @Nwa;"OUTPMARK;"
4830         ENTER @Nwa;Mdata(I),Pdata(I)
4831         WAIT 1
4832         PRINT "     ";CHR$(130);"MOVING";CHR$(128);
4840         OUTPUT 709 USING "K";"I3"
4852         WAIT 14*Mrange
4853         OUTPUT 709 USING "K";"C30.0"
4860         NEXT I
4870         OUTPUT @Nwa;"OUTPMARK;"
4880         ENTER @Nwa;Mdata(Length/Mrange+1),Pdata(Length/Mrange+1)
```

```
4890       SUBEND
4900       !
5260    SUB Clear_crt
5270      OUTPUT KBD:" K";
5280    SUBEND
5290    !
5300    ! THIS SUBROUTINE NORMALIZES THE DATA
5310    !
5310    !
5520    SUB Normalize(Pdata(*),Length,Mrange,Viewp(*),Mdata(*),Viewm(*),Dir$)
5521    OPTION BASE 1
5530    REAL Tempm(365),Tempp(365)
5535    Pnorm=Pdata(((Length/Mrange)/2)+1)
5536    Mnorm=Mdata(((Length/Mrange)/2)+1)
5537    !
5545    FOR I=1 TO (Length/Mrange)+1
5550    Viewm(I)=Mdata(I)-Mnorm
5551    Viewp(I)=Pdata(I)-Pnorm
5560    NEXT I
5561    !
5570    FOR I=2 TO (Length/Mrange)+1
5580     IF Viewp(I-1)-Viewp(I)>40 THEN Viewp(I)=Viewp(I)+360
5590     IF Viewp(I-1)-Viewp(I)<-40 THEN Viewp(I)=Viewp(I)-360
5600    NEXT I
5601    !
5610    IF Viewp(((Length/Mrange)/2)+1)<>0. THEN
5620     FOR I=1 TO (Length/Mrange)+1
5630     Tempp(I)=Viewp(I)-Viewp(((Length/Mrange)/2)+1)
5631     NEXT I
5632     Doit=1
5634    END IF
5635    !
5636    IF Doit=1 THEN
5637      Doit=0
5639      GOTO Fillit
5640     ELSE
5641      GOTO Passit
5642     END IF
5643   Fillit: FOR I=1 TO (Length/Mrange)+1
5644    Viewp(I)=Tempp(I)
5645    NEXT I
5652    !
5653   Passit: IF Dir$="2" THEN
5654    FOR I=1 TO (Length/Mrange)+1
5655    Tempm(I)=Viewm((Length/Mrange)+2-I)
5656    Tempp(I)=Viewp((Length/Mrange)+2-I)
5657    NEXT I
5658    FOR I=1 TO (Length/Mrange)+1
5659    Viewm(I)=Tempm(I)
5660    Viewp(I)=Tempp(I)
5661    NEXT I
5662    END IF
5663    !
5671    SUBEND
```

```
5672  !
5682  ! THIS SUBROUTINE STORES THE DATA
5692  !
6060  SUB Stre(Date$,Pre_gate$,View(*))
6080  CALL Clear_crt
6081  OPTION BASE 1
6090  PRINT ""
6100  PRINT ""
6110  PRINT ""
6120  PRINT ""
6130  PRINT "          Insert storage disk into the right-hand disk drive."
6140  PRINT ""
6150  PRINT "               Press   ":CHR$(129):"CONTINUE":CHR$(128):"    when yo
u are ready."
6160  PAUSE
6170  CALL Clear_crt
6180 Name:PRINT "The file name must have at least one UPPER CASE letter."
6190  PRINT ""
6200  INPUT "  Enter the file name for the current set of data.",Dt_file2$
6210  File_name2$=LWC$(Dt_file2$)
6220 Disk: CREATE BDAT Dt_file2$,1,2960
6230        ASSIGN @Dt_file2 TO Dt_file2$
6240        OUTPUT @Dt_file2;View(*)
6250        ASSIGN @Dt_file2 TO *
6260        CREATE BDAT File_name2$,2,30
6270        ASSIGN @File_name2 TO File_name2$
6280        OUTPUT @File_name2,1;Date$
6290        OUTPUT @File_name2,2;Pre_gate$
6300        ASSIGN @File_name TO *
6310  CALL Clear_crt
6320  SUBEND
6330  !
6340  ! THIS SUBROUTINE MAKES SURE THE USER HAS REMEMBERED TO SAVE THE DATA.
6350  !
6360  SUB Check(Chk$)
6370  PRINT ""
6380  PRINT ""
6390  PRINT ""
6400  PRINT ""
6410  PRINT "     Have you saved your data?  It will be lost if you haven't."
6420  PRINT ""
6430  Chk$=""
6440  INPUT "DO YOU WANT TO SAVE DATA? (Enter 'Y' or 'N':  Default is no)",Chk$
6450  CALL Clear_crt
6460  SUBEND
6470  !
6480  !THIS SUBROUTINE DISPLAYS THE FIELD PATTERN ON THE CRT.
6490  !
6500  SUB Show_crt(Meas_freq,Pol,Date$,Pre_gate$,Choice,View(*),J,Icount,Retrn,C
oord)
```

```
6510 Start:   CALL Clear_crt
6520     GINIT
6530     PLOTTER IS 3,"INTERNAL"
6540     Ymin=View(1)
6550     Ymax=Ymin
6560     FOR I=1 TO Icount
6570       IF View(I)<Ymin THEN Ymin=View(I)
6580       IF View(I)>Ymax THEN Ymax=View(I)
6590     NEXT I
6600     Ymax=Ymax+10
6610     Ymax=PROUND(Ymax,1)
6620     Ymin=Ymin-10
6630     Ymin=PROUND(Ymin,1)
6640     Range=Ymax-Ymin
6650     GRAPHICS ON
6660     MOVE 0,95
6670     CSIZE 3
6680     LABEL Name$
6690     CSIZE 6
6700     LORG 6
6710     FOR I=-.3 TO .3 STEP .1
6720       MOVE 70+I,100
6730       LABEL "LOW OBSERVABLES"
6740     NEXT I
6750     LORG 1
6760     CSIZE 4
6770     MOVE 0,62
6771     IF J=0 THEN
6772         Label$="LOG MAG"
6773         FOR I=1 TO 7
6774           LABEL Label$[I,I]
6775         NEXT I
6776       ELSE
6780         Label$="PHASE"
6790         FOR I=1 TO 5
6800           LABEL Label$[I,I]
6810         NEXT I
6811     END IF
6820     MOVE 56,15
6830     LABEL "ASPECT ANGLE"
6840     VIEWPORT 15,125,30,90
6850     FRAME
6860     WINDOW 0,Icount,Ymin,Ymax
6870     AXES 5,3,0,Ymin,9,5,2
6880     CSIZE 3
6890     LORG 6
6900     CLIP OFF
```

```
6910    FOR I=0 TO Icount STEP 10
6920      MOVE I,Ymin-1
6930      LABEL I
6940    NEXT I
6950    LORG 8
6960    FOR I=Ymin TO Ymax STEP 10
6970      MOVE -1,I
6980      LABEL I
6990    NEXT I
7000    FOR I=0 TO Icount
7010      PLOT I,View(I+1)
7020    NEXT I
7021    PLOT Icount,View(Icount+1)
7030    ON KEY 0 LABEL "PLOT" GOTO Plotr
7040    ON KEY 1 GOTO Idle
7050    ON KEY 2 LABEL "STORE THE DATA" GOTO C_stre
7060    ON KEY 3 GOTO Idle
7070    ON KEY 4 LABEL "NEW FP" GOTO C_new
7080    ON KEY 5 LABEL "DUMP TO PRNTR" GOTO Ddump
7090    ON KEY 6 GOTO Idle
7091    IF J=1 THEN
7100        ON KEY 7 GOTO Idle
7101      ELSE
7102        ON KEY 7 LABEL "PHASE" GOTO Bottom
7103    END IF
7110    ON KEY 8 GOTO Idle
7120    ON KEY 9 LABEL "TO BASIC" GOTO C_strt
7130    ON KBD GOTO Bottom
7140 Idle:DISP CHR$(131);"";CHR$(128);"";TIME$(TIMEDATE)
7150    WAIT 1
7160    GOTO Idle
7170 Ddump:PRINTER IS 701
7180    OUTPUT KBD;" N";
7190    PRINTER IS CRT
7200    GOTO Idle
7430 C_stre:  OFF KEY
7440    CALL Clear_crt
7450    GRAPHICS OFF
7460      View(361)=Meas_freq
7470      View(362)=Pol
7480    CALL Stre(Date$,Pre_gate$,View(*))
7490    CALL Clear_crt
7500    GOTO Start
7510 C_new:  OFF KEY
7520    GRAPHICS OFF
7530    CALL Clear_crt
7540    Choice=1
7550    CALL Check(Chk$)
```

```
7560     IF ChkS="Y" THEN GOTO C_stre
7570     SUBEXIT
7580 C_strt:  GRAPHICS OFF
7590     CALL Clear_crt
7600     Choice=0
7610     CALL Check(ChkS)
7620     IF ChkS="Y" THEN GOTO C_stre
7630     SUBEXIT
7631 Plotr:GRAPHICS OFF
7632         CALL Clear_crt
7634         Choice=3
7635         Retrn=0
7636         Coord=0
7637         SUBEXIT
7640 Bottom:GRAPHICS OFF
7650     CALL Clear_crt
7660  SUBEND
7670  !
7680  ! THIS SUBROUTINE CONTROLS THE PLOTTING OF THE DATA
7690  !
12960 SUB Pat_procplot(Icount,J,Choice)
12980 OPTION BASE 1
12990 DIM Ptrace_data(365),View(365)
13000 Input:CALL Pat_input(Ptrace_data(*),Meas_freq,DateS,File_name2$,Pol,Pre_ga
teS)
13010 View:CALL Show_crt(Meas_freq,Pol,DateS,Pre_gateS,Choice,Ptrace_data(*),J,I
count,Retrn,Coord)
13011       IF Choice=3 THEN GOTO Pmenu
13020 IF Retrn=2 OR Choice=1 OR Choice=0 THEN SUBEXIT
13030 IF Retrn=1 THEN GOTO Input
13040 Pmenu:ON KEY 0 GOTO Idle
13050 ON KEY 1 LABEL "LINE TYPE" GOTO Lin_typ
13060 ON KEY 2 GOTO Idle
13070 ON KEY 3 GOTO Idle
13080 ON KEY 4 GOTO Idle
13090 ON KEY 5 LABEL "PLOT GRID" GOTO Pgrid
13100 ON KEY 6 GOTO Idle
13110 ON KEY 7 LABEL "PLOT DATA" GOTO Pdata
13120 ON KEY 8 GOTO Idle
13130 ON KEY 9 LABEL "EXIT" GOTO Pexit
13140 Idle:DISP "ENTER APPROPRIATE SOFT KEY"
13150 GOTO Idle
13160 Lin_typ:CALL Clear_crt
13170 ON KEY 0 LABEL "0" GOTO Zero
13180 ON KEY 1 LABEL "1" GOTO One
13190 ON KEY 2 LABEL "2" GOTO Two
13200 ON KEY 3 LABEL "3" GOTO Three
13210 ON KEY 4 LABEL "4" GOTO Four
13220 ON KEY 5 LABEL "5" GOTO Five
13230 ON KEY 6 LABEL "6" GOTO Six
13240 ON KEY 7 GOTO Lidle
13250 ON KEY 8 GOTO Lidle
```

```
13260 ON KEY 9 GOTO Licle
13270 Licle:DISP "SELECT LINE TYPE"
13280 GOTO Licle
13290 Zero:Lin_typ=0
13300 GOTO Pmenu
13310 One:Lin_typ=1
13320 GOTO Pmenu
13330 Two:Lin_typ=2
13340 GOTO Pmenu
13350 Three:Lin_typ=3
13360 GOTO Pmenu
13370 Four:Lin_typ=4
13380 GOTO Pmenu
13390 Five:Lin_typ=5
13400 GOTO Pmenu
13410 Six:Lin_typ=6
13420 GOTO Pmenu
13430 Perio:    CALL Clear_crt
13440 CALL Pscale_ch(Ymax,Ymin,Ptrace_data(*),Icount)
13450 CALL Clear_crt
13460 IF Coord=0 THEN CALL Pdraw_pl(Ymax,Ymin,Num_traces,Icount)
13480 GOTO Pmenu
13490 Pdata: CALL Clear_crt
13500 IF Coord=0 THEN CALL Pdraw_data(Ptrace_data(*),Ymax,Ymin,File_name2$,Meas_
freq,Pol,Pre_gate$,Date$,Num_traces,Lin_typ,Icount)
13520 GOTO Pmenu
13530 Pexit:  CALL Clear_crt
13540  GRAPHICS OFF
13541  Choice=1
13542 Retrn=2
13550 SUBEXIT
13560 SUBEND
13570 !
13571 ! THIS SUBROUTINE RETRIEVES THE DATA FROM A DISK
13580 !
13590 SUB Pat_input(Ptrace_data(*),Meas_freq,Date$,File_name2$,Pol,Pre_gate$)
13600 !  Written by Dana J. Bergey, May 1989
13610 OPTION BASE 1
13620   DIM View(365)
13630   CALL Clear_crt
13640 Start:PRINT ""
13650   PRINT ""
13660   PRINT "            Insert disc containing data file into right hand disk d
rive."
13670   PRINT ""
13680   PRINT "                    Press ":CHR$(131):"CONTINUE":CHR$(128):
" when ready."
13690   PAUSE
13700   ON ERROR GOTO Err2
```

```
13710    CALL Clear_crt
13720    INPUT "Do you wish to see listing of disk (Y or N)?  Default is NO.",Lis
t$
13730    IF List$="Y" THEN
13740      CAT
13750      ON KBD GOTO Again
13760      DISP CHR$(131);"Press space bar when ready.";CHR$(128)
13770 Lloop:GOTO Lloop
13780    ELSE
13790      GOTO Again
13800    END IF
13810 Again:CALL Clear_crt
13820    OFF KBD
13830    OFF ERROR
13840 Name:INPUT "Enter the file name of the stored file.",File_name2$
13850    ON ERROR GOTO Err1
13860    GOTO Inbound
13870 Err1:PRINT ERRM$
13880    GOTO Name
13890 Inbound:ASSIGN @File2 TO File_name2$
13900    ENTER @File2;View(*)
13910    ASSIGN @File2 TO *
13920    FOR I=1 TO 365
13930    Ptrace_data(I)=View(I)
13940    NEXT I
13950    Meas_freq=View(362)
13960    Pol=View(363)
13970    Dte_file2$=LWC$(File_name2$)
13980    ASSIGN @Dte_file2 TO Dte_file2$
13990    ENTER @Dte_file2,1;Date$
14000    ENTER @Dte_file2,2;Pre_gate$
14010    ASSIGN @Dte_file2 TO *
14020    SUBEXIT
14030 Err2:CALL Clear_crt
14040    DISP ERRM$
14050    BEEP
14060    OFF ERROR
14070    GOTO Start
14080 SUBEND
14090     !
14091     ! THIS SUBROUTINE SCALES THE DATA FOR PLOTTING
14100     !
14110 SUB Pscale_ch(Ymax,Ymin,Ptrace_data(*),Icount)
14120 !  Written by Dana J. Bergey, May 1989
14121 !  Modified by Anthony J. Hunt, April 1990
14130  GRAPHICS OFF
14140   Ymin=Ptrace_data(1)                !   INITIALIZE
14150   Ymax=Ymin
14160     FOR J=1 TO Icount+1
14170       IF Ptrace_data(J)<Ymin THEN Ymin=Ptrace_data(J)
14180       IF Ptrace_data(J)>Ymax THEN Ymax=Ptrace_data(J)
14190     NEXT J
14200     CALL Clear_crt
```

```
14210   PRINT "        *
*"
14220   PRINT "        *                        SCALING CHOICES
*"
14230   PRINT "        *
*"
14240   PRINT "        ***************************************************
********"
14250   PRINT ""
14260   PRINT "        The maximum value of the current data is ";Ymax;
14270   PRINT "        The minimum value of the current data is ";Ymin;
14280   PRINT ""
14290   PRINT "        ";CHR$(129);"AUTO SCALE";CHR$(128);"..........Computer gen
erates scale."
14300   PRINT ""
14310   PRINT "        ";CHR$(129);"USER";CHR$(128);"................User defines
 scale."
14320   PRINT ""
14330   ON KEY 5 LABEL "    AUTO SCALE" GOTO Auto
14340   ON KEY 7 LABEL "       USER" GOTO User
14350   ON KEY 9 GOTO Idle
14360   ON KEY 0 GOTO Idle
14370   ON KEY 1 GOTO Idle
14380   ON KEY 2 GOTO Idle
14390   ON KEY 3 GOTO Idle
14400   ON KEY 4 GOTO Idle
14410   ON KEY 6 GOTO Idle
14420   ON KEY 8 GOTO Idle
14430 Idle:DISP "Enter appropriate soft key."
14440   GOTO Idle
14450 User:CALL Clear_crt
14460   PRINT "        *
*"
14470   PRINT "        *                        USER DEFINED SCALE
*"
14480   PRINT "        *
*"
14490   PRINT "        ***************************************************
*******"
14500   PRINT ""
14510   PRINT ""
14520   INPUT "Enter the maximum value of scale desired.",Ymax
14530   INPUT "Enter the minimum value of scale desired.",Ymin
14540   Range=Ymax-Ymin
14550   IF Range>0 THEN GOTO Good_rge
14560   BEEP
14570   IF Range=0 THEN PRINT "              You have entered the same value fo
r Ymin and Ymax."
14580   IF Range<0 THEN PRINT "                    Your Ymin is greater than y
our Ymax."
14590   PRINT ""
14600   PRINT "                        Try again!"
```

```
14610   GOTO 14520
14620 Good_rge:CALL Clear_crt
14630   OFF KEY
14640   SUBEXIT
14650 Auto:CALL Clear_crt
14660   Ymax=Ymax+10
14670   Ymax=PROUND(Ymax,1)
14680   Ymin=Ymin-10
14690   Ymin=PROUND(Ymin,1)
14700   OFF KEY
14710 SUBEND
14720 !
14721 ! THIS SUBROUTINE DRAWS THE GRID
14730 !
14740 SUB Pdraw_pl(Ymax,Ymin,Num_traces,Icount)
14750 !  Written by Dana J. Bergey, May 1989
14751 !  Modified by Anthony J. Hunt, April 1990
14760   Num_traces=0
14770   CALL Clear_crt
14780   PRINT ""
14790   PRINT ""
14800   PRINT ""
14810   PRINT "              Ensure that paper and two pens are in the plotter at thi
s time."
14820   PRINT ""
14830   PRINT "                                    Press ";CHR$(129);"CONTINUE";CHR$(128)
;" when ready."
14840   PAUSE
14850   CALL Clear_crt
14860   !GRAPHICS ON
14870   PRINTER IS 705
14880   E$=CHR$(3)
14890   PRINT "IN;SP1;IP 1500,2000,9500,7500;"
14900   PRINT "SC0",Icount,"0,100;"
14910   PRINT "PU 0,0 PD ",Icount,"0",Icount,"100,0,100,0,0 PU;"
14920   PRINT "SI .2,.3;TL 3,0;"
14930   FOR X=10 TO 110 STEP 10
14940     PRINT "PA",X,"0,XT;"
14950   NEXT X
14960   PRINT "TL 1.5,0"
14970   FOR X=1 TO 119 STEP 1
14980     PRINT "PA",X,"0,XT"
14990   NEXT X
15000   PRINT "TL 0,3;"
15010   FOR X=10 TO 110 STEP 10
15020     PRINT "PA",X,"100,XT;"
15030   NEXT X
15040   PRINT "TL 0,1.5"
15050   FOR X=1 TO 119 STEP 1
```

```
15060     PRINT "PA",X,"100,XT"
15070    NEXT X
15080    FOR X=0 TO Icount STEP 10
15090      PRINT "PA",X,"0"
15100      IF X<10 THEN PRINT "CP -1.5,-1;LB";X;ES
15110      IF X>9 AND X<100 THEN PRINT "CP -2,-1;LB";X;ES
15120      IF X>99 THEN PRINT "CP -2.5,-1;LB";X;ES
15130    NEXT X
15140    PRINT "PA 60,0;CP -11,-2.5; LBTRANSLATION (CM)";ES
15150    PRINT "SC0",Icount,Ymin,Ymax;"TL 3,0"
15160    Range=Ymax-Ymin
15170    FOR Y=Ymin+10 TO Ymax-10 STEP 10
15180      PRINT "PA0",Y,"YT"
15190    NEXT Y
15200    PRINT "TL 1.5,0"
15210    IF Range>49 THEN Little_tick=2.5
15220    IF Range<51 THEN Little_tick=2
15230    IF Range<31 THEN Little_tick=1
15240    FOR Y=Ymin+Little_tick TO Ymax-Little_tick STEP Little_tick
15250      PRINT "PA 0",Y,"YT"
15260    NEXT Y
15270    PRINT "TL 0,3"
15280    FOR Y=Ymin+10 TO Ymax-10 STEP 10
15290      PRINT "PA ",Icount,Y,"YT"
15300    NEXT Y
15310    PRINT "TL 0,1.5"
15320    FOR Y=Ymin+Little_tick TO Ymax-Little_tick STEP Little_tick
15330      PRINT "PA ",Icount,Y,"YT"
15340    NEXT Y
15350    PRINT "TL 3,0"
15360    FOR Y=Ymin TO Ymax STEP 10
15370      PRINT "PA 0",Y;
15380      Ynum=Y
15390      Ynum=PROUND(Ynum,-2)
15400      IF Ynum<-99.99 THEN Offset=6
15410      IF Ynum>-100 AND Ynum<-9.99 THEN Offset=5
15420      IF Ynum>-10 AND Ynum<-.99 THEN Offset=4
15430      IF Ynum>-1 AND Ynum<0 THEN Offset=3
15440      IF Ynum=0 THEN Offset=0
15450      IF Ynum>0 AND Ynum<1 THEN Offset=2
15460      IF Ynum>.99 AND Ynum<10 THEN Offset=3
15470      IF Ynum>9.99 AND Ynum<100 THEN Offset=4
15480      IF Ynum>99.99 THEN Offset=5
15490      PRINT "CP",(-2.5)-Offset,"-.25;LB";Ynum;ES
15500    NEXT Y
15510 !  PRINT "PA0",Ymin+Range/2;"DI0,1;CP -5,5"
15520 !  PRINT "LBRCS (dBsm)";ES
15530    PRINT "DI1,0"
15540    PRINT "PU;PA0",Ymin,";SI .15,.225;CP5,-5;"
15550    PRINT "LBFile Name        Frequency       Polarization      Soft gate
  Date";ES
15560    PRINT "SP0"
15570    PRINTER IS CRT
15580 SUBEND
```

```
15590 !
15591 ! THIS SUBROUTINE PLOTS THE DATA ON THE GRID
15600 !
15610 SUB Pcraw_data(Ptrace_data(*),Ymax,Ymin,File_name2$,Meas_freq,Pol,Pre_gate
$,Date$,Num_traces,Lin_typ,Icount)
15620 !  Written by Dana J. Bergey, May 1989
15621 !  Modified by Anthony J. Hunt, April 1990
15630   PRINTER IS 705
15640   PRINT "SC0",Icount,Ymin,Ymax
15650   PRINT "SP2;"
15651   IF Ptrace_data(2)<Ymin THEN Ptrace_data(2)=Ymin
15660   PRINT "PU0",Ptrace_data(2);
15670   PRINT "LT2,";Lin_typ;";"
15680   IF Lin_typ=0 THEN PRINT "LT;"
15690   FOR I=2 TO Icount+2
15700     IF Ptrace_data(I)<Ymin THEN Ptrace_data(I)=Ymin
15710     IF Ptrace_data(I)>Ymax THEN Ptrace_data(I)=Ymax
15720     PRINT "PD",I-2,Ptrace_data(I)
15730   NEXT I
15740   Num_traces=Num_traces+1
15750   PRINT "PU;PA0",Ymin,";SI .15,.225;CP5,-5;"
15760   E$=CHR$(3)
15770   IF Pol=1 THEN
15780     Pol$="VERTICAL"
15790   ELSE
15800     Pol$="HORIZONTAL"
15810   END IF
15820   FOR I=0 TO Num_traces
15830     PRINT "CP0,-1;"
15840   NEXT I
15850   PRINT "LB";File_name2$;E$
15860   PRINT "CP;CP20,1;"
15870   PRINT "LB";Meas_freq;"GHz";E$
15880   PRINT "CP;CP30,1;"
15890   PRINT "LB";Pol$;E$
15900   PRINT "CP;CP59,1;"
15910   PRINT "LB";Pre_gate$;E$
15920   PRINT "CP;CP69,1;"
15930   PRINT "LB";Date$;E$
15940 Bottom:PRINT "SI .2,.3;PU0",Ymin,"SP ;"
15950   PRINTER IS CRT
15960 SUBEND
```

# Appendix B. *Quiet Zone Magnitude and Phase Plots*

*Horizontal Translation, Vertical Polarization*

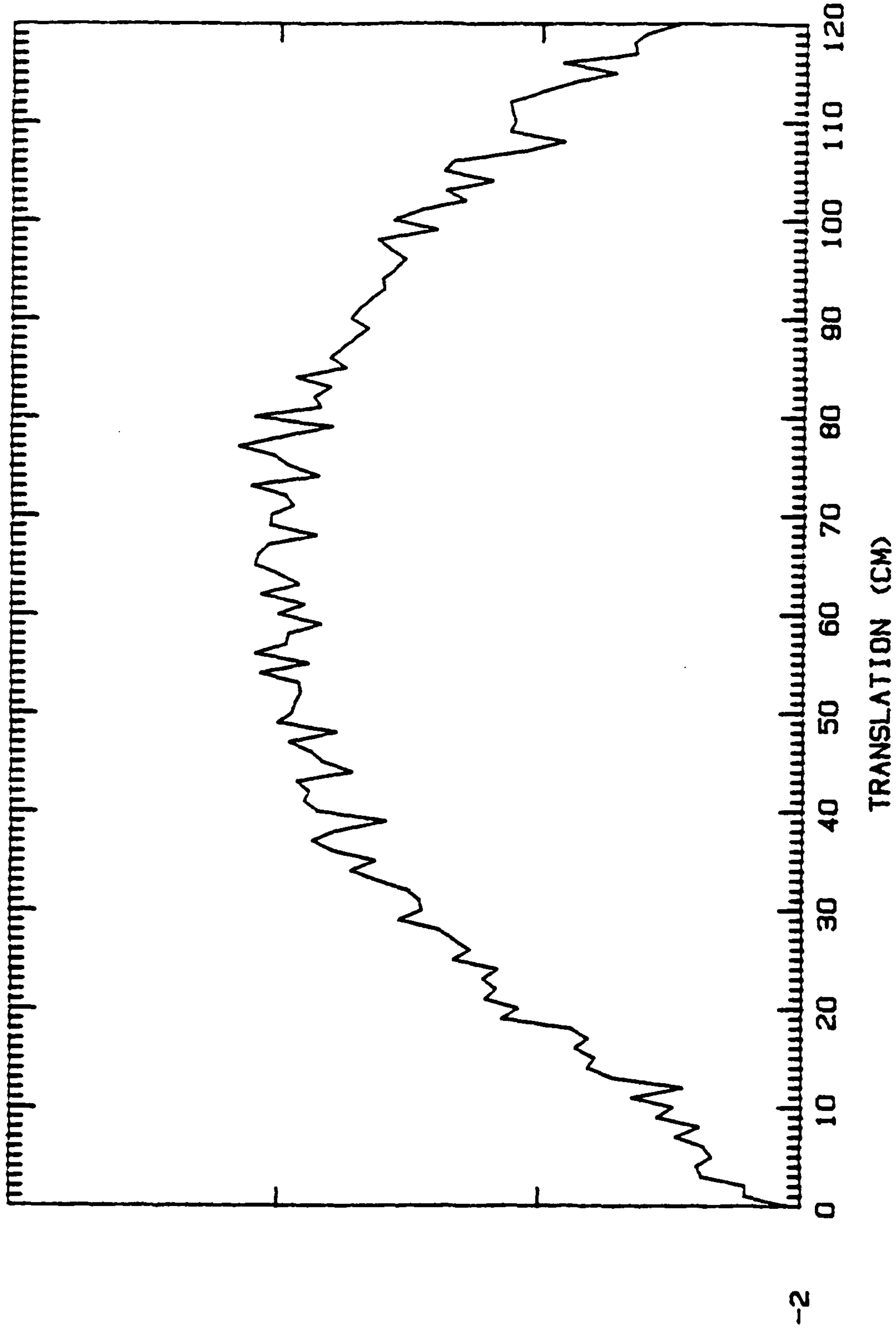


Figure 32. Magnitude, 6 GHz

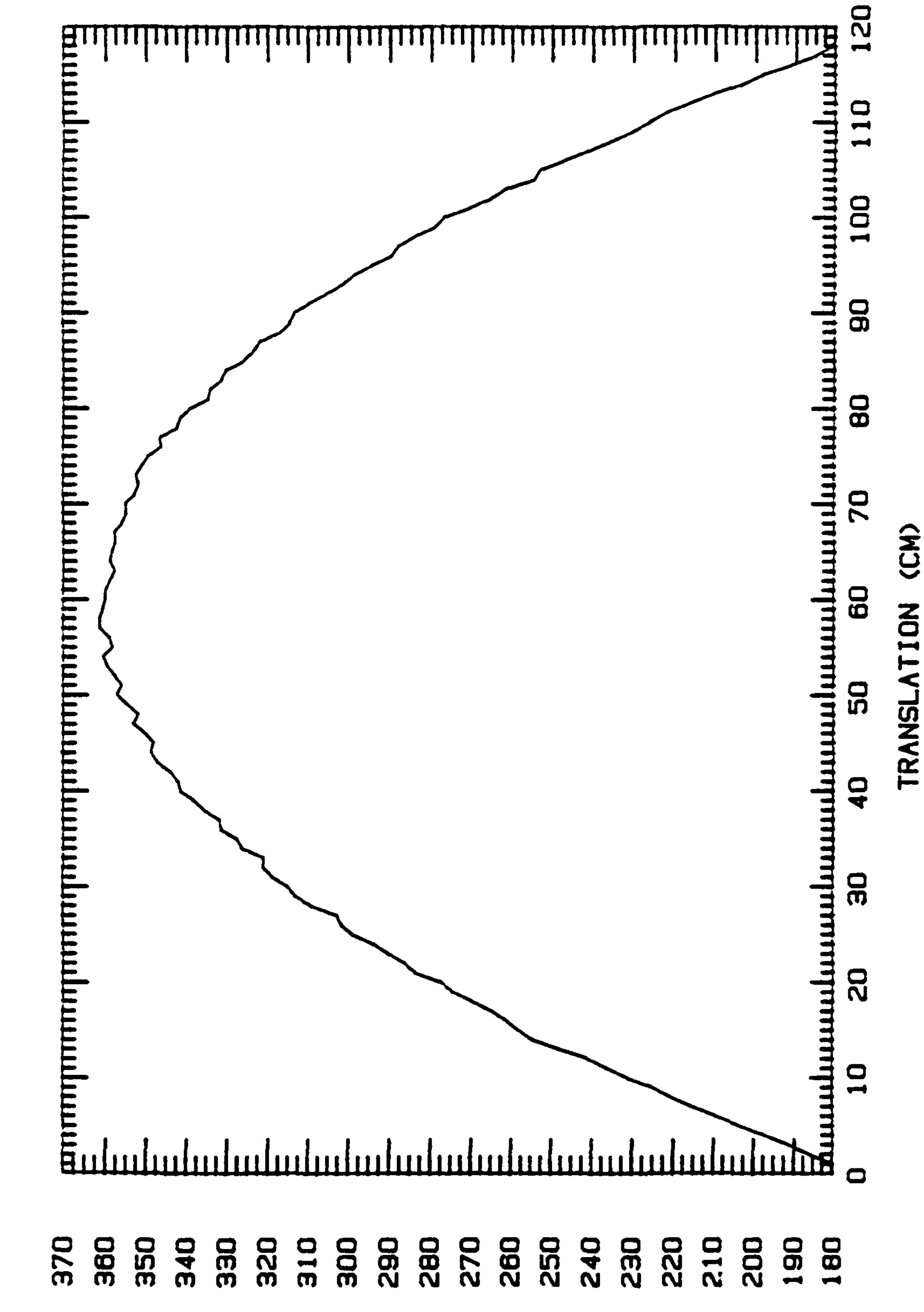


Figure 33. Phase, 6 GHz

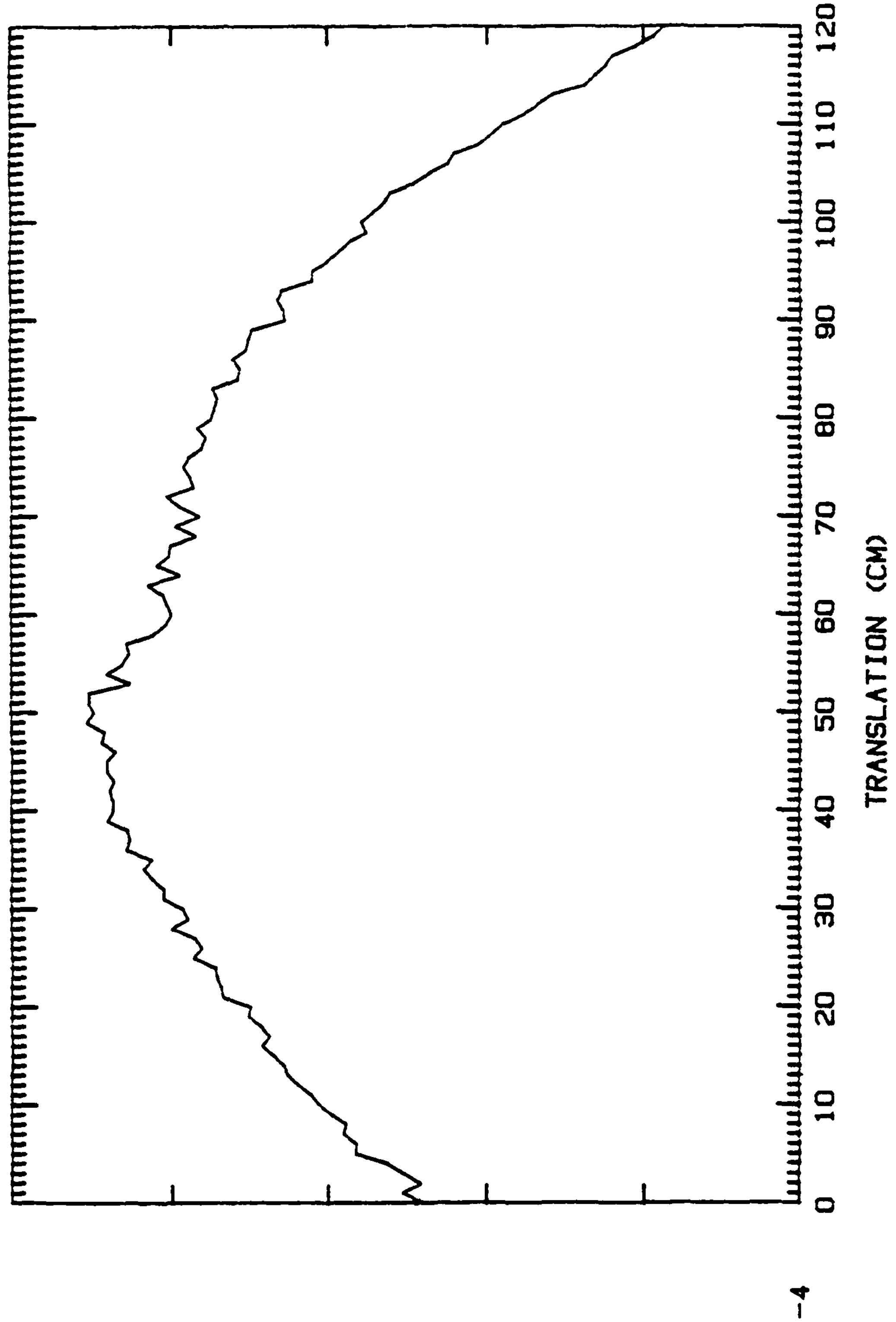


Figure 34. Magnitude, 8 GHz

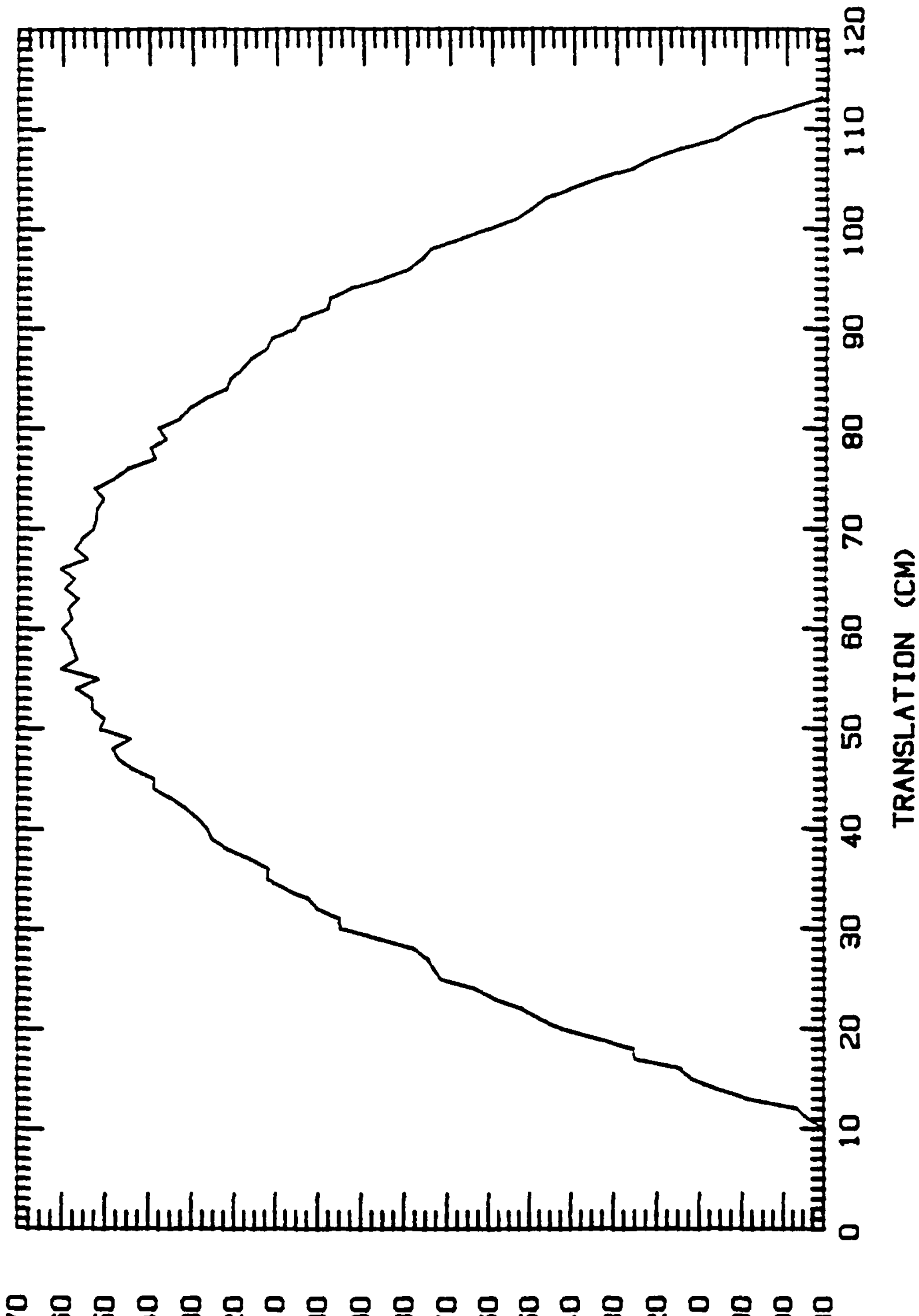


Figure 35. Phase, 8 GHz

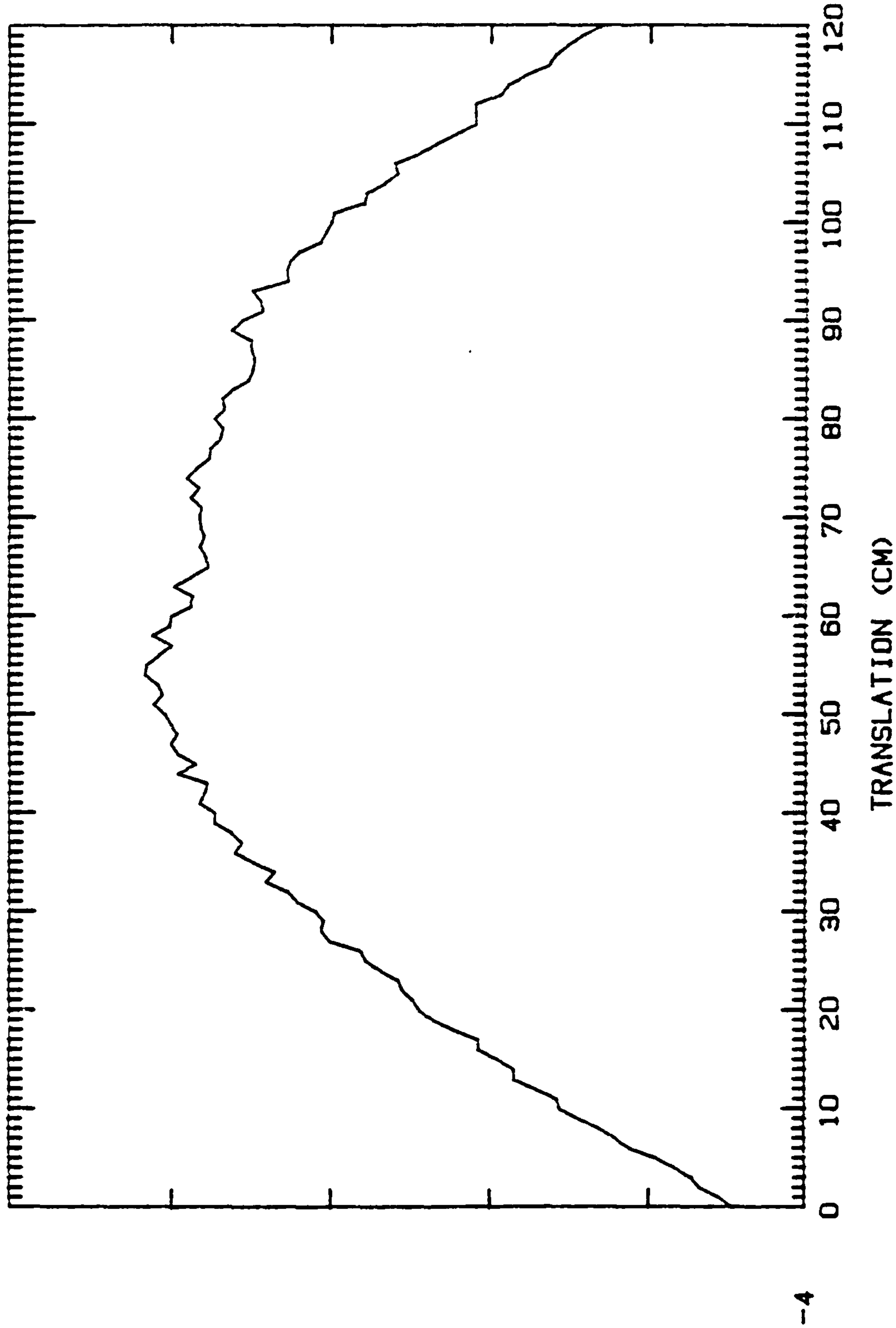


Figure 36. Magnitude, 10 GHz

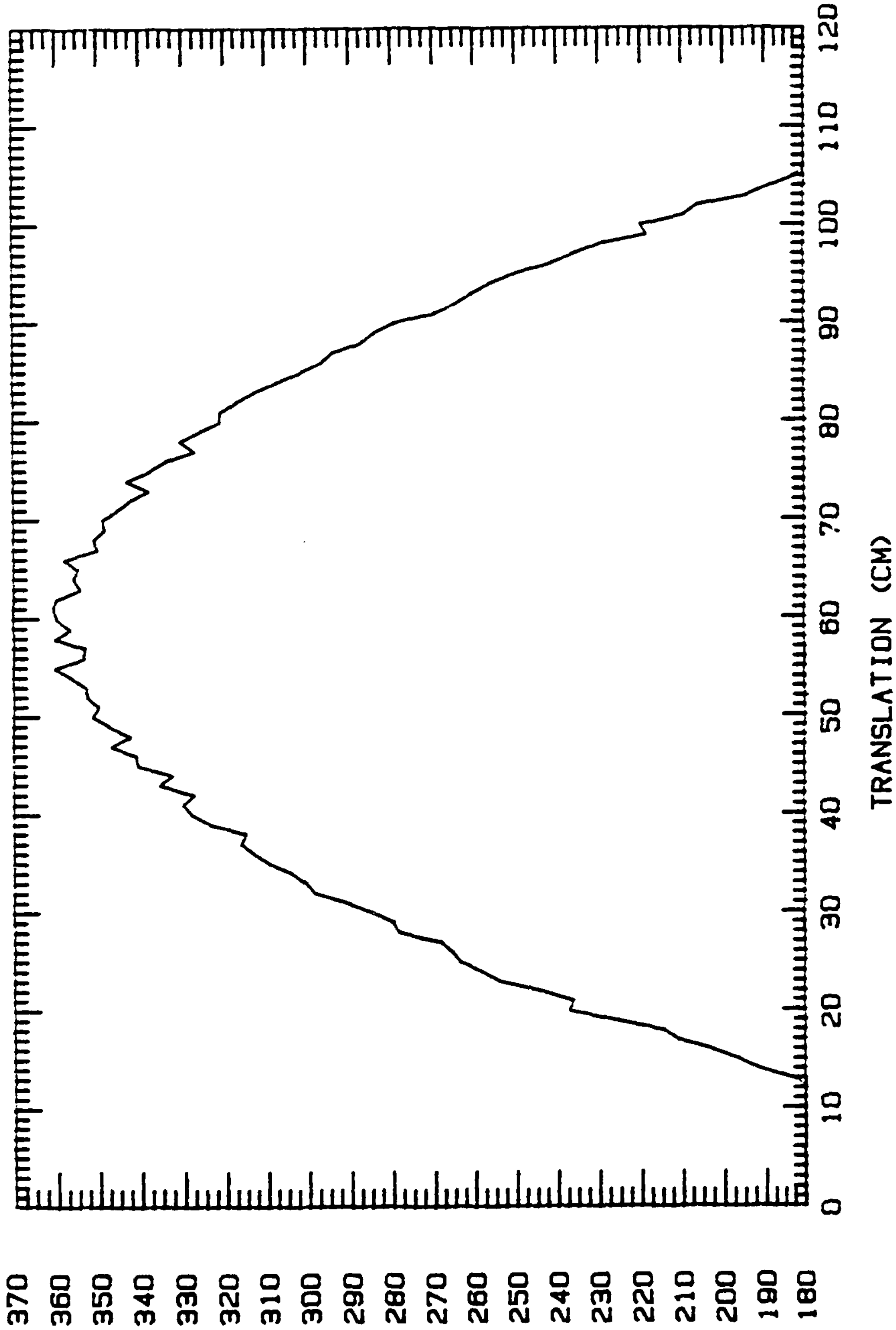


Figure 37. Phase, 10 GHz

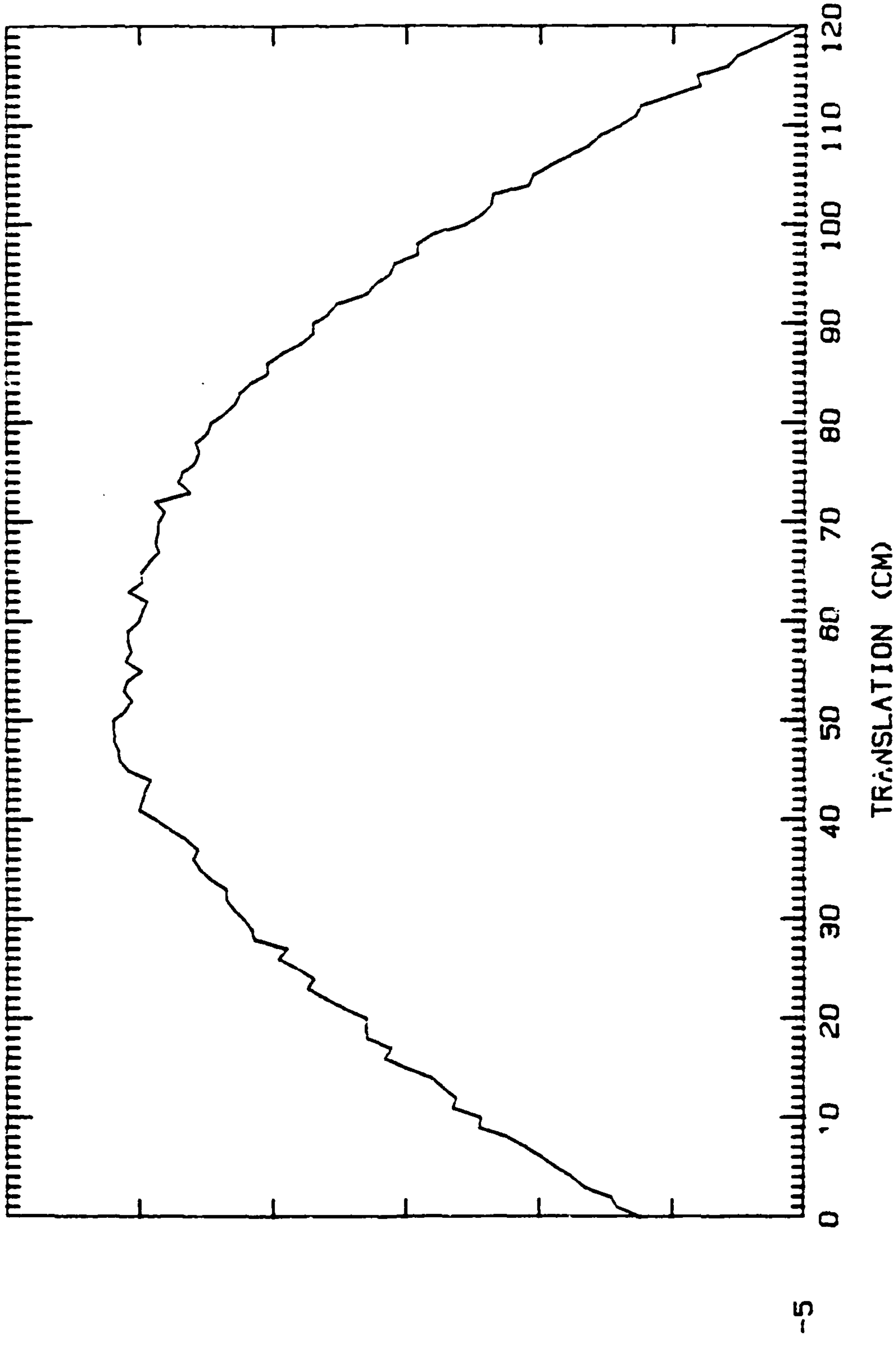


Figure 38. Magnitude, 12 GHz

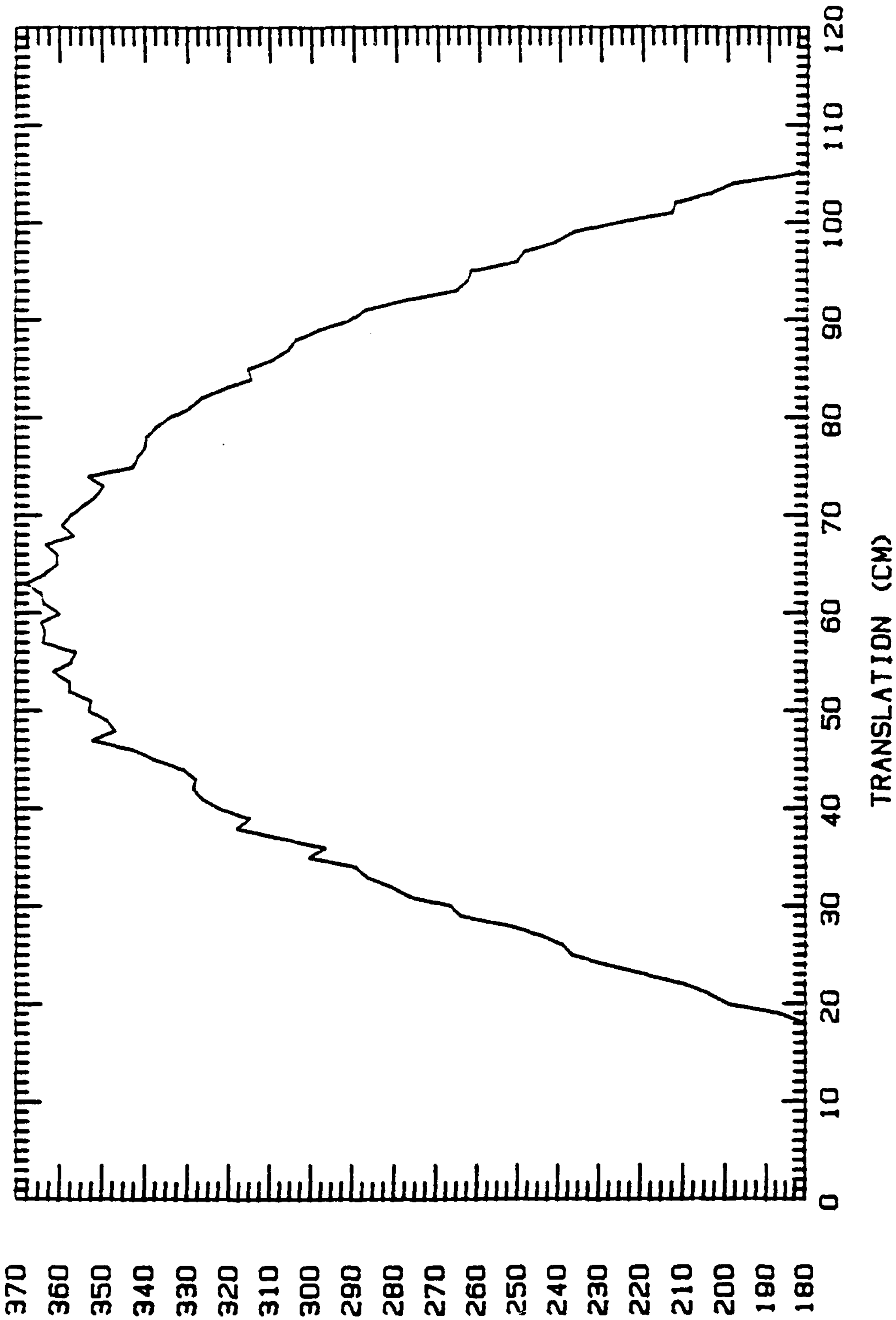


Figure 39. Phase, 12 GHz

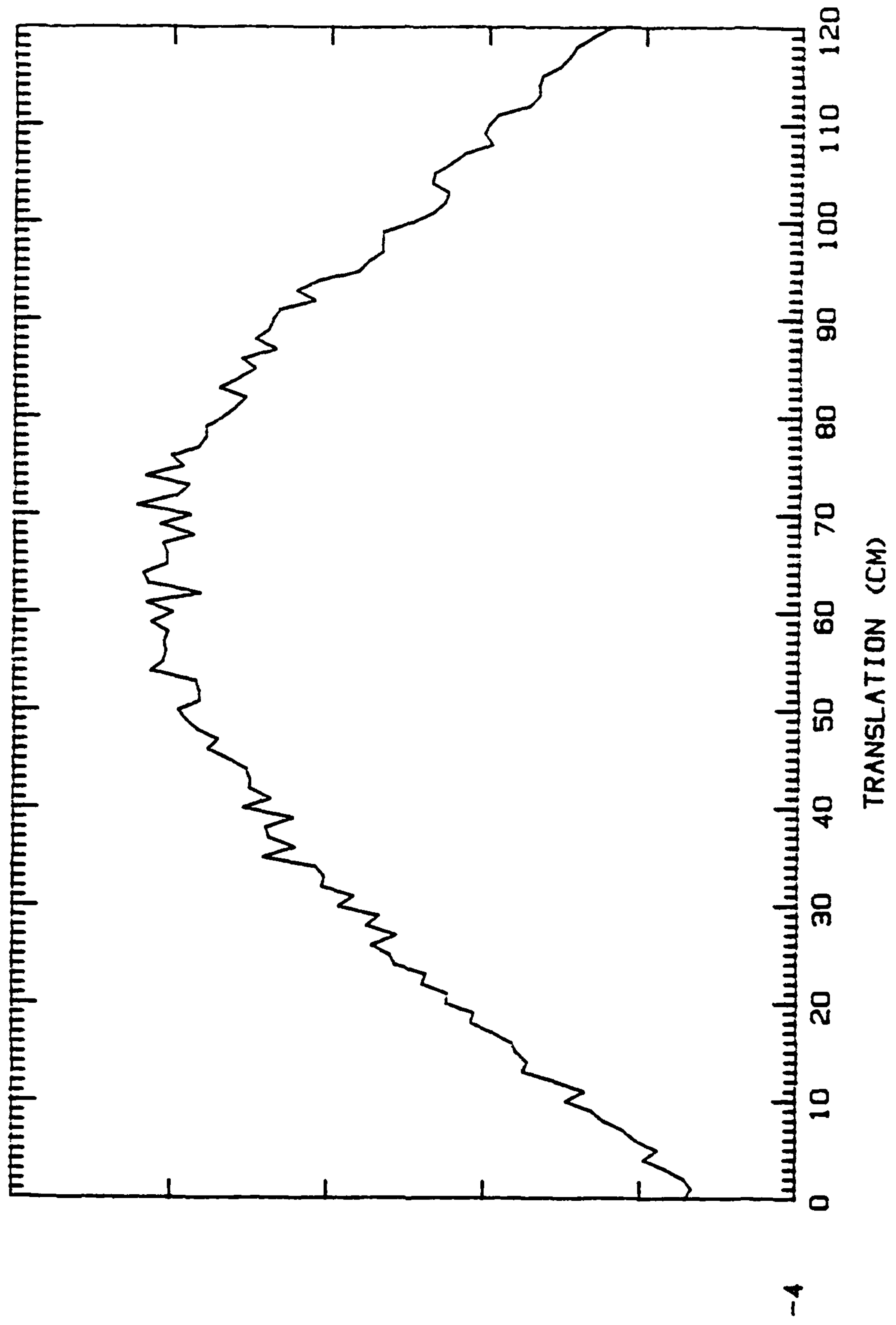


Figure 40. Magnitude, 14 GHz

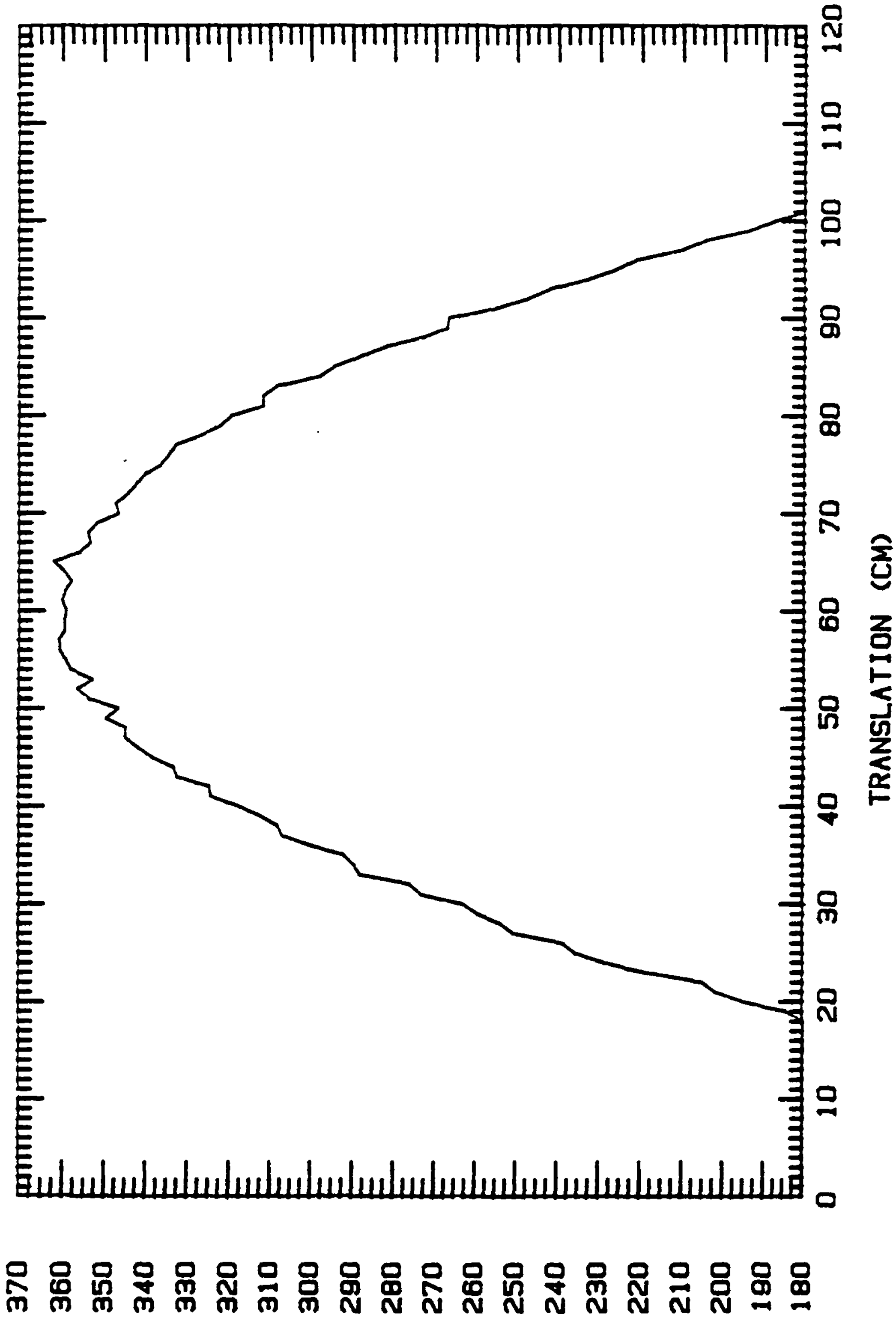


Figure 41. Phase, 14 GHz

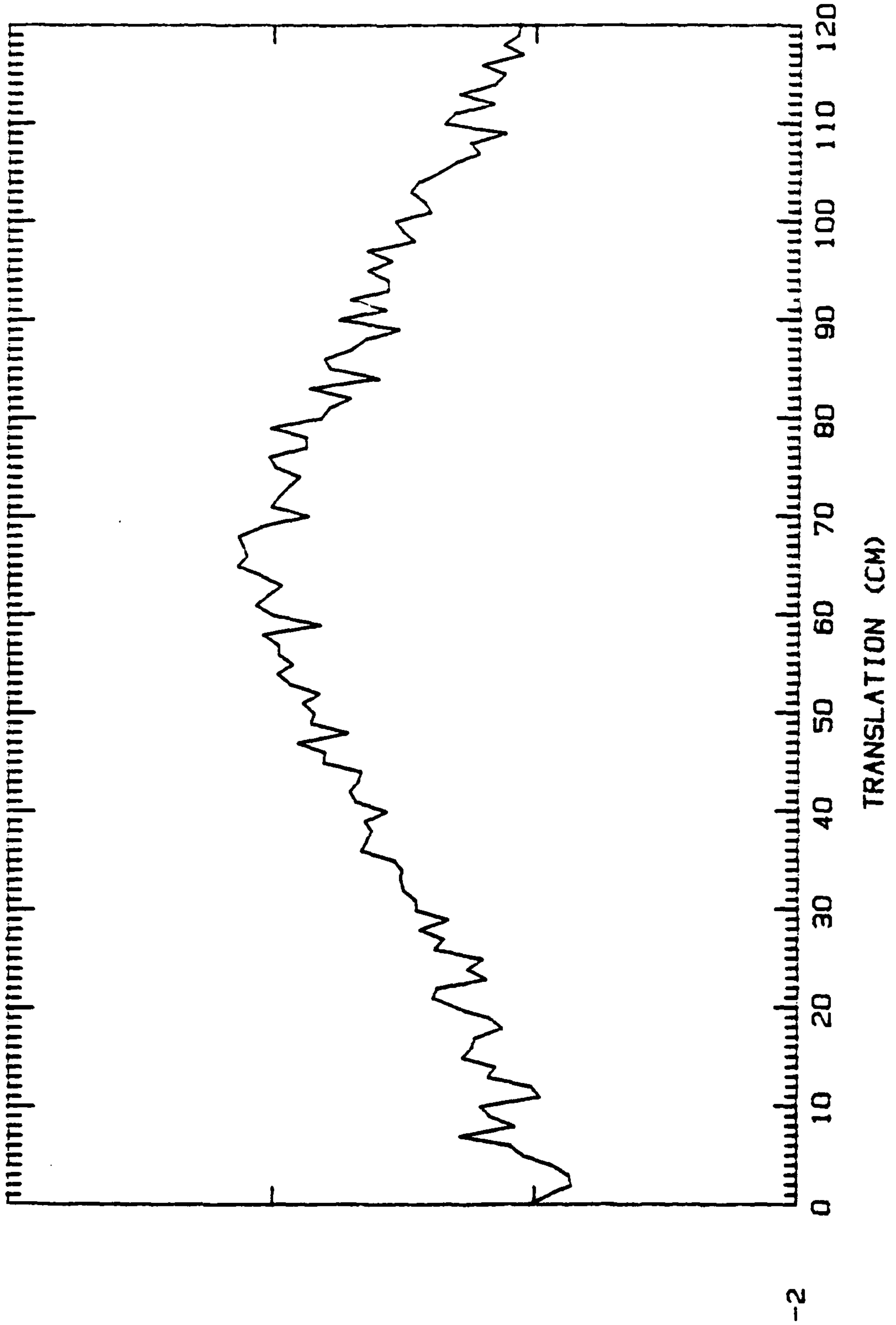


Figure 42. Magnitude, 16 GHz

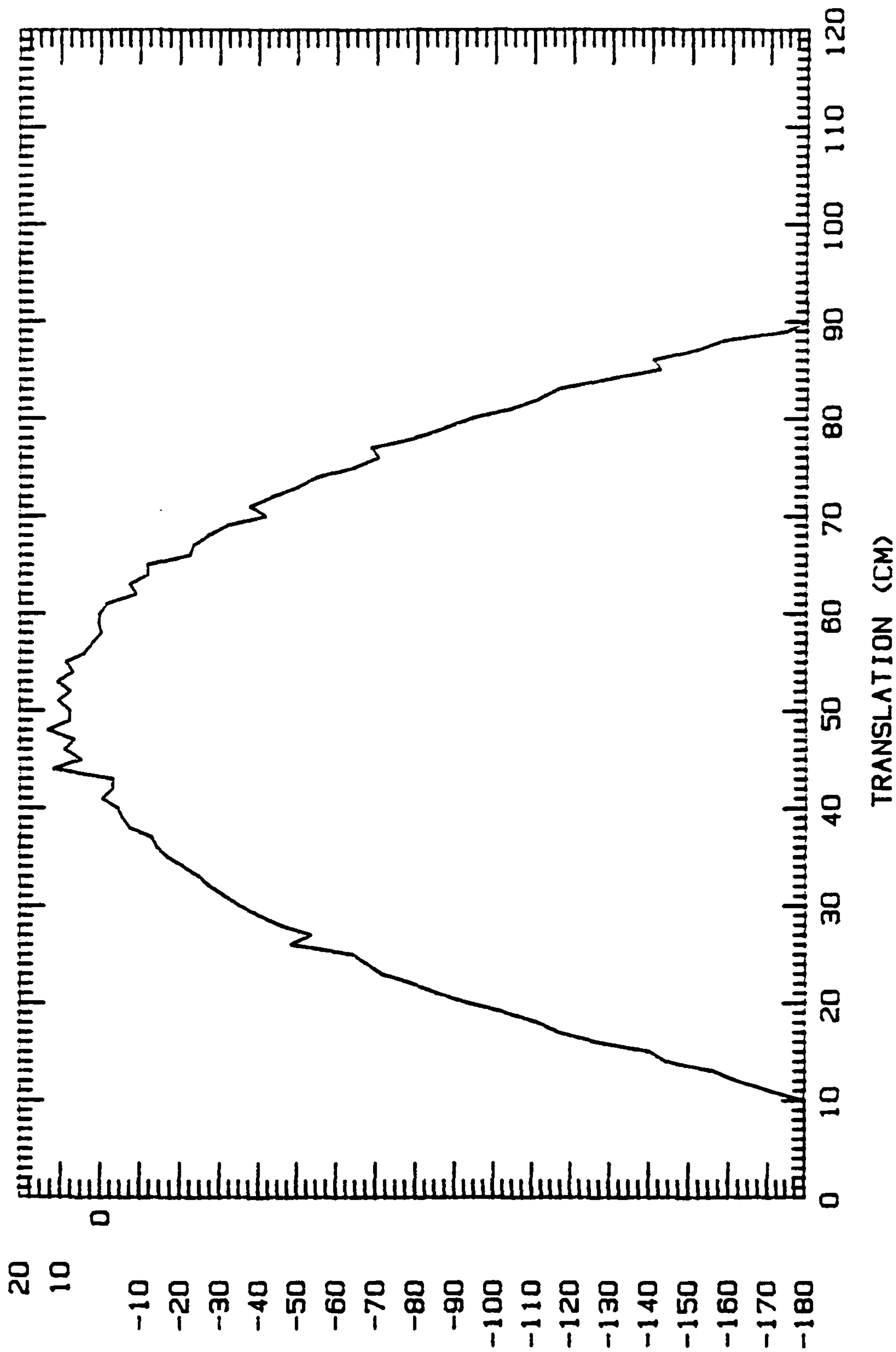


Figure 43. Phase, 16 GHz

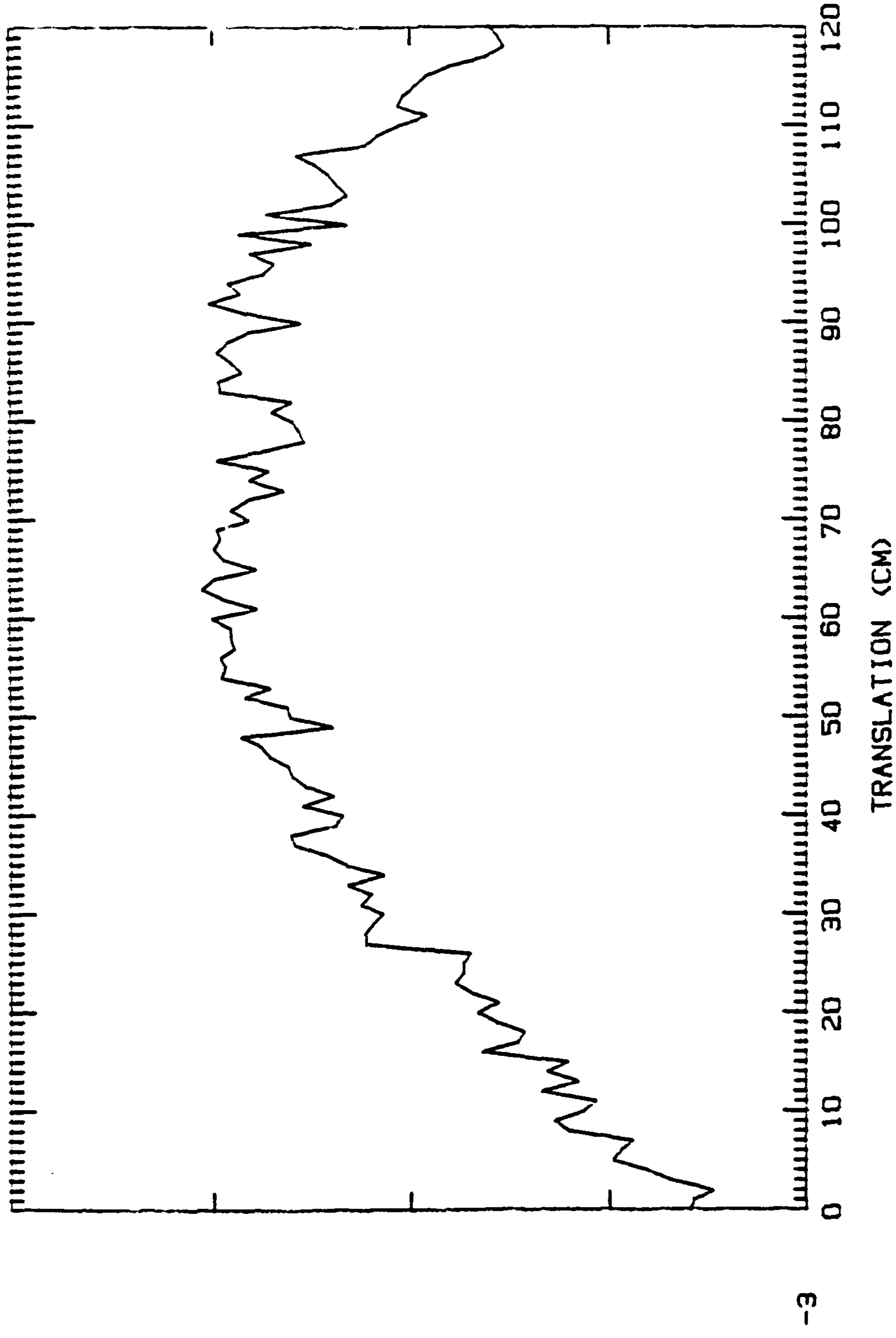


Figure 44. Magnitude, 18 GHz

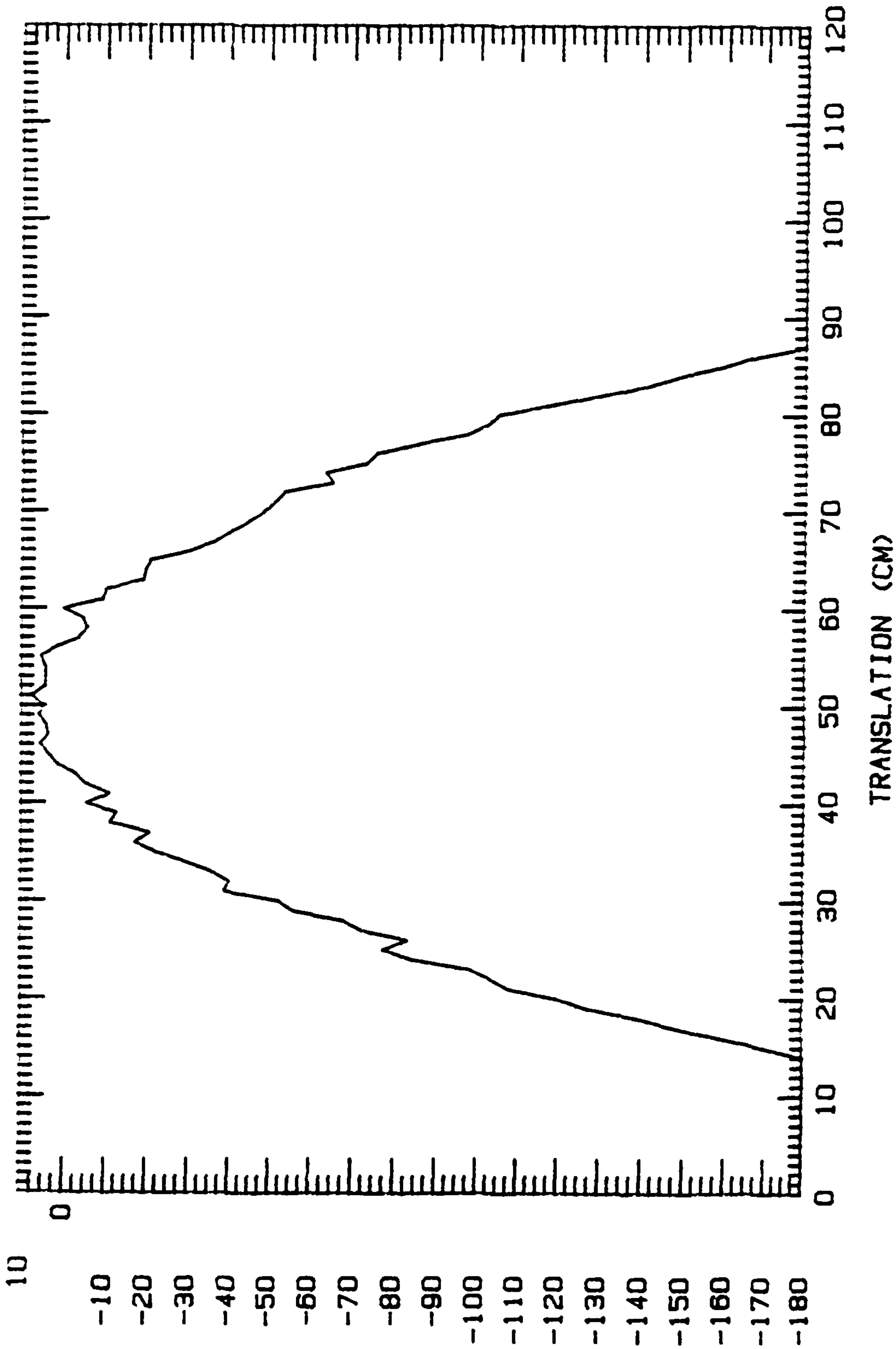


Figure 45. Phase, 18 GHz

*Horizontal Translation, Horizontal Polarization*

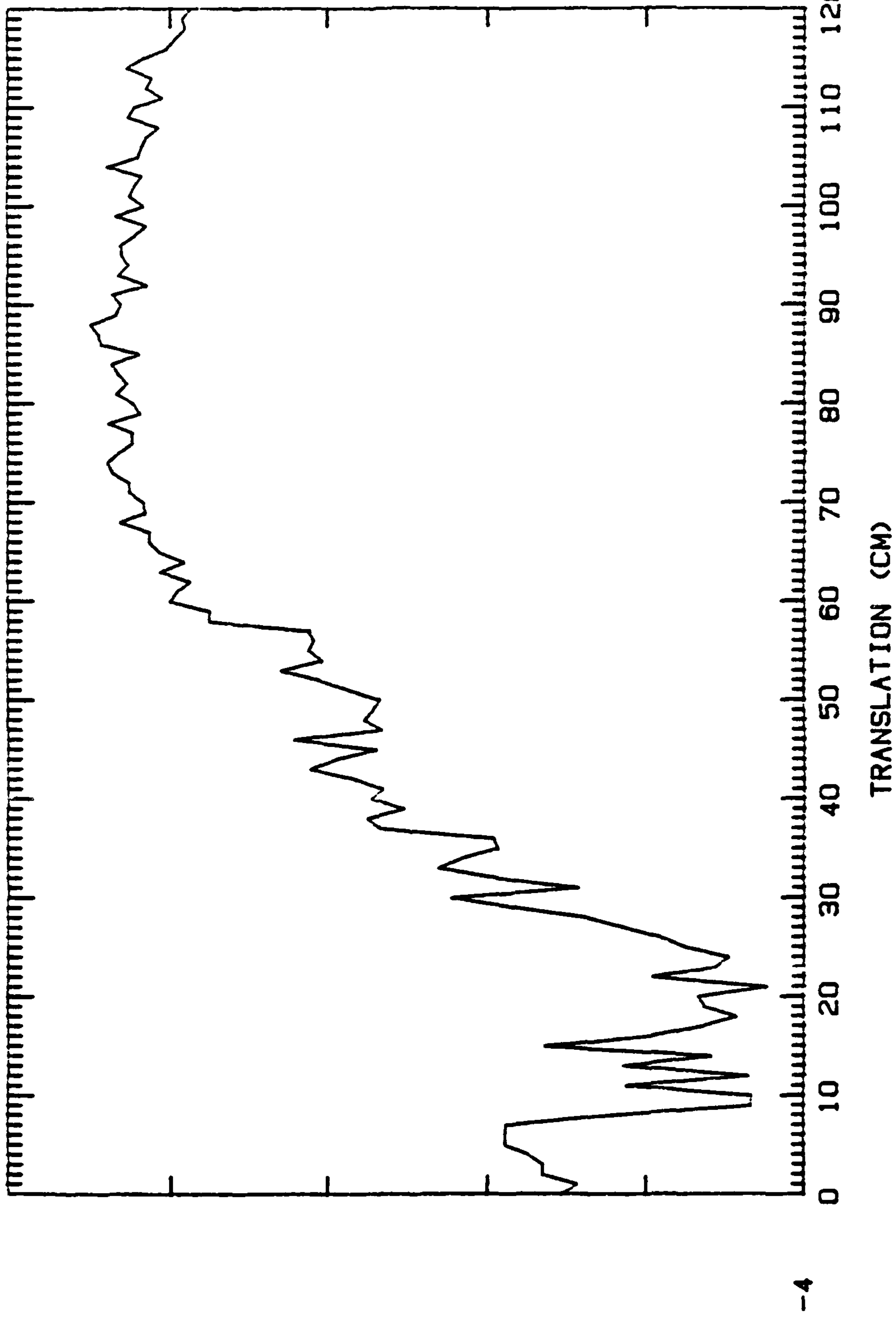


Figure 46. Magnitude, 6 GHz

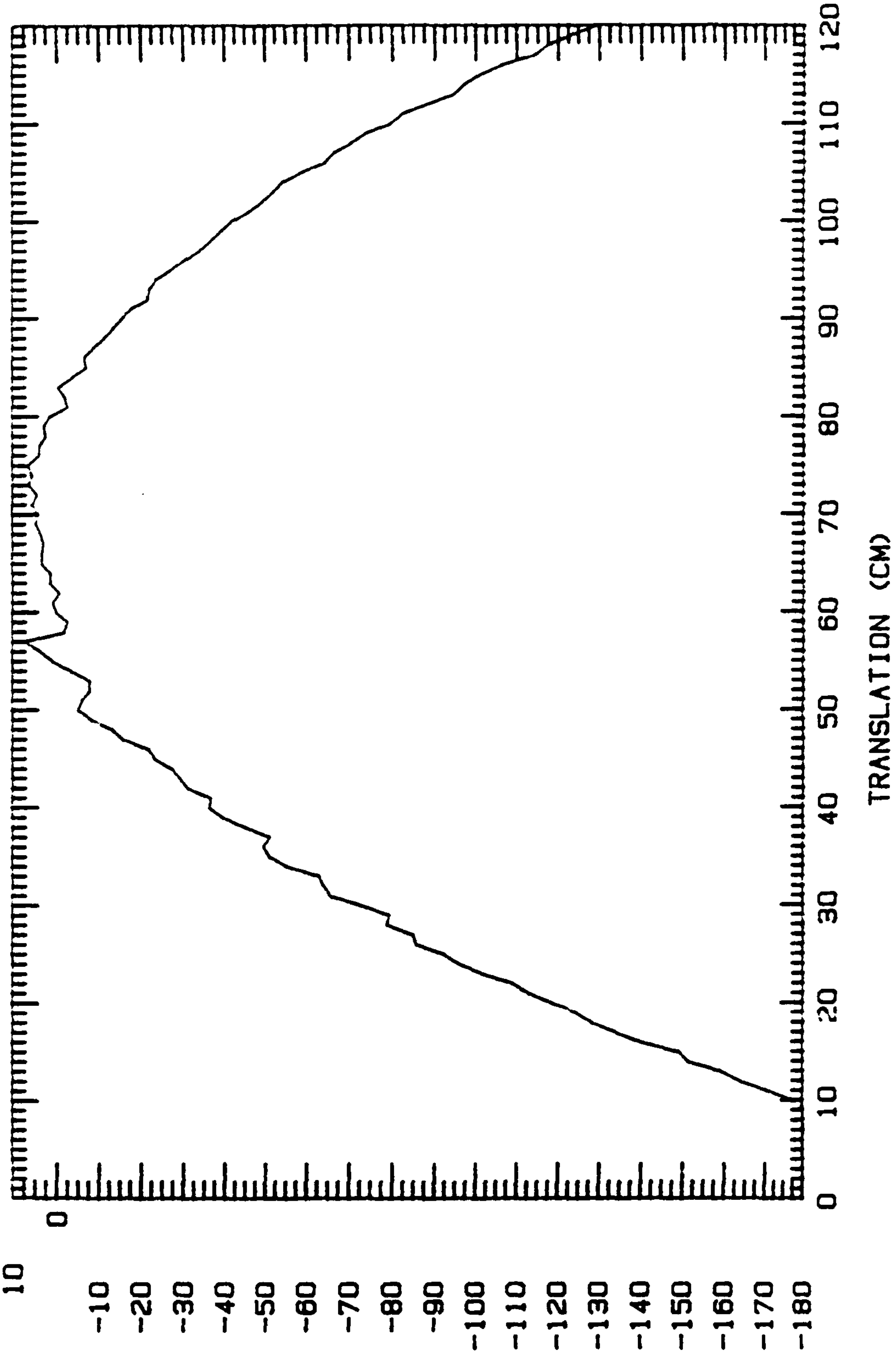


Figure 47. Phase, 6 GHz

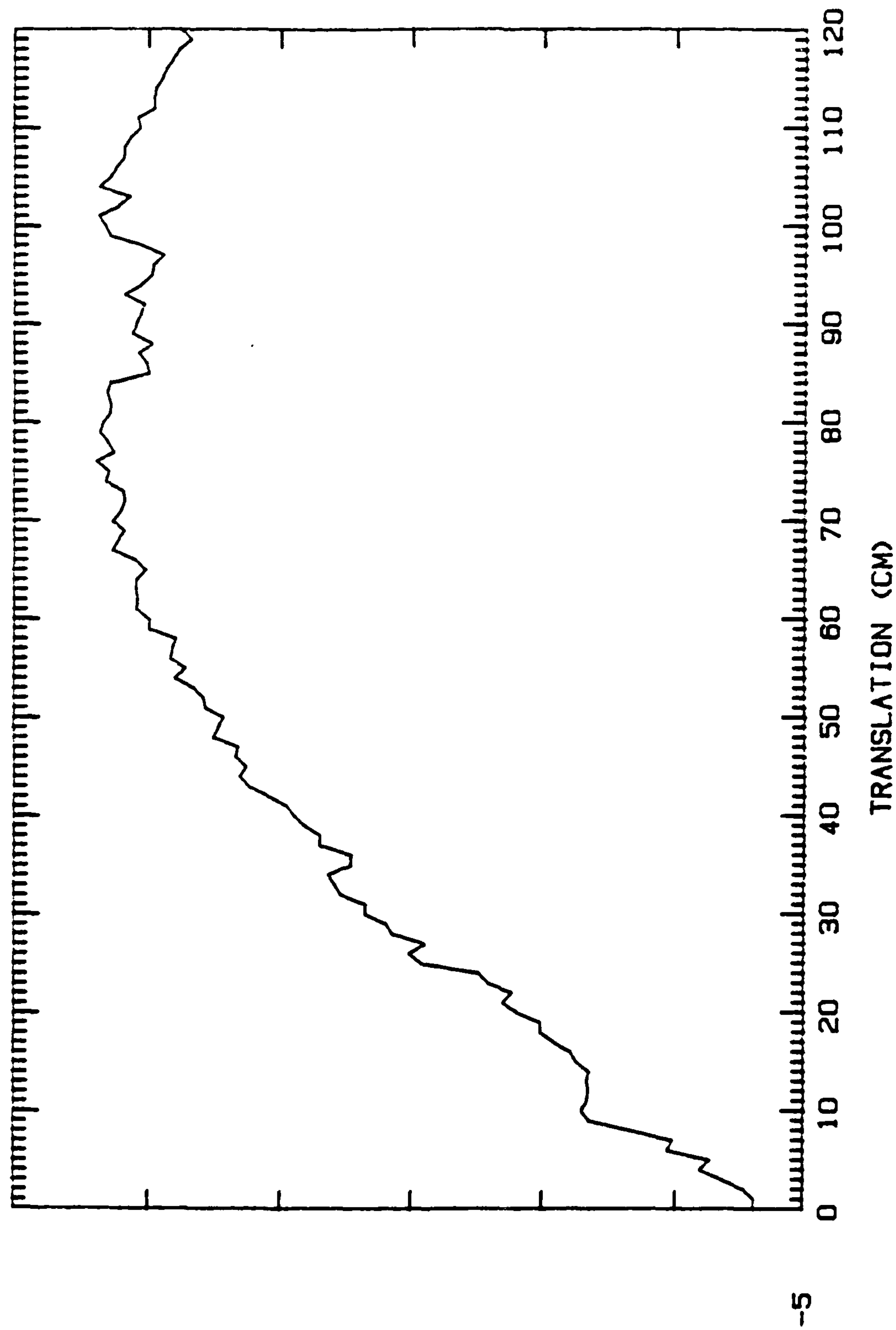


Figure 48. Magnitude, 8 GHz

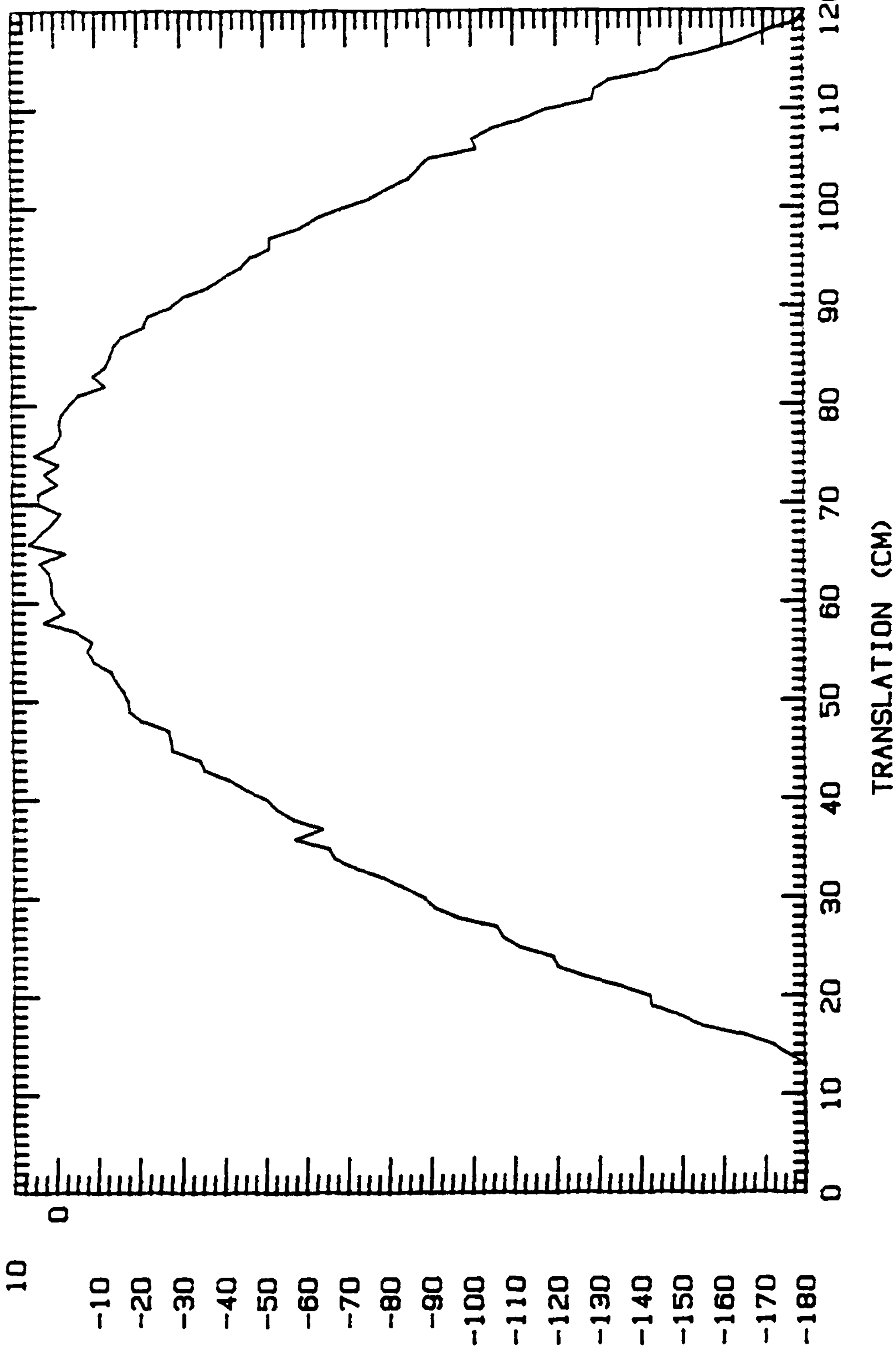


Figure 49. Phase, 8 GHz

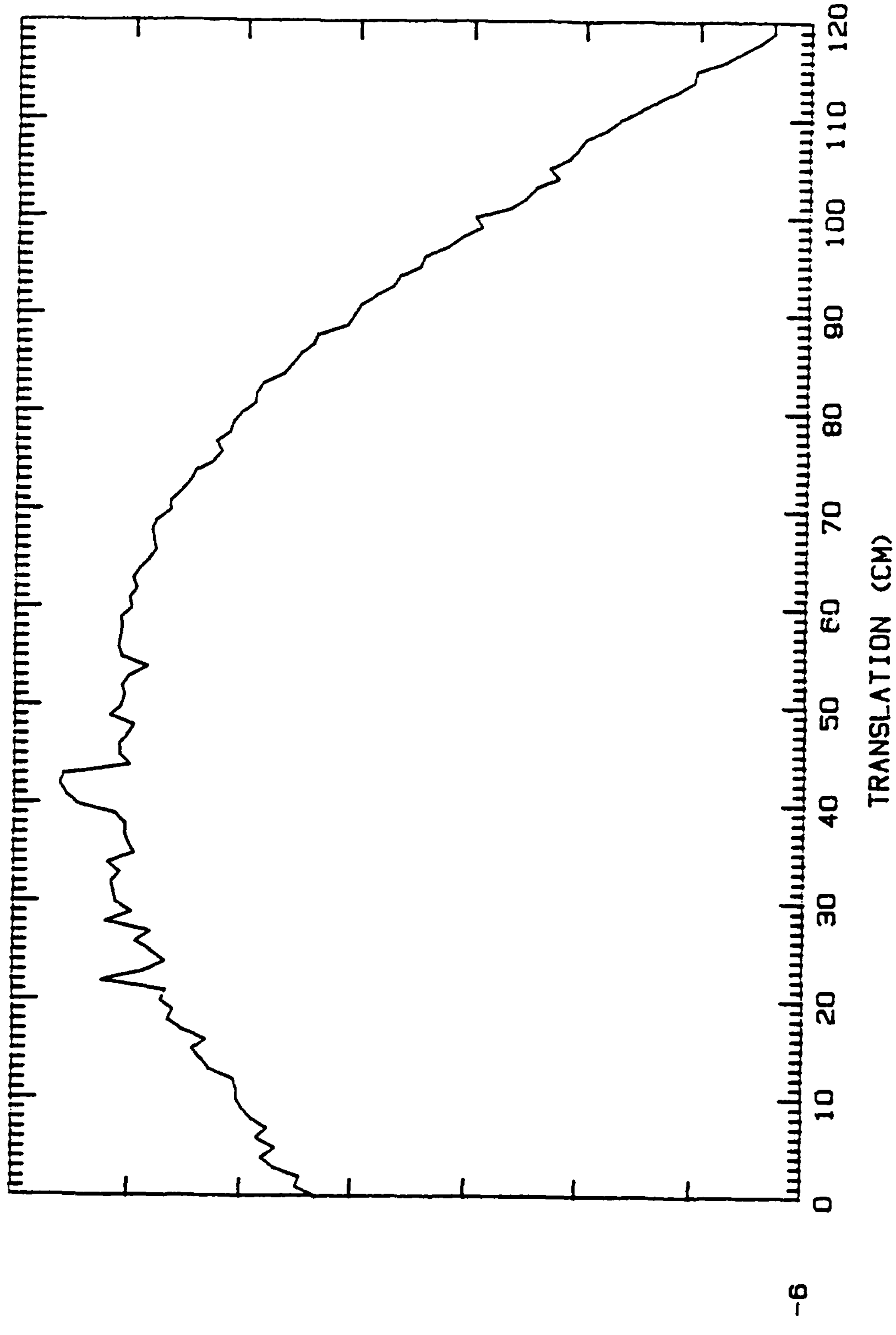


Figure 50. Magnitude, 10 GHz, Antenna 1 Transmitting

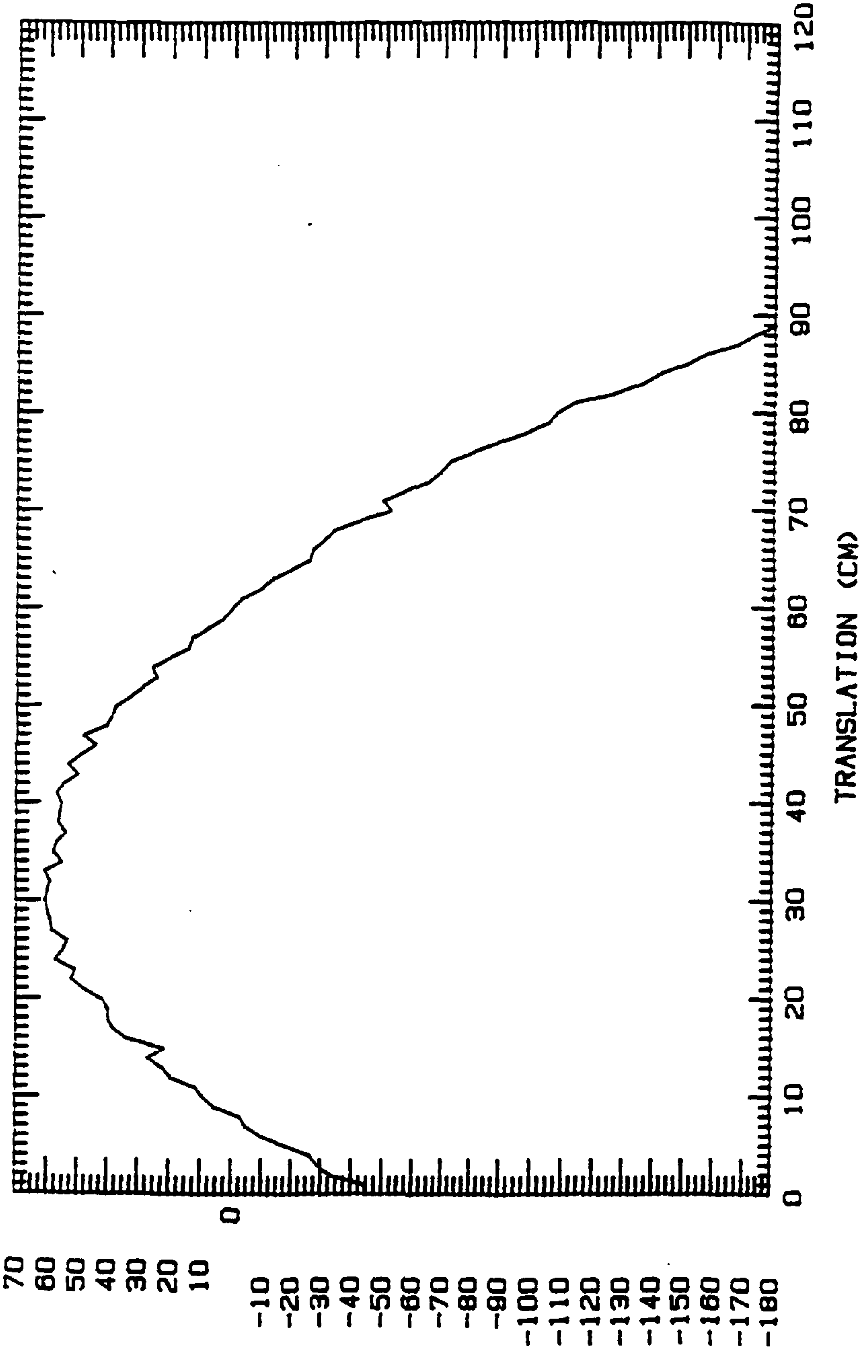


Figure 51. Phase, 10 GHz, Antenna 1 Transmitting

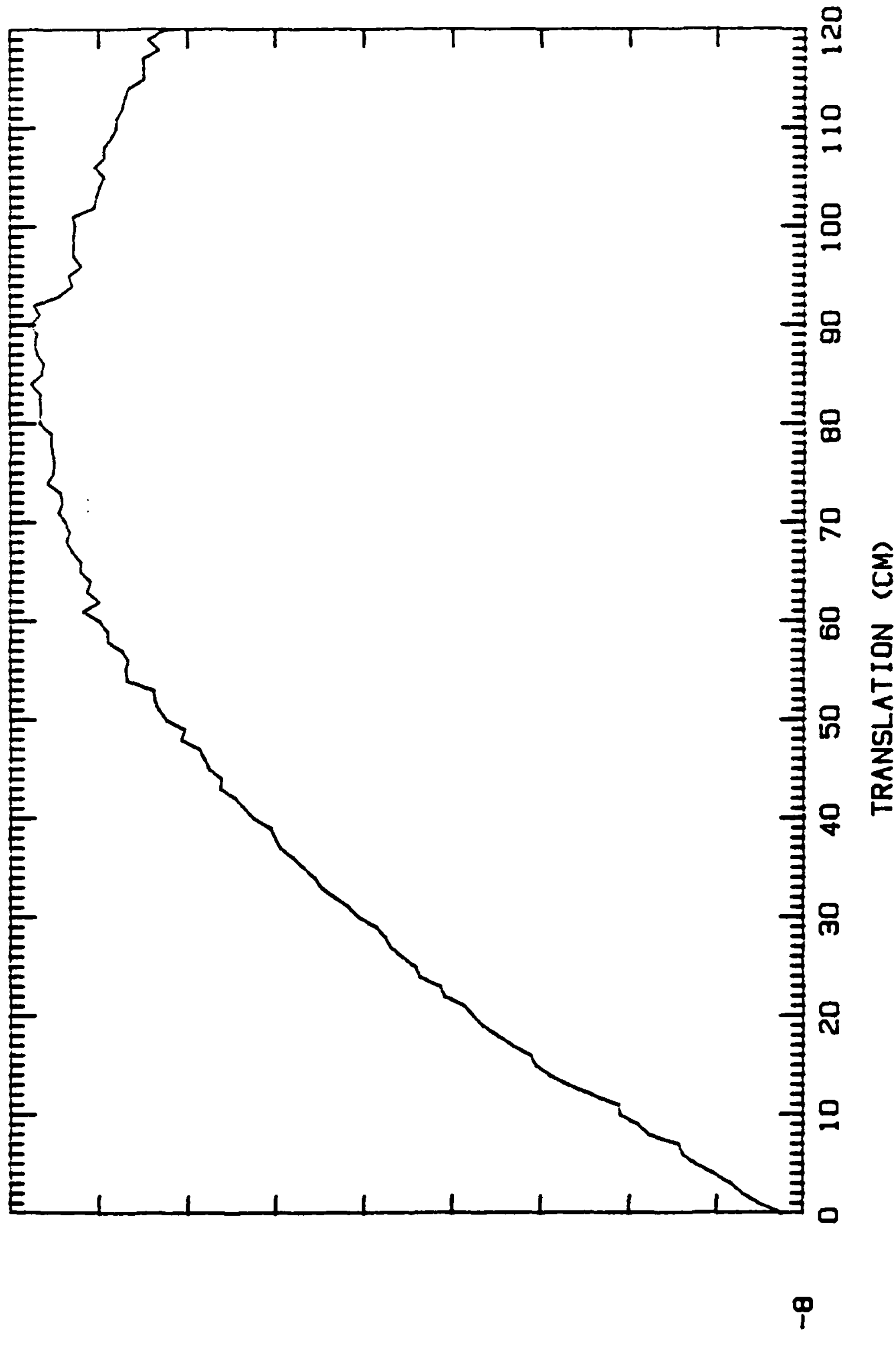


Figure 52. Magnitude, 10 GHz, Antenna 2 Transmitting

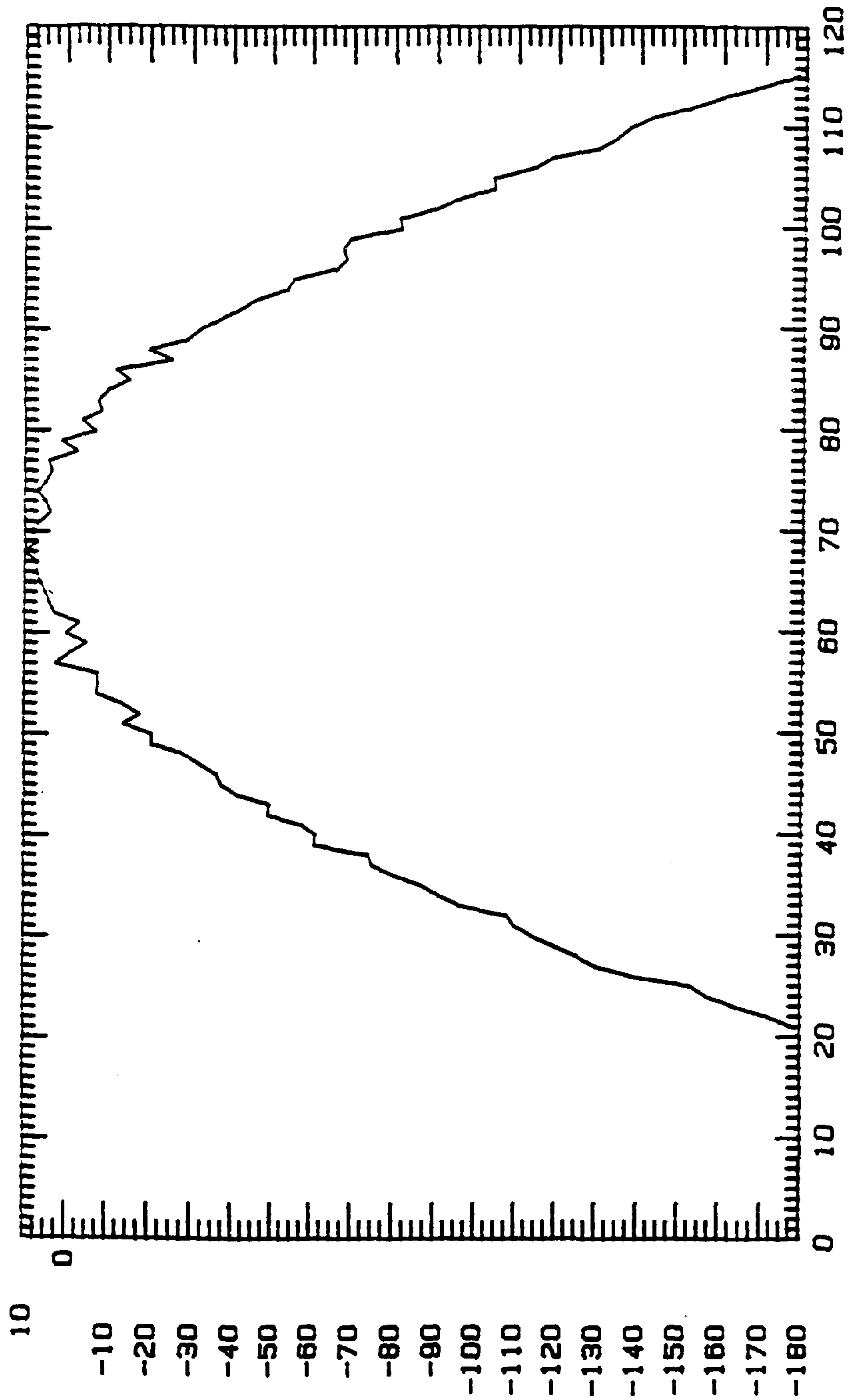


Figure 53. Phase, 10 GHz, Antenna 2 Transmitting

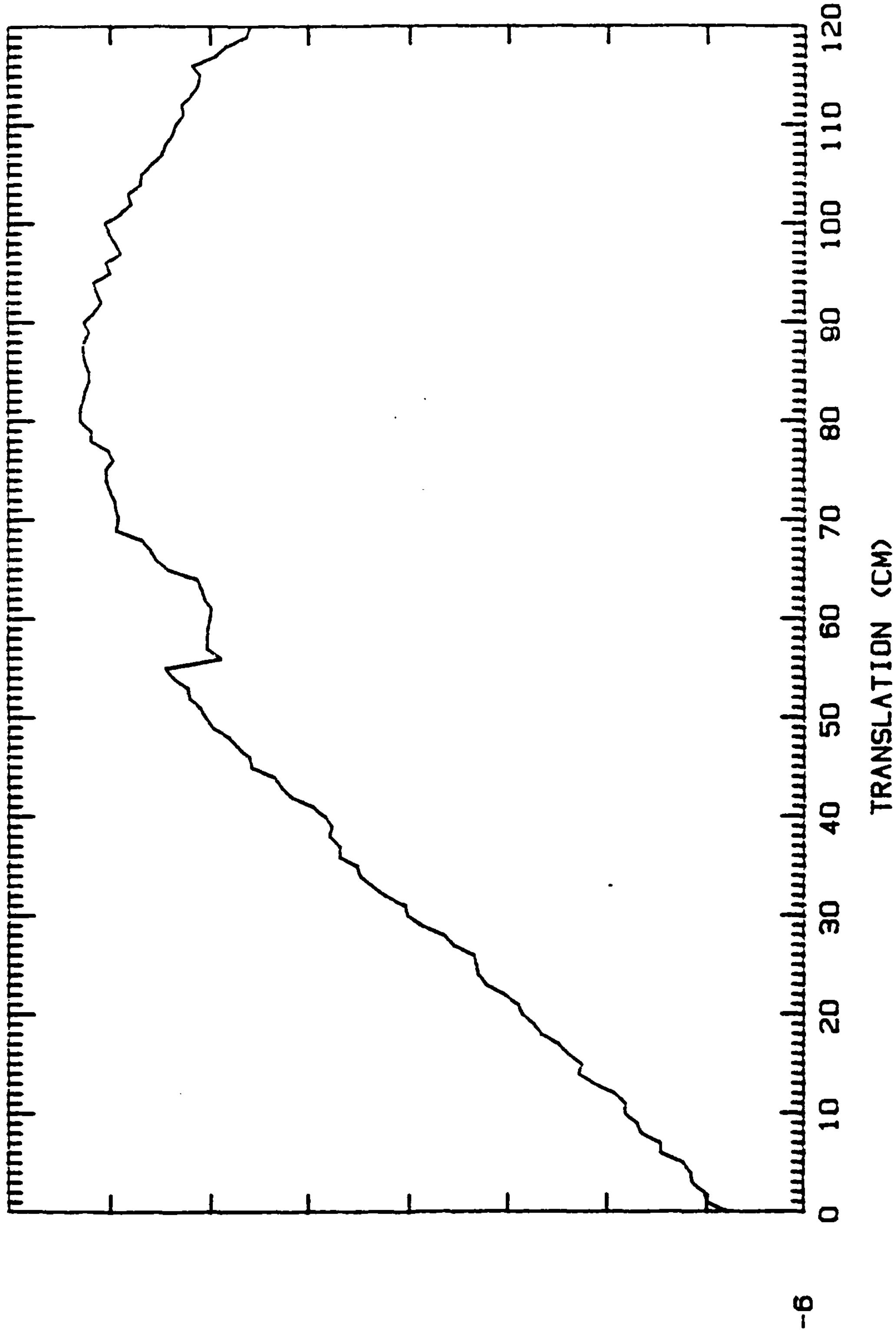


Figure 54. Magnitude, 12 GHz

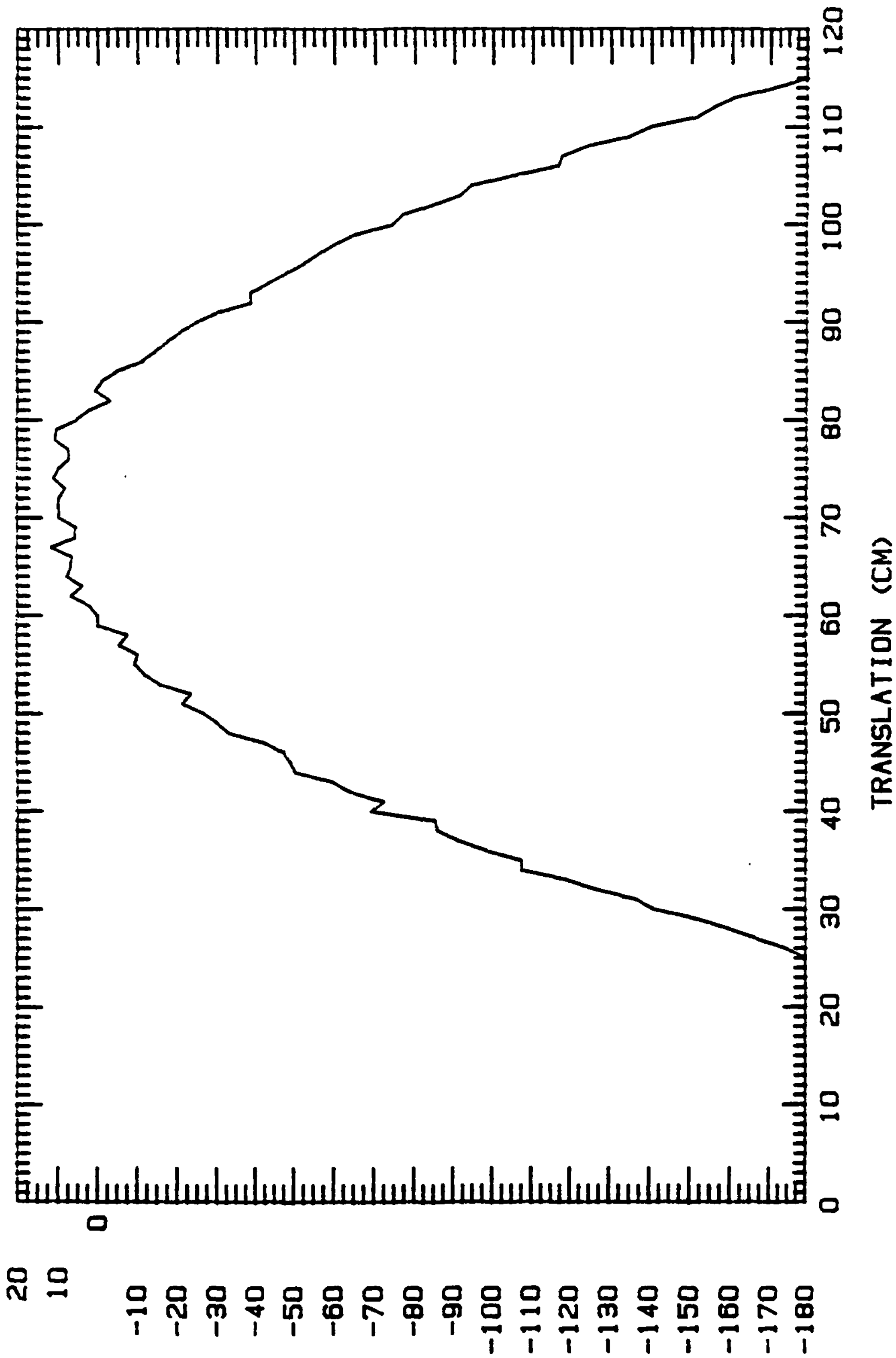


Figure 55. Phase, 12 GHz

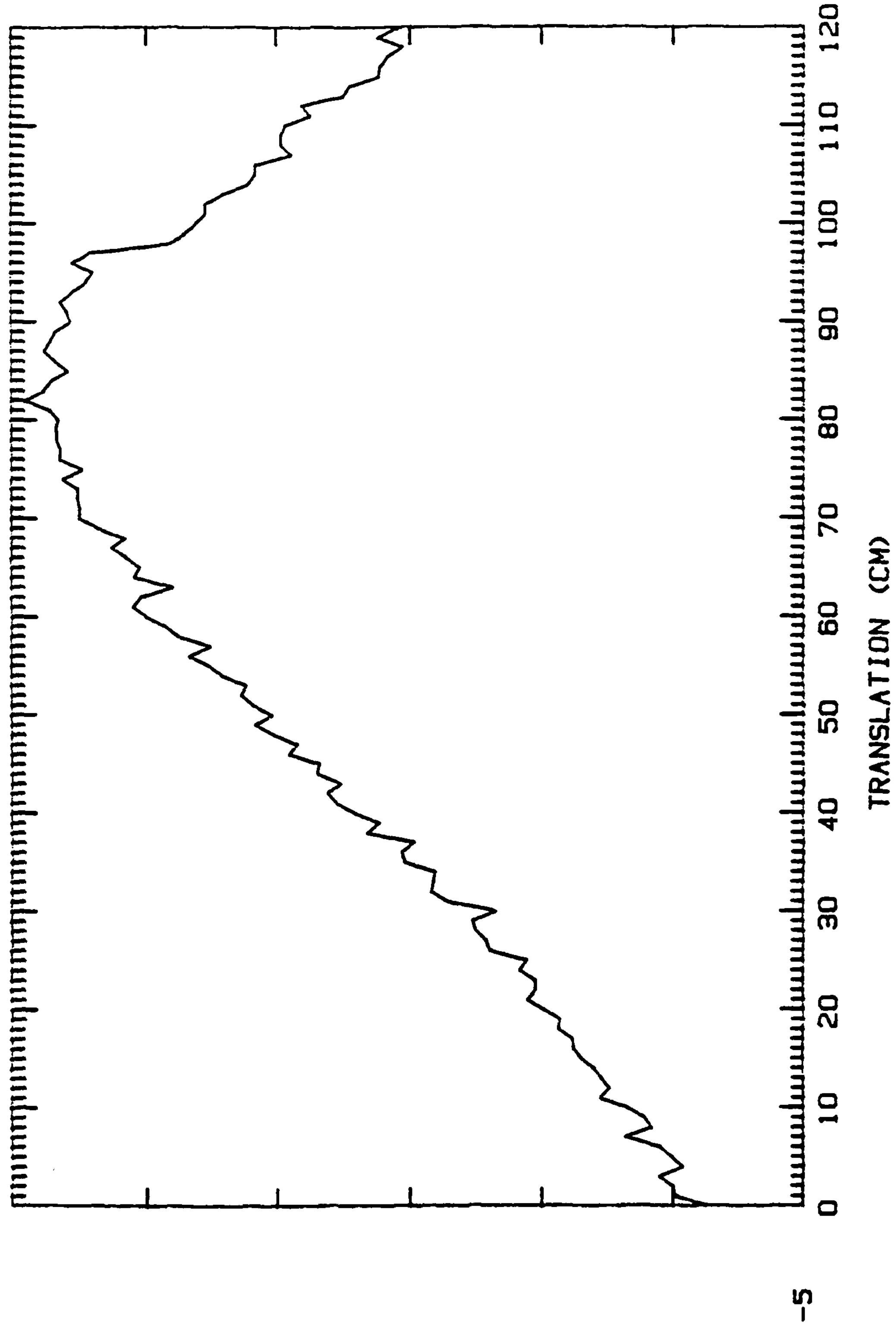


Figure 56. Magnitude, 14 GHz

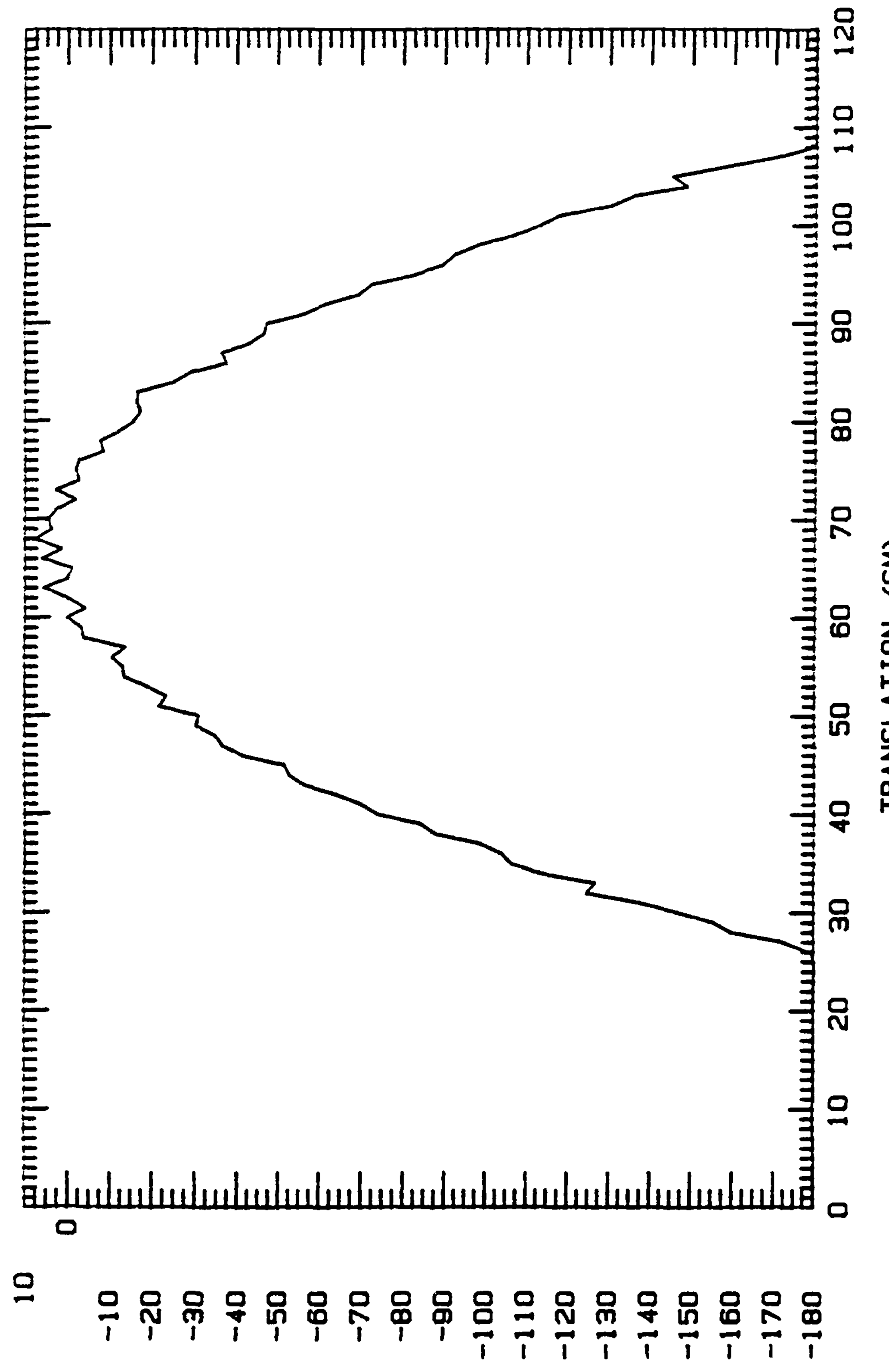


Figure 57. Phase, 14 GHz

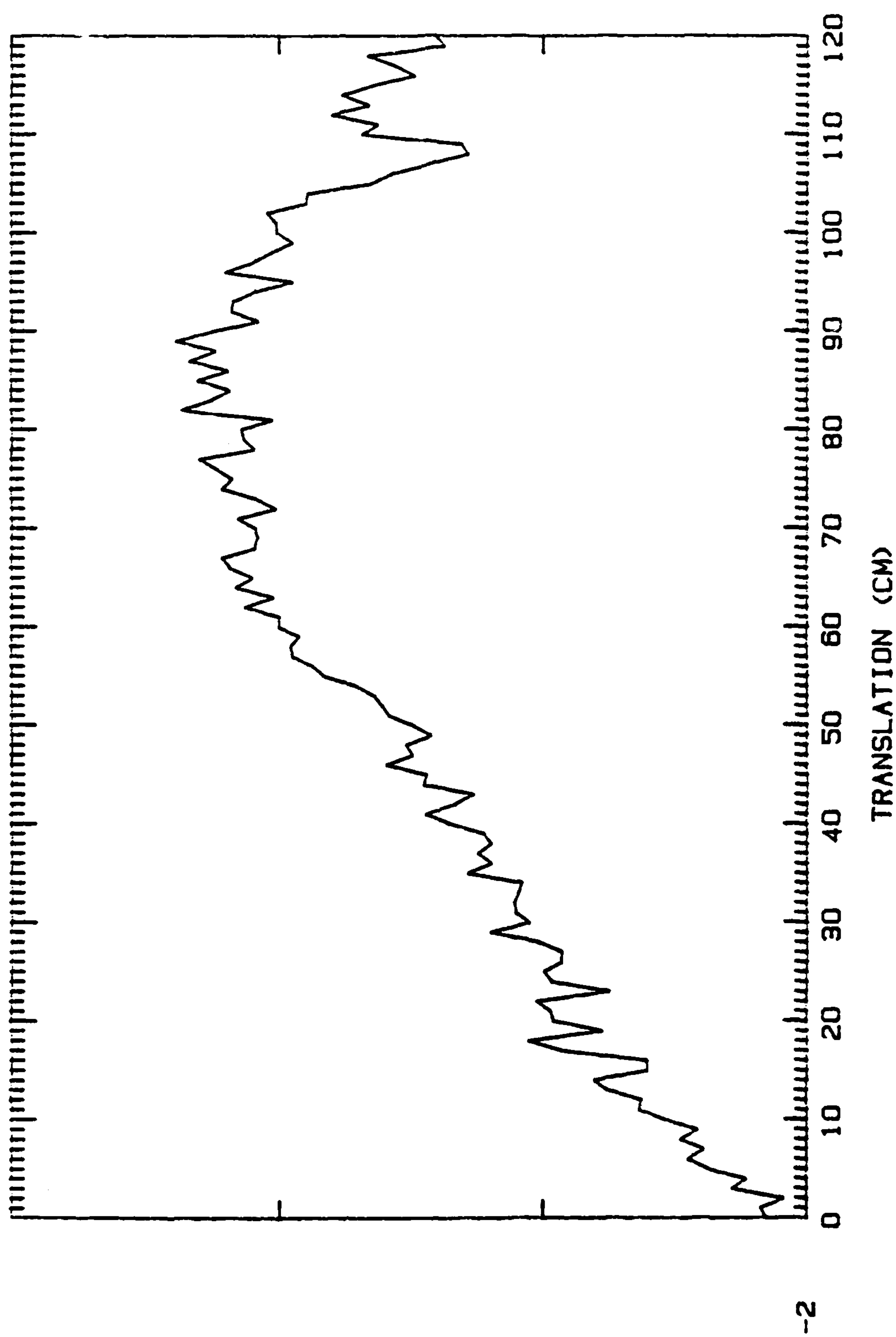


Figure 58. Magnitude, 16 GHz

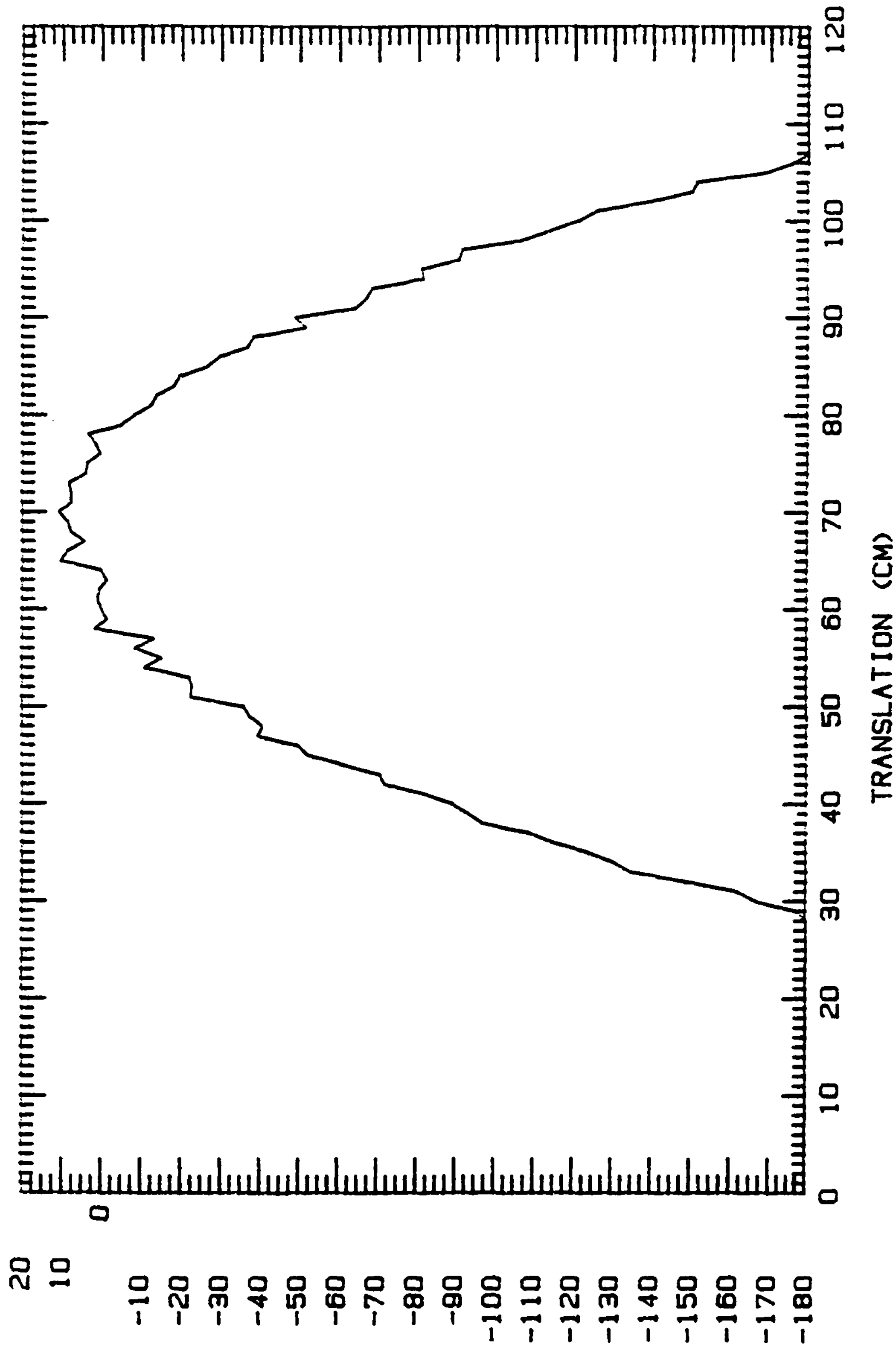


Figure 59. Phase, 16 GHz

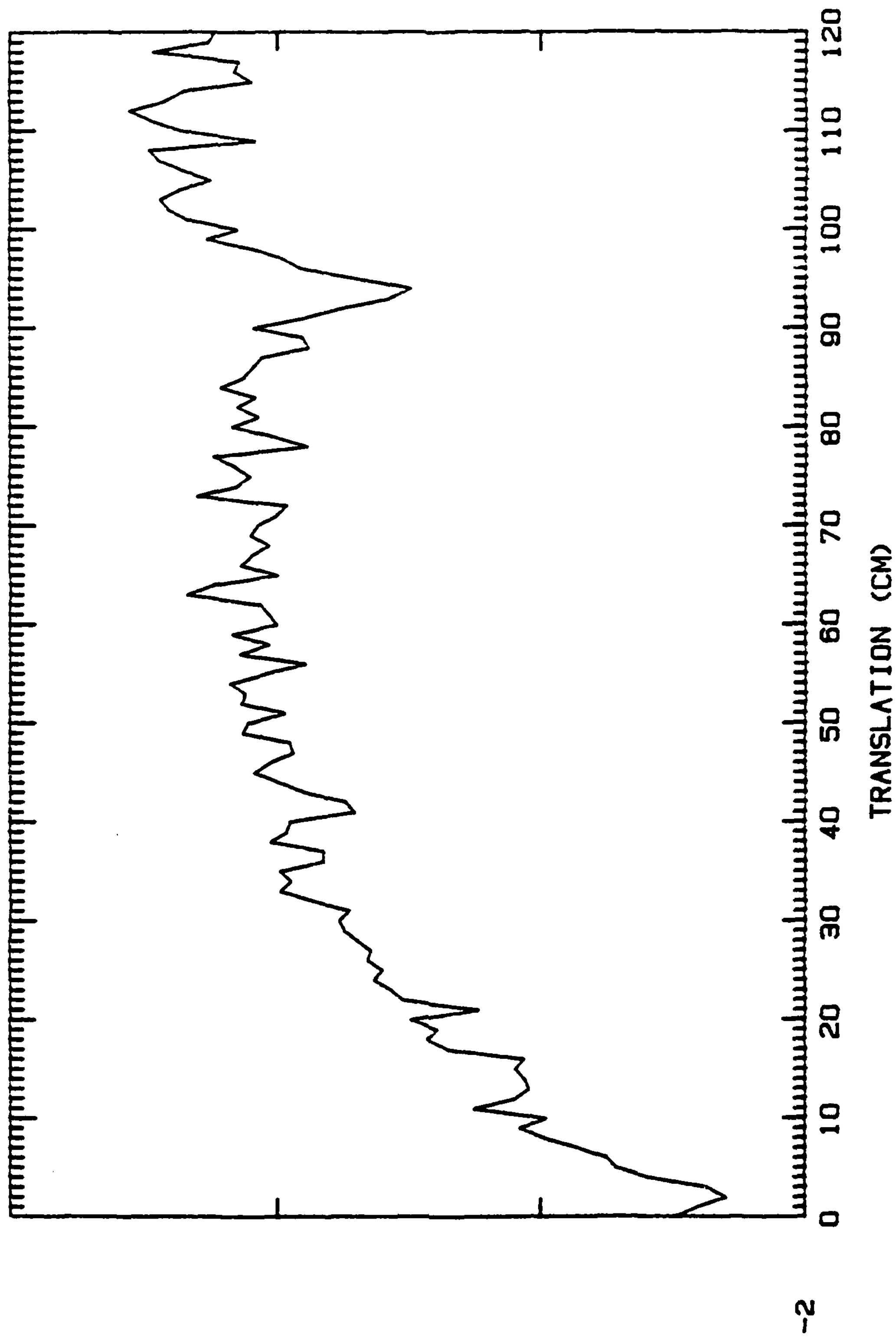


Figure 60. Magnitude, 18 GHz

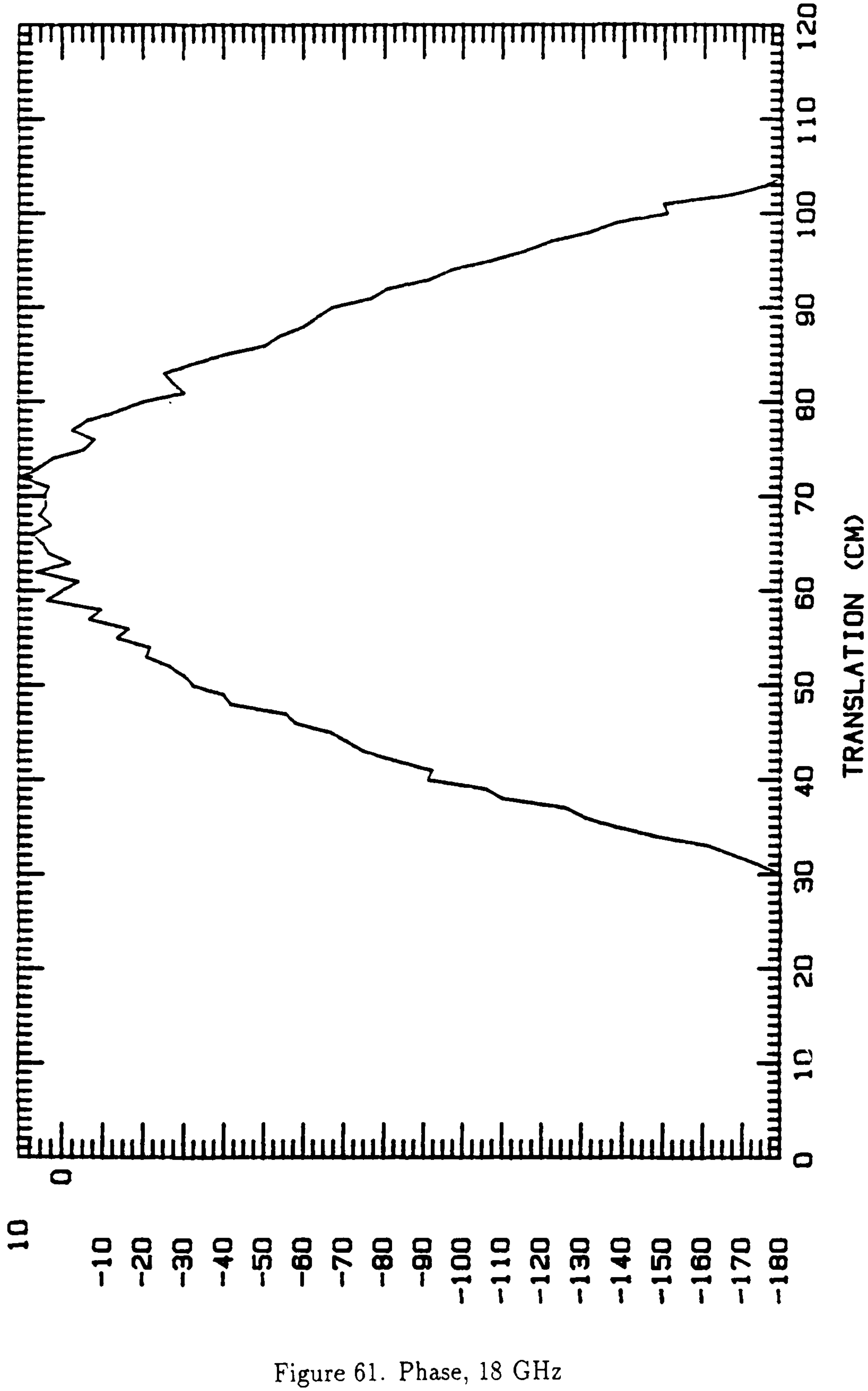


Figure 61. Phase, 18 GHz

*Vertical Translation*

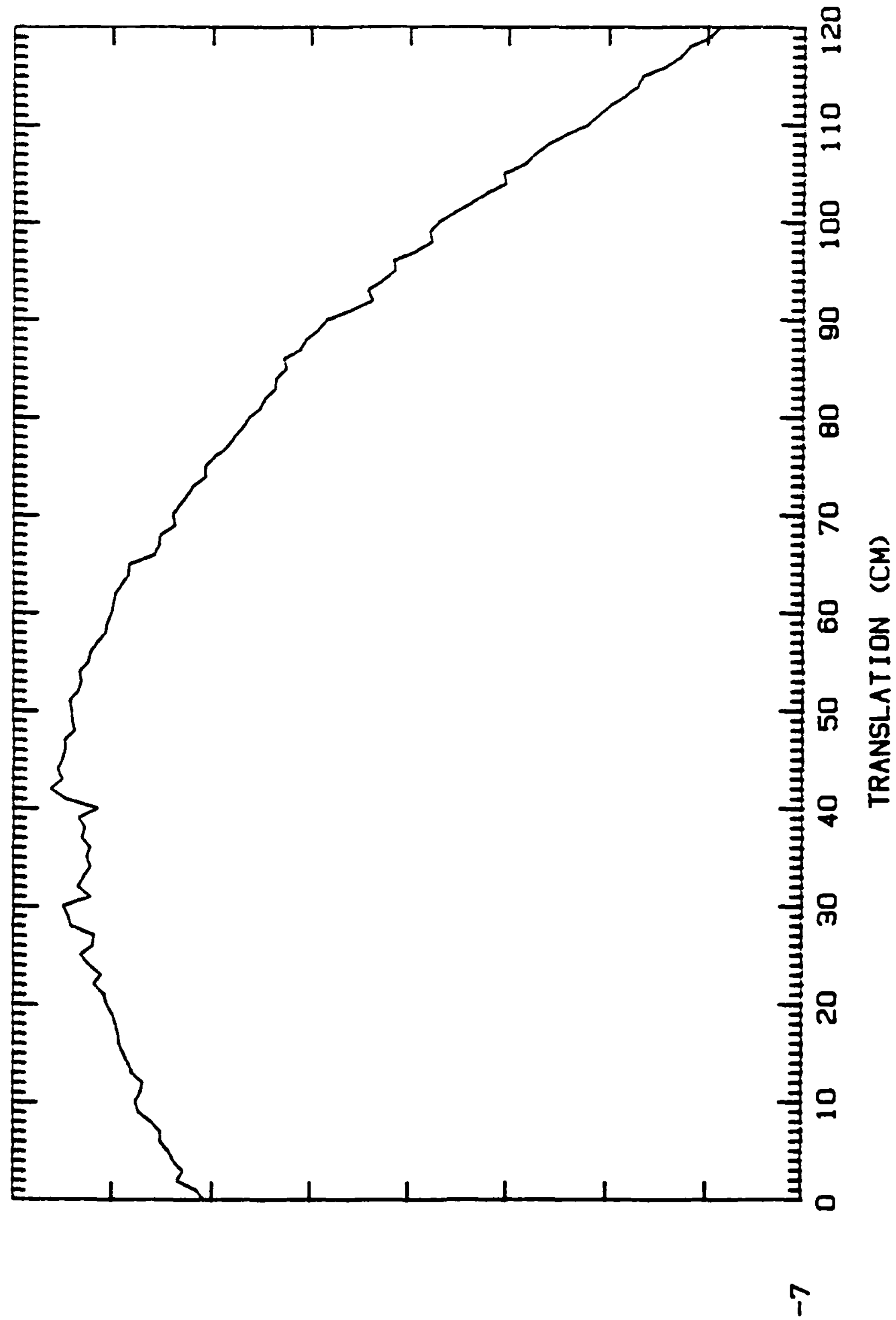


Figure 62. Magnitude, 10 GHz, Vertical Polarization, Antenna 2 TX

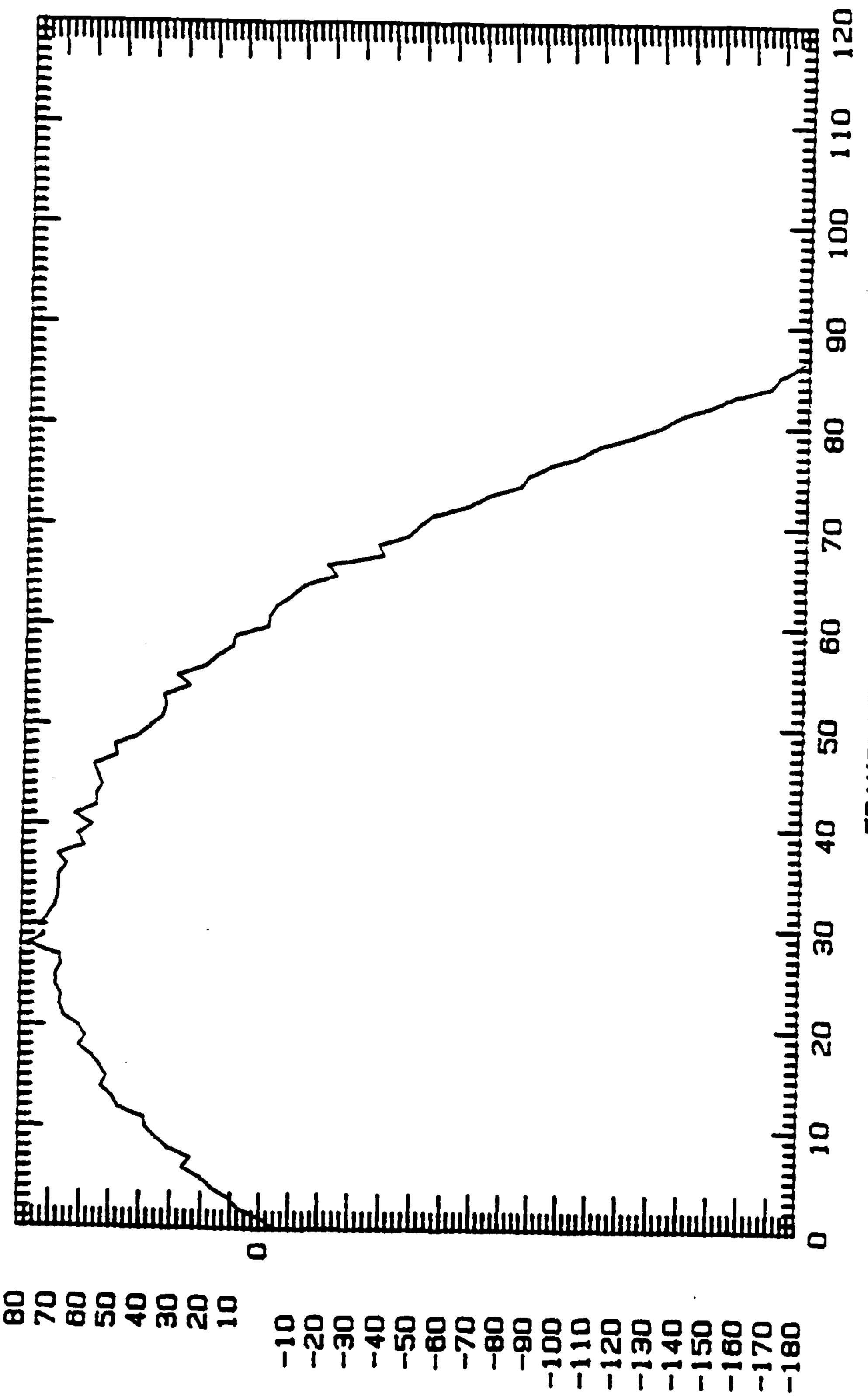


Figure 63. Phase, 10 GHz, Vertical Polarization, Antenna 2 TX

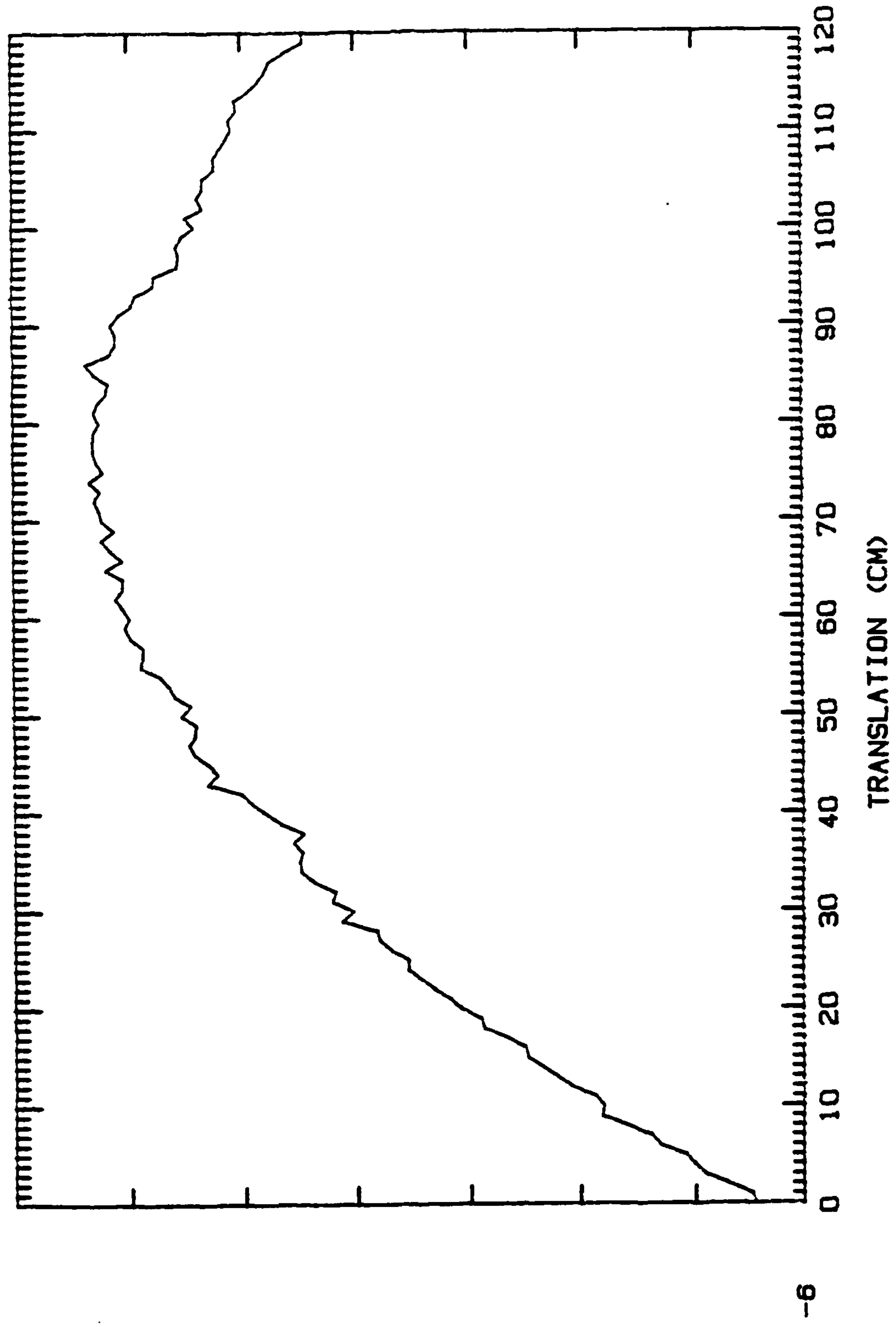


Figure 64. Magnitude, 10 GHz, Vertical Polarization, Antenna 1 TX

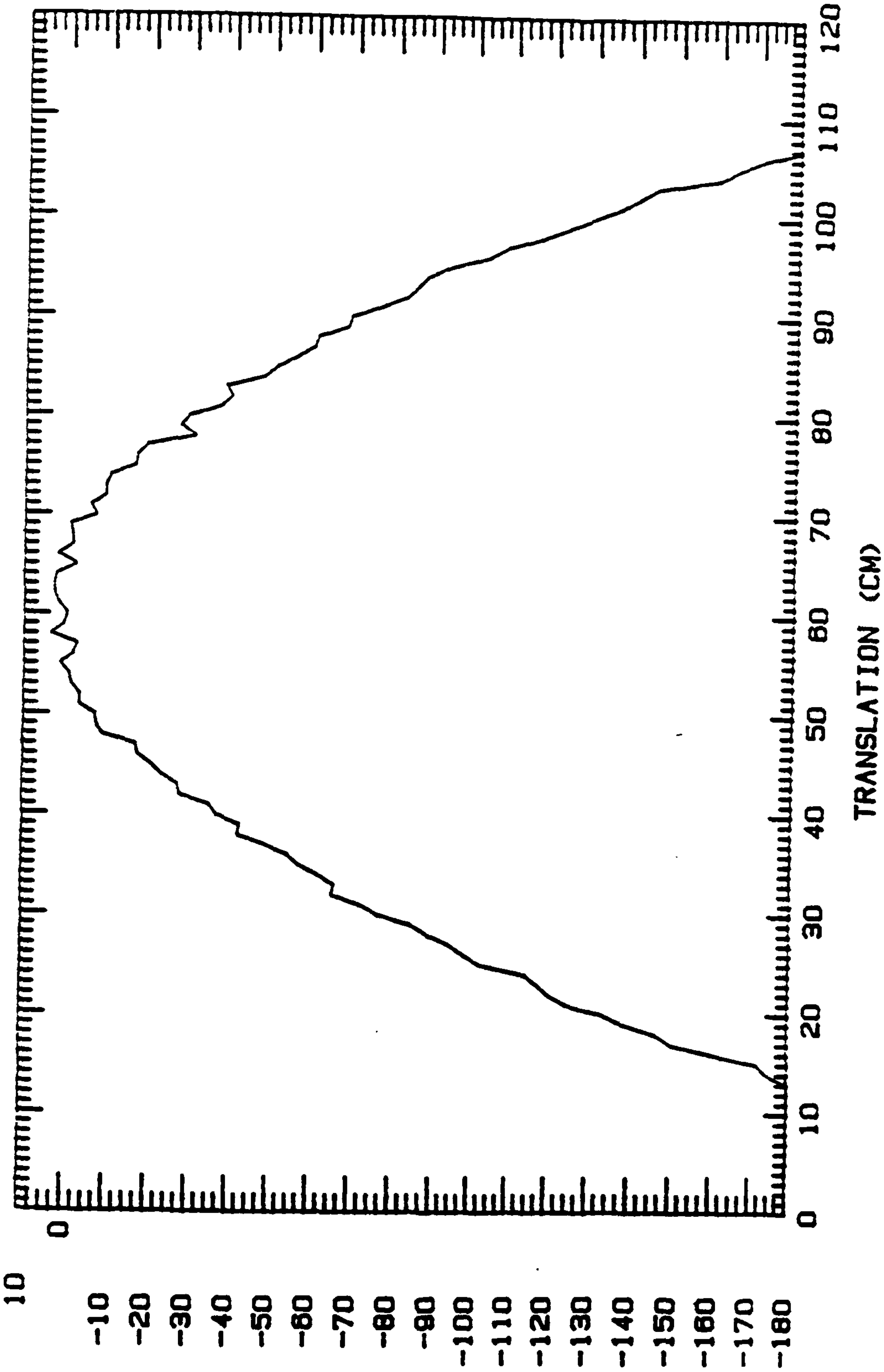


Figure 65. Phase, 10 GHz, Vertical Polarization, Antenna 1 TX

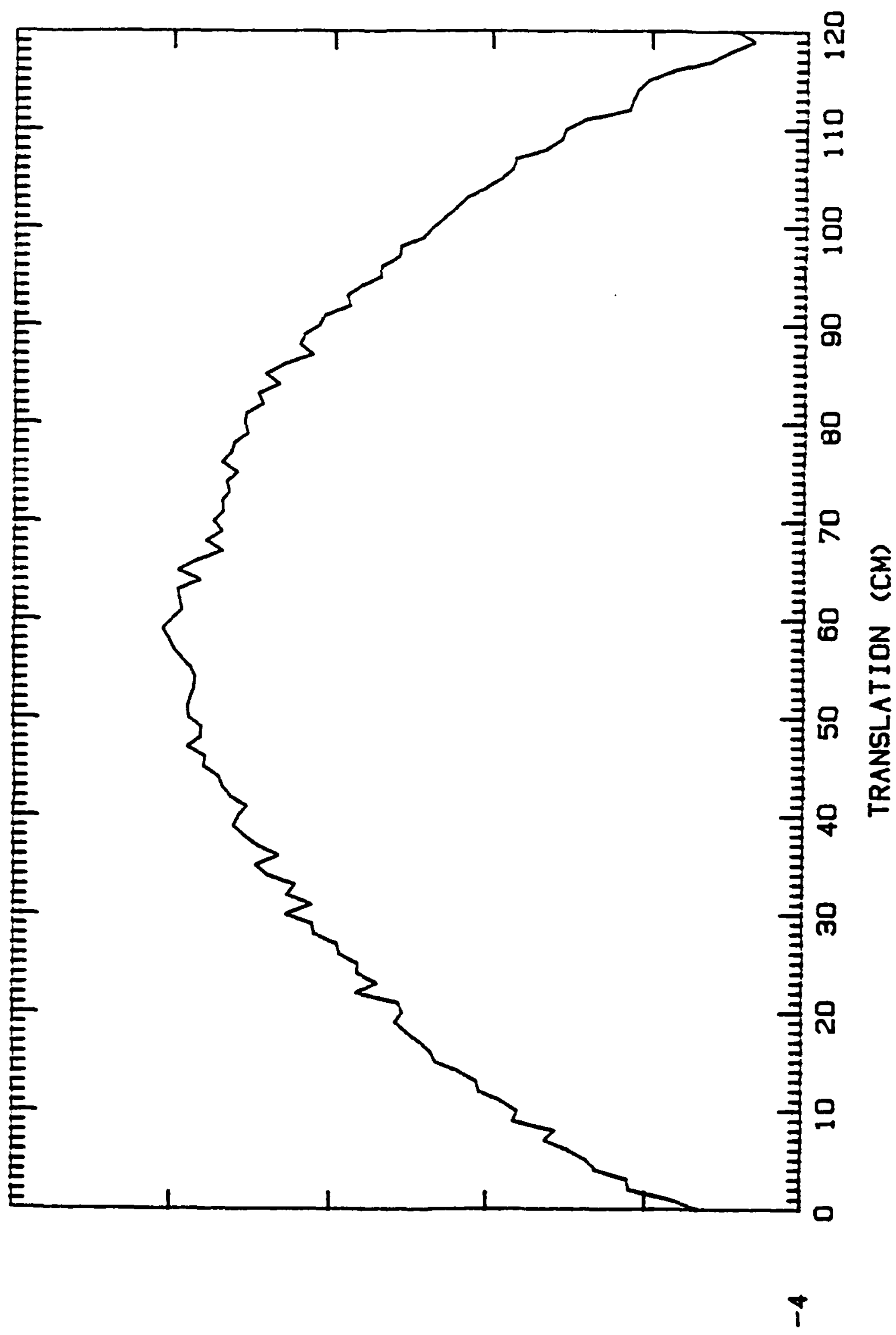


Figure 66. Magnitude, 10 GHz, Horizontal Polarization, Antenna 2 TX

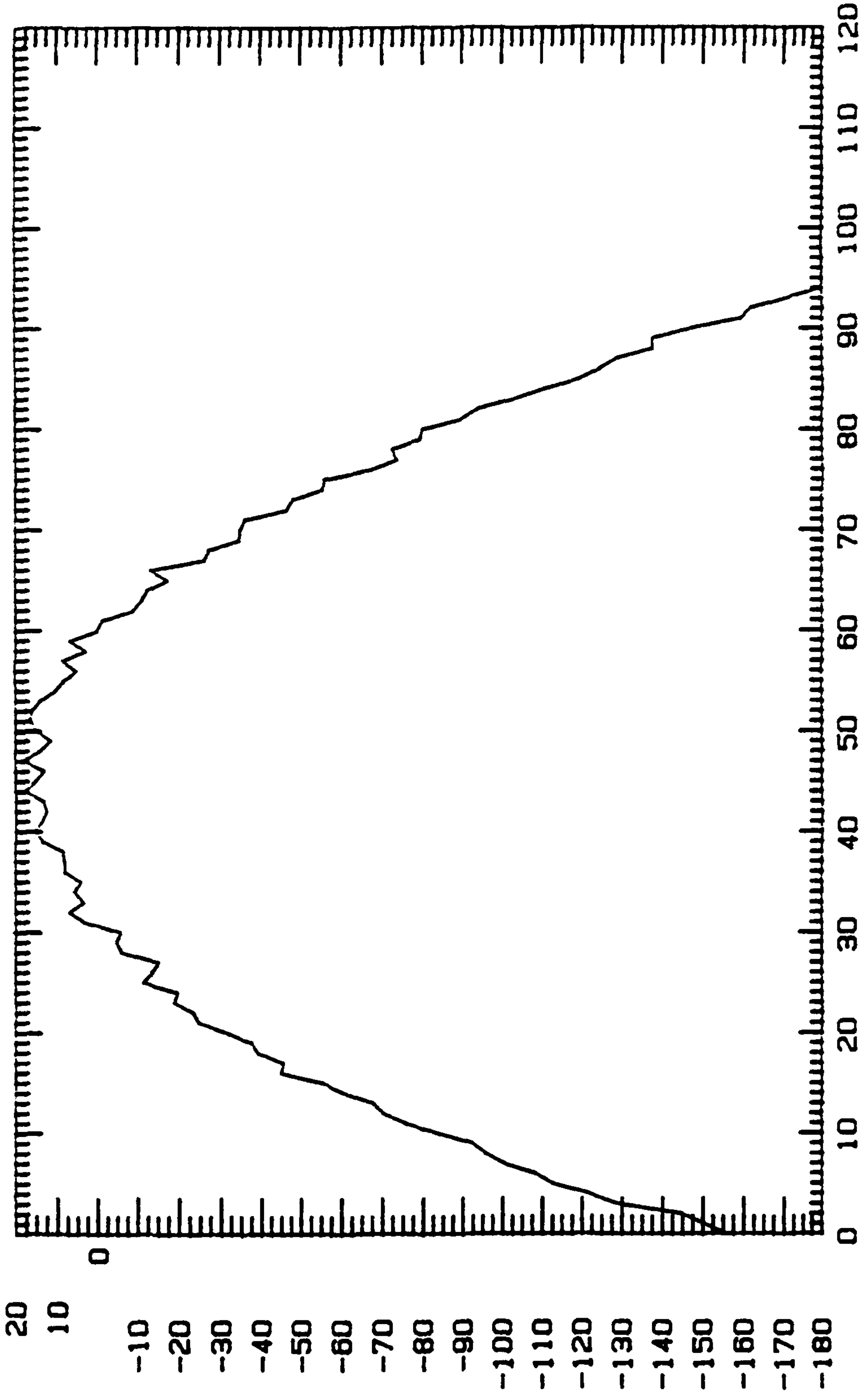


Figure 67. Phase, 10 GHz, Horizontal Polarization, Antenna 2 TX

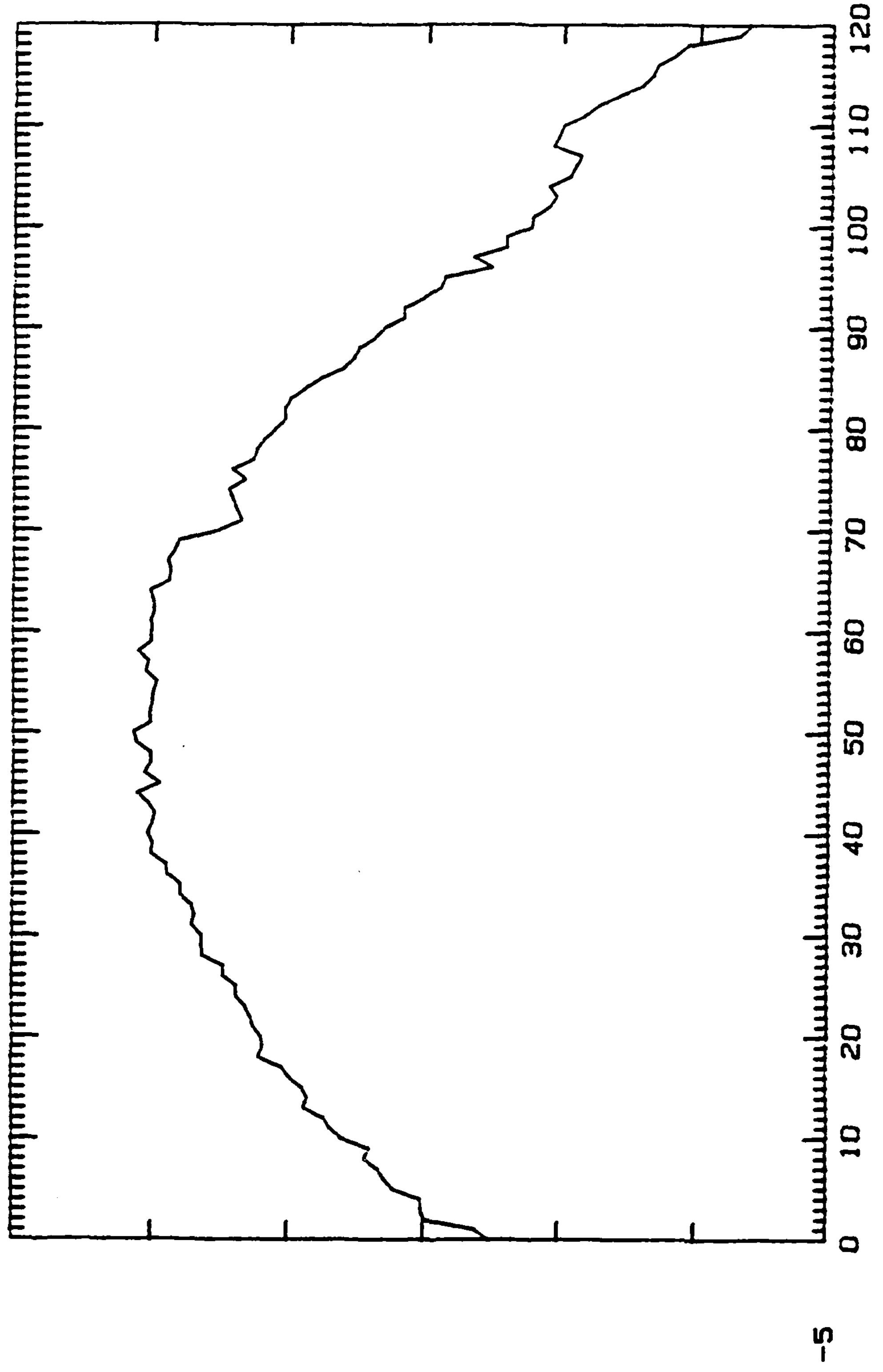


Figure 68. Magnitude, 10 GHz, Horizontal Polarization, Antenna 1 TX

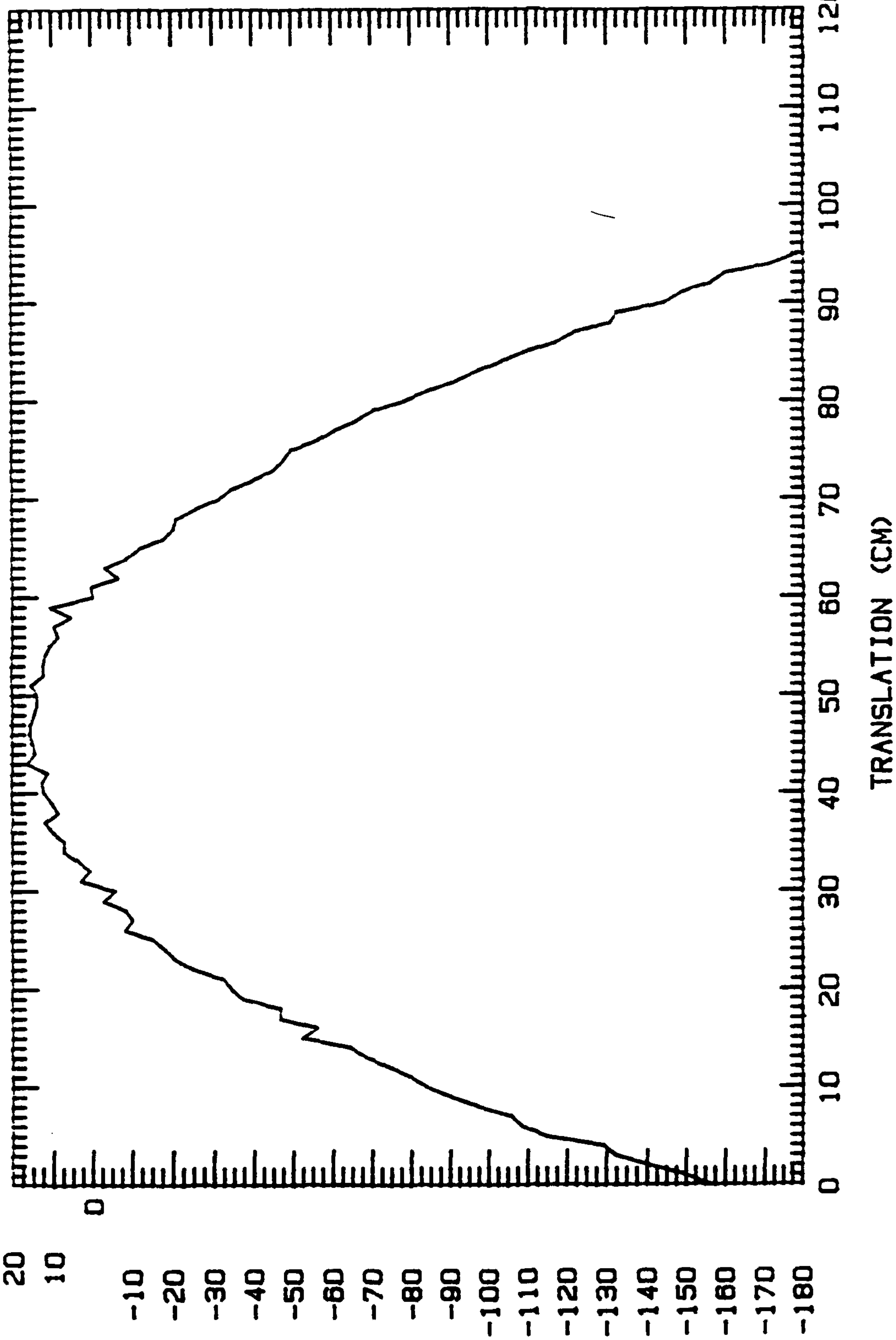


Figure 69. Phase, 10 GHz, Horizontal Polarization, Antenna 1 TX

## *Vita*

Captain Anthony J. Hunt [redacted]. Within two years, he moved to Oklahoma where he spent most of his childhood. After graduating from High School, he enlisted in the Army as an Electronic Warfare Noncommunications Intercepter/Analyst. After two years, he attended the U.S. Military Academy at West Point, New York. He graduated in 1980 and was commissioned as a Second Lieutenant in Military Intelligence. His military training includes Airborne, Military Basic and Advanced Courses, and Combined Arms Services Staff School. His assignments include Platoon Leader, Executive Officer, Armor Battalion Intelligence Officer, and CEWI Battalion Assistant Operations Officer at Fort Hood, Texas and Mission Control Officer, Battalion Operations Officer, and Company Commander in West Germany. In May of 1988 he entered the Air Force Institute of Technology in pursuit of a Master of Science degree in Electrical Engineering.

[redacted]

# *Bibliography*


1. W. D. Burnside. Reflector edge, target support and feed antenna design for compact range. A workshop presentation by Ohio State University, September 1985.
2. S. J. Foti and D. D. McGahey. Diagonal horn improves anechoic chamber tests. *Microwaves and RF*, pages 105,107–110,134, March 1984.
3. C. C. Freeny and R. A. Ross. Radar cross section target supports — metal columns and suspension devices. Technical Documentary Report RADC-TDR-64-382, General Dynamics/ Fort Worth, June 1964.
4. P. J. Joseph. A utd scattering analysis of pyramidal absorber for design of compact range chambers, 1988. PhD Dissertation, The Ohio State University.
5. E. F. Knott et al. *Radar Cross Section.* Artech House, Inc., Norwood, Mass., 1985.
6. R. G. Kouyoumjian and L. Peters Jr. Range requirements in radar cross-section measurements. In *Proceedings of the IEEE*, volume 53, pages 920–928, August 1965.
7. A. W. Love. The diagonal horn. *Microwave Journal*, V:117,122, March 1962.
8. Hewlett Packard. The fundamentals of signal analysis. Application Note 243.
9. M. A. Plonus. Theoretical investigations of scattering from plastic foams. In *IEEE Transactions on Antennas and Propagation*, pages 88–94, 1964.
10. L. A. Robinson. Design of anechoic chambers for antenna and radar-cross-section measurements. Technical Report 2, Office of Naval Research, 800 North Quincy Street, Arlington, VA 22217, November 1982.
11. T. B.A. Senior et al. Designing foamed-plastic target supports. *Microwaves*, pages 38–43, December 1964.
12. W. G. Swarner et al. Sixth status report on contract number or-549651-b28. Electro Science Laboratory, The Ohio State University, Columbus, OH.

ABSTRACT:

This research effort investigated improvements and characterization of the AFIT RCS measurement chamber. The two main areas of improvement included the support pedestal and antennas. Characterization included antenna and system performance as pertains to aliasing, noise floor and quiet zone definition.

Support pedestal improvement involved consideration of the three primary types used; the suspension line support, foamed plastic columns, and ogive-shaped metal pylon. Antenna improvement imcluded installing broad bandwidth, low sidelobe antennas. These were mounted so that they could be easily rotated for polarization selection, and so that they provided a good approximation to a backscatter angle of zero degrees without incurring high antenna coupling.

System aliasing measurements and anlaysis was performed to ensure that the full bandwidth capacity of the antennas was achievable without causing alias error signals to enter the target zone. Noise floor data was taken to determine the degree of sensitivity improvement after modifications. Quiet zone characterization was designed to verify predictions and provide actual dimensions for measurement analysis. Additionally, the quiet zone measurements provided information as to the pedestal location relative to the focus of the antenna.

UNCLASSIFIED

SECURITY CLASSIFICATION OF THIS PAGE

# REPORT DOCUMENTATION PAGE

*Form Approved OMB No. 0704-0188*

| | |
|---|---|
| 1a. REPORT SECURITY CLASSIFICATION<br>UNCLASSIFIED | 1b RESTRICTIVE MARKINGS |
| 2a. SECURITY CLASSIFICATION AUTHORITY | 3. DISTRIBUTION/AVAILABILITY OF REPORT<br>Approved for public release; distribution unlimited |
| 2b. DECLASSIFICATION/DOWNGRADING SCHEDULE | |
| 4. PERFORMING ORGANIZATION REPORT NUMBER(S)<br>AFIT/GE/ENG/90J-03 | 5. MONITORING ORGANIZATION REPORT NUMBER(S) |
| 6a. NAME OF PERFORMING ORGANIZATION<br>School of Engineering<br>6b. OFFICE SYMBOL *(If applicable)*<br>AFIT/ENG | 7a. NAME OF MONITORING ORGANIZATION |
| 6c. ADDRESS *(City, State, and ZIP Code)*<br>Air Force Institute of Technology<br>Wright-Patterson AFB, Ohio 45433-6583 | 7b. ADDRESS *(City, State, and ZIP Code)* |
| 8a. NAME OF FUNDING/SPONSORING ORGANIZATION<br>School of Engineering<br>8b. OFFICE SYMBOL *(If applicable)*<br>AFIT/ENG | 9 PROCUREMENT INSTRUMENT IDENTIFICATION NUMBER |
| 8c. ADDRESS *(City, State, and ZIP Code)*<br>Air Force Institute of Technology<br>Wright-Patterson AFB, Ohio 45433-6583 | 10. SOURCE OF FUNDING NUMBERS<br>PROGRAM ELEMENT NO / PROJECT NO. / TASK NO / WORK UNIT ACCESSION NO. |

11. TITLE *(Include Security Classification)*
ANALYSIS AND DESIGN OF MODIFICATIONS FOR IMPROVED PERFORMANCE OF THE AFIT RADAR CROSS SECTION MEASUREMENT CHAMBER

12. PERSONAL AUTHOR(S)
Anthony J. Hunt, CPT, USA

| 13a. TYPE OF REPORT | 13b. TIME COVERED | 14. DATE OF REPORT *(Year, Month, Day)* | 15. PAGE COUNT |
|---|---|---|---|
| MS Thesis | FROM ______ TO ______ | 1990 June | 120 |

16. SUPPLEMENTARY NOTATION

| 17. COSATI CODES | | | 18. SUBJECT TERMS *(Continue on reverse if necessary and identify by block number)* |
|---|---|---|---|
| FIELD | GROUP | SUB-GROUP | |
| 14 | 02 | | Anechoic Chambers |
| | | | |

19. ABSTRACT *(Continue on reverse if necessary and identify by block number)*

Thesis Advisor: Philip J. Joseph, Captain, USAF
Assistant Professor of Electrical Engineering

Abstract: See reverse side

| | |
|---|---|
| 20. DISTRIBUTION/AVAILABILITY OF ABSTRACT<br>☐ UNCLASSIFIED/UNLIMITED ☒ SAME AS RPT. ☐ DTIC USERS | 21. ABSTRACT SECURITY CLASSIFICATION<br>UNCLASSIFIED |
| 22a. NAME OF RESPONSIBLE INDIVIDUAL<br>Philip J. Joseph, Captain, USAF | 22b TELEPHONE *(Include Area Code)*<br>(513) 255-3576<br>22c OFFICE SYMBOL<br>AFIT/ENG |